

QuaesitUM

The Undergraduate Research Journal of The University of Memphis

Spring 2020

<http://www.memphis.edu/quaesitum/>

QuaesitUM is an annual publication that provides an academic forum where University of Memphis undergraduate students can showcase research from all disciplines.

QuaesitUM © 2020
The University of Memphis
<http://www.memphis.edu/quaesitum/>

ISSN 2375-5423

Editorial Board

Editor-in-Chief

Dr. Sage Graham

Technical Editor

Scott Dutt

*Do research. Feed your talent.
Research not only wins the war on cliché,
it's the key to victory over fear and its cousin, depression.*

-- Robert McKee

To Our Readers

In the Spring of 2020, the world was confronted with the COVID-19 pandemic. Times of upheaval and uncertainty such as this illustrate (in a concrete way) that research and expanding our knowledge is vital to our very existence. This is true not only in laboratories developing vaccines, but also in research that examines wider implications and perspectives. Explorations of how global events are discussed, how societal structures and practices are altered, how tools and resources can be adapted to changing needs, and how depictions of human experience impact our outlook and attitudes all enhance our understanding of the world and the circumstances around us.

Since its inception, *Quaesitum's* mission has been to showcase multidisciplinary research that reflects the excellence of our students' scholarship. In many cases, the students who contributed the papers included here encountered unanticipated challenges due to the COVID-19 pandemic. In some cases they were unable to present their work at scholarly conferences, in others they had reduced access to library resources, and in others they were diverted from their projects because of family and health concerns. Despite these obstacles, they persisted and the results are contained in this volume. Their work reflects the excellence and capability of our students.

Producing this volume relies on the efforts and expertise of many people. I am immeasurably grateful for the efforts of our technical editor Mr. Scott Dutt, who has played a critical role in the development of the journal for the past 5 years. His efforts have set the stage for ongoing excellence and his influence will be felt in the journal from here onward. I am similarly grateful to Dr. Melinda Jones, Director of the Honors College, a committed member of the editorial team whose expertise and resources have ensured a quality publication since the inaugural issue.

Mr. Gary Golightly has graciously continued to create the artwork for the journal, capturing its spirit in each image year-after-year. The Honors College, under Dr. Jones' leadership, also generously funded the awards for the best paper, thereby supporting the research climate that exists on our campus.

In addition, Dr. Jones, Mr. Dutt and I also owe thanks to the faculty reviewers who helped ensure the quality of the final publication: Dr. Gustav Borstad, Dr. Colin Chapell, Dr. David Freeman, Dr. Ronald Fuentes, Dr. Arleen Hill, Dr. Jessica Jennings, Dr. Sanjay Mishra, Dr. Max Paquette, Dr. Melissa Pappa, and Dr. Kris-Stella Trump. Their feedback was a critical part of the publication process and we could not produce a quality publication without their efforts.

The faculty who have mentored and sponsored the student contributors also deserve thanks: Dr. Rebecca Adams, Dr. Gary Bowlin, Dr. Aram Goudsouzian, Dr. Eric Groenendyk, Dr. Mohammed Lardji, Dr. Deranda Lester, Dr. Francisco Muller Sanchez, Dr. Esra Ozdenerol, Dr. Douglas Powell, and Dr. Firouzeh Sabri. Without their guidance and encouragement these students would not have entered the scholarly conversation that comes from publishing their work.

Finally, congratulations and thanks go to the student authors themselves. Despite the benefits of research, exposing oneself to the potential criticism of reviewers and laboring through the multi-stage publication process can be difficult. They should be commended for the perseverance and commitment to excellence that they displayed throughout this project. Their efforts will set the stage for continued research in their fields moving into the future.

With gratitude for ongoing discovery,

Dr. Sage Graham
Quaesitum Editor-in-Chief

Table of Contents

Engineering

- | | | |
|---|---|--|
| 1 | Evaluating the Effect of Incorporation of Fibrinogen into Electrospun Templates of Polydioxanone on their Mechanical Properties | William Cain,
Allison Fetz,
Gary Bowling |
|---|---|--|

Humanities

- | | | |
|----|---|--------------------|
| 21 | “The Chaplain of the New Left”:
Reverend Richard Moon’s Community of Influence and the 1968 Memphis Sanitation Workers’ Strike | Amanda
Campbell |
|----|---|--------------------|

Life and Health Sciences

- | | | |
|----|---|---------------|
| 39 | Effects of Stride Length on Knee Loading in Simulated Obese Populations | Alexis Nelson |
|----|---|---------------|

Physical and Applied Sciences

- | | | |
|-----|---|--------------------|
| 57 | Physical Characteristics of the Nuclear Region of NGC 4388 | Christian
Brown |
| 75 | The Synthesis and Preparation of Upconverting and Downconverting Phosphors for Sensing Applications | Daniel Duong |
| 87 | Mars Dust Adhesion: Characterizing Adhesion Behavior of JSC Mars-1 Regolith on Aerogel Substrates | Jacob Parks |
| 103 | Assessing Tornado Vulnerability in Tennessee through Tornado Incidence and Societal Exposure | Jacob Seboly |
| 121 | A Molecular Dynamics Study of Lipid Membranes Cushioned by Polymer Brushes | Jeremy Walker |

Social and Behavioral Sciences

- | | | |
|-----|---|---|
| 137 | Who Do You Belong To?: Social Sorting Between Gender and Partisan Identity Groups | Aeona Seymour |
| 161 | Environmental Enrichment Alters Mesolimbic Dopamine Release in Mice | Shelby Towers,
Josiah Comstock,
Nick Paige,
Price Dickson,
Deranda Lester |
| 179 | Communication Across Cultural Boundaries Within Memphis ESL Classrooms | Johnda Washington |

Publication and Review Process

- | | |
|-----|-------------------------|
| 205 | Faculty Reviewers Board |
| 209 | Submission Guidelines |

William J. Cain graduated *summa cum laude* from the University of Memphis in May 2020 with a major in biomedical engineering and minors in biology and chemistry. He also earned Honors in Biomedical Engineering and University Honors with Thesis designations. Throughout his time at the University of Memphis, he has been involved in multiple tissue engineering research projects under Dr. Gary Bowlin and has presented at various research conferences. He has worked extensively with various humanitarian projects and hopes to use his engineering background to help improve the condition of the less fortunate. William plans to earn a higher degree in bioengineering or the medical field before entering the workforce.

William Cain, Allison E. Fetz, Gary L. Bowlin

Evaluating the Effect of Incorporation of Fibrinogen
into Electrospun Templates of Polydioxanone on
their Mechanical Properties

Faculty Sponsor

Dr. Gary Bowlin

Abstract

Research has shown that the enzyme matrix metalloproteinase-9 (MMP9) is a critical factor responsible for angiogenesis. Since MMP9 secretion by neutrophils can be induced by fibrinogen, our goal is to stimulate the secretion of MMP9 from template interacting neutrophils via the incorporation of fibrinogen into an electrospun template. The aims of this preliminary research study were (1) to create electrospun templates of five different concentrations of the synthetic polymer, polydioxanone, and the natural polymer, fibrinogen, (2) to analyze the fiber diameters of these templates, and (3) to characterize the mechanical properties of these templates. The results indicate that increased fibrinogen incorporation into polydioxanone templates correlates with a decrease in the fiber diameter of their resultant electrospun templates. Additionally, uniaxial tensile testing revealed that increasing the fibrinogen content of electrospun templates decreased both the ultimate tensile strength and the maximum strain of the electrospun template. This work shows that incorporation of fibrinogen into electrospun polydioxanone templates changes the mechanical properties of the templates, and thus alters the potential of the biomaterial to be used in applications which are subject to different stresses and strains. Future work will evaluate the effect that fibrinogen concentration makes on neutrophil secretion of MMP9 and its efficacy in inducing angiogenesis.

Introduction

Various pathologies are characterized by a lack of functional vascularization. One of the most prevalent conditions is peripheral arterial disease (PAD), which presents with atherosclerotic narrowing of the arteries of the limbs, especially the legs. PAD leads to pain and movement disabilities, secondary to muscle atrophy and non-healing ulcers. If the condition is left untreated, injury or ulcers in the ischemic tissue may lead to tissue death and gangrene and necessitate total limb amputation [1]. Treatment strategies include bypass surgery to restore blood flow to the ischemic tissues using allografts, autografts, and synthetic grafts. Since there is typically poor neointimal regeneration of these vascular grafts, thrombosis can occur, occlude the vessel, and cause the graft to fail at high rates [2]. This high failure rate indicates the need for a better system which can guide blood flow to targeted tissues. Ideally, a resorbable small diameter vascular graft could guide the in situ regeneration of a functional native blood vessel. To generate this functional graft, the template must guide robust angiogenesis by recruiting endothelial cells into the lumen of the graft and supporting their proliferation. This neointimal regeneration is essential for the success of the implant so that a confluent endothelium, neointima, can form [3-5].

The white blood cells that lead the immune system in the inflammatory response, the neutrophils, release an enzyme, MMP9, which has been identified as a critical factor responsible for angiogenesis [6-8]. Because implanted vascular grafts immediately interact with large numbers of neutrophils upon implantation and ligation of a receptor which binds fibrinogen (FBG) is known to induce neutrophil secretion of MMP9, we anticipate that we may be able to harness the angiogenic capabilities of neutrophils by incorporating FBG into electrospun templates of polydioxanone (PDO). Achievement of this aim will create more efficacious grafts for restoring blood flow to ischemic tissues.

To create these templates, we electrospun solutions containing different concentrations of PDO and FBG. Electrospinning is a process by which templates composed of nano- to microfibers are fabricated. This template fabrication process involves the application of a voltage source to a polymer solution which is stored in a syringe. Due to the potential difference between the liquid surface at the tip of the syringe and a grounded target opposite the syringe, a liquid jet extrudes from the syringe and is drawn across an airgap to deposit small diameter fibers onto the grounded target. This process creates mats of nonwoven, randomly distributed fibers, which are biomimetic of native extracellular matrix (ECM). These templates can be fabricated with an array of physical, chemical, and mechanical properties which create

efficacious biomaterials for diverse application in guided tissue regeneration.

Since FBG plays a key role in the secretion of MMP9 from neutrophils, we sought to incorporate this protein into our electrospun templates and determine if the physical and mechanical properties of these FBG containing templates differed significantly depending on their concentration ratio of PDO and FBG. The morphological characteristics of the templates were evaluated by fiber diameter analysis, which indicated that increasing the percentage of FBG in the templates decreases the average fiber size. The mechanical properties were evaluated by uniaxial tensile testing to determine Young's modulus (YM), Ultimate Tensile Strength (UTS), and maximum strain for each template. The data indicate an inverse correlation between the percentage of FBG and both UTS and maximum strain. Additionally, mechanical testing data displayed a non-uniform correlation between FBG concentration and YM, which indicated that some intermediate percentage of FBG incorporation may maximize the stiffness of the material. These results indicate that FBG incorporation into electrospun templates of PDO changes the properties of the templates, and, with these tailorable templates, we should be able to fabricate and optimize the FBG incorporation into templates to promote optimal MMP9 secretion.

Null Hypothesis

Incorporating FBG into electrospun PDO templates will not affect the mechanical properties of YM, UTS, or maximum strain.

Materials And Methods

Electrospinning

In this study, PDO (Bezwada Biomedical LLC, Lot. No. BB0306-234D) and FBG (Sigma, Fibrinogen from bovine plasma, F8630-5G, Lot. No. SLBW1275) were combined in different volume-to-volume ratios (vol/vol) to create templates with variable compositions of FBG (Table 1). The two polymers were dissolved in solution in separate vials. The PDO was mixed for 24 hours in a vial of 1,1,1,3,3,3-hexafluoro-2-propanol (HFP, Oakwood Products, Inc., Pro. No. 003409), and the FBG was mixed in a solution of 1 part 10x Gibco Minimum Essential Medium with Earle Salts (MEM, ThermoFisher Scientific, Cat. No. 11430030) to 9 parts HFP for 24 hours [9]. The PDO solution was added to the FBG vial after 24 hours, vortexed for 60 seconds, and then loaded into a 3-mL syringe (Becton, Dickinson, and Company, Pro. No. 309657). This syringe was attached to an 18-gauge blunt needle McMaster-Carr, Pro. No. 6710A25) which

was connected to the positive lead of a Spellman CZE1000R power source (Spellman High Voltage Electronic Corp.). The syringe was placed on a syringe pump (Fisher Scientific, Model No. 78-01001) which dispensed the solution at a rate between 0.25 mL/h and 2.00 mL/h. Fibers were collected on the parchment side of non-stick Pan Lining Paper (Reynolds Wrap, Model No. B0068TZUXO) which was attached to a grounded, stainless steel 200 x 750 x 5 mm rectangular mandrel, which was rotating at 1250 RPM and translating 6.5 cm/s over 13 cm. Polymer concentration, applied voltage, flow rate, and airgap distance between the needle tip and mandrel are shown in Table 1. The parameters were optimized for each electrospun template to produce templates composed of uniform fiber diameter which were non-beaded. The templates (thickness 0.07 - 0.13 mm) were stored in a desiccator at 25°C until analysis connected to the positive lead of

PDO/FBG (vol/vol)	PDO Concentration (mg/mL)	FBG Concentration (mg/mL)	Voltage (kV)	Flow Rate (mL/h)	Airgap Distance (cm)
100/0	67	N/A	+14	0.25	14
75/25	60	100	+28	2.00	15
50/50	100	100	+28	2.00	15
25/75	100	100	+28	2.00	15
0/100	N/A	100	+28	2.00	15

Table 1. Electrospinning parameters optimized for PDO/FBG templates.

a Spellman CZE1000R power source (Spellman High Voltage Electronic Corp.). The syringe was placed on a syringe pump (Fisher Scientific, Model No. 78-01001) which dispensed the solution at a rate between 0.25 mL/h and 2.00 mL/h. Fibers were collected on the parchment side of non-stick Pan Lining Paper (Reynolds Wrap, Model No. B0068TZUXO) which was attached to a grounded, stainless steel 200 x 750 x 5 mm rectangular mandrel, which was rotating at 1250 RPM and translating 6.5 cm/s over 13 cm. Polymer concentration, applied voltage, flow rate, and airgap distance between the needle tip and mandrel are shown in Table 1. The parameters were optimized for each electrospun template to produce templates composed of uniform fiber diameter which were non-beaded. The templates (thickness 0.07 - 0.13 mm) were stored in a desiccator at 25°C until analysis.

Imaging and Fiber Diameter Analysis

To characterize the templates by scanning electron microscopy, each template was sputter coated with 5 nm of gold-palladium in an argon gas field. The templates were then imaged using a scanning electron microscope (SEM, FEI Nova NanoSEM™ 650) with a field emission gun at + 20 kV and a working distance of 5 mm. Both the inside (mandrel facing) and outside (external facing) surfaces of each template were imaged at 1000x and 5000x to ensure the templates were composed of non-fused, non-beaded fibers. If the SEM image revealed a template composed of beaded or fused fibers, the template was discarded, and the fabrication and characterization process was repeated until optimal electrospinning parameters were found. The fiber diameters were subsequently quantified by analyzing the SEMs in FibraQuant 1.3 software (nanoTemplate Technologies, LLC). A minimum of 200 semi-automated random measurements were taken per image to generate averages and corresponding standard deviations.

Mechanical Testing

After fabrication and SEM characterization, the electrospun templates were cut into dogbone shaped samples (2.75 mm at the narrowest point) in two directions: axial (parallel to the axis of rotation) and perpendicular (perpendicular to the axis of rotation). The thickness of each specimen was measured using calipers (Mitutoyo Absolute, Pro. No. 547-516), and the dogbone shape samples were loaded into a TestResources frame (model no. 220Q with 111 N load cell) with a gauge length of 7.5 mm. Uniaxial tensile testing was then performed ($n \geq 7$ punches of each orientation) at a strain rate of 10 mm/min until failure. The resultant data were recorded in the software associated with the testing frame (TestResources XY Series Software) and exported to Microsoft Excel.

Data and Statistical Analysis

Microsoft Excel was used to generate stress strain curves for each replicate, which was then used to calculate YM, UTS, and maximum strain. YM for each template was found using a line of best fit to approximate the slope of the initial linear elastic region of the stress strain curve. The slope of each linear elastic region, equivalent to the YM of that piece of electrospun material, was recorded and saved for statistical analysis. Similarly, the UTS was identified by finding the maximum stress on the stress strain curve. This peak stress occurs just before the material fails under uniaxial tensile testing. Last, the maximum strain was found and corresponds to elongation at the point of failure. The data were grouped by the orientation of the dogbone punch and exported to Graphpad Prism 6 for statistical analysis.

The normality of the data was tested using the Shapiro-Wilk normality test to determine the appropriate analysis of variance. Fiber diameter and each mechanical property was then analyzed with either Kruskal-Wallis analysis of variance and Dunn's multiple comparison procedure for non-normal data sets or Tukey's multiple comparisons test for normal data. All analyses were performed in GraphPad Prism 6 at a significance level of 0.05.

Results

Electrospinning and Fiber Diameter Analysis

The electrospinning parameters for each PDO/FBG mixture were optimized to produce fibers which were approximately equivalent to those of the lowest concentration of PDO. After these parameters were optimized such that the electrospun fibers were non-fused, non-beaded, and roughly the same diameter, full templates of each composition were fabricated. Figure 1 shows representative SEMs which display the fiber morphology of each template. As shown in Figure 1, there appears to be some inconsistency in the fiber deposition patterns between the five templates including relative alignment of the fibers and presence of both large and small fibers in some templates (Figure 1D). Worthy of note, the PDO/FBG template 0/100 (Figure 1E) has a single fiber which has an elongated bead and appears to have fibers packed in greater density than the other templates. As fiber anisotropy and density of the templates were outside of the scope of this project, we did not further investigate these properties.

The results of fiber diameter analysis are shown in Figure 2 and Table 2. As indicated in Figure 2, the average fiber diameter of the templates correlates inversely to the percentage of FBG incorporated into the electrospun templates. The average fiber diameter of each PDO containing electrospun template decreased with increasing proportions of FBG incorporation. Notably, the $0.28 \pm 0.14 \mu\text{m}$ fibers for the PDO/FBG 100/0 template were significantly larger ($p < 0.05$) than all other templates while the $0.17 \pm 0.09 \mu\text{m}$ fibers for the PDO/FBG 25/75 template were significantly smaller ($p < 0.05$) than for all other templates. The PDO/FBG 0/100 electrospun template did not continue the same trends as the blended templates which contained PDO.

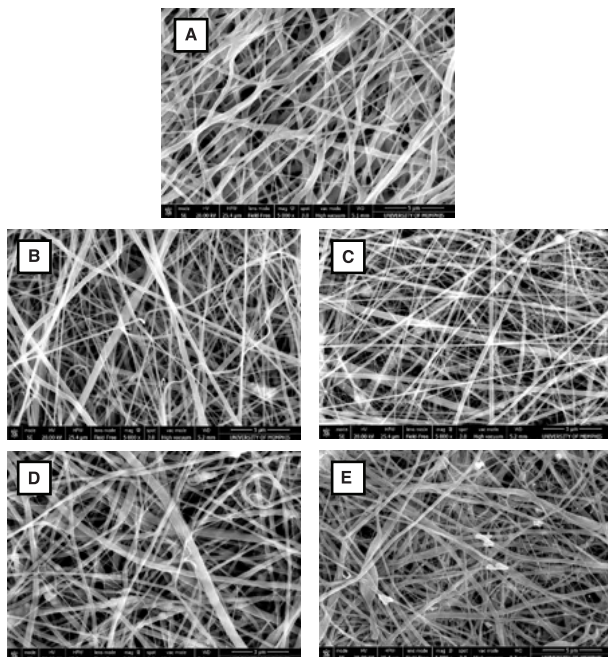


Figure 1. Electrospun templates of PDO/FBG vol/vol A)100/0, B) 75/25, C) 50/50, D) 25/75, and E) 0/100 (images taken at 5000x (A, B, C, E) and 8000x (D), scale bars = 5 μm (A, B, C, E) and 3 μm (D)).

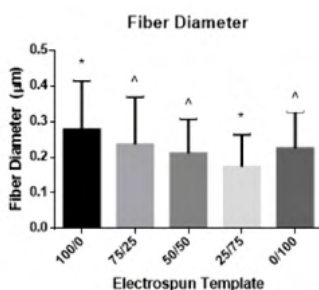


Figure 2. Fiber diameter for each electrospun template. *indicates significant difference from all other templates. ^ indicates significant difference from 100/0 and 25/75 ($p < 0.05$).

PDO/FBG (vol/vol)	Fiber Diameter (μM)
100/0	0.28 \pm 0.14
75/25	0.24 \pm 0.13
50/50	0.21 \pm 0.10
25/75	0.17 \pm 0.09
0/100	0.23 \pm 0.10

Table 2. Mean and standard deviation for fiber diameter.

Mechanical Testing

Results for the mechanical testing are shown in tabular format in Table 3. Results are reported as mean \pm standard deviation for at least 7 replicates. Units for YM and UTS are megapascals (MPa) and units for maximum strain are strain (ϵ) which is a unitless measurement for distance/distance.

PDO/FBG (vol/vol)	YM (MPa)		UTS (MPa)		Maximum Strain (ϵ)	
	Axial	Perpendicular	Axial	Perpendicular	Axial	Perpendicular
100/0	33 \pm 4	26 \pm 10	7.8 \pm 0.8	10.0 \pm 2.0	0.65 \pm 0.14	0.50 \pm 0.05
75/25	85 \pm 43	70 \pm 30	9.6 \pm 1.9	8.6 \pm 2.2	0.27 \pm 0.07	0.27 \pm 0.09
50/50	57 \pm 22	22 \pm 7	5.7 \pm 0.9	4.1 \pm 0.6	0.19 \pm 0.03	0.25 \pm 0.02
25/75	72 \pm 27	66 \pm 23	3.8 \pm 0.5	3.2 \pm 0.4	0.12 \pm 0.01	0.12 \pm 0.06
0/100	35 \pm 9	27 \pm 12	1.0 \pm 0.3	1.0 \pm 0.3	0.08 \pm 0.01	0.09 \pm 0.02

Table 3. Mean and standard deviation for YM, UTS, and maximum strain.

Figure 3 shows the results for YM and indicate variability in stiffness of the templates. Mechanical testing data shown in Figure 3 revealed larger average YM for PDO/FBG 75/25 and 25/75 templates than for PDO/FBG 100/0, 50/50, and 0/100 templates. These trends were significant for the perpendicular orientation (i.e. 75/25 and 25/75 template YM were significantly greater than all other templates of that orientation). For axial orientation data, the same peaks and troughs were indicated; however, there was no significant difference for the PDO/FBG 50/50 template.

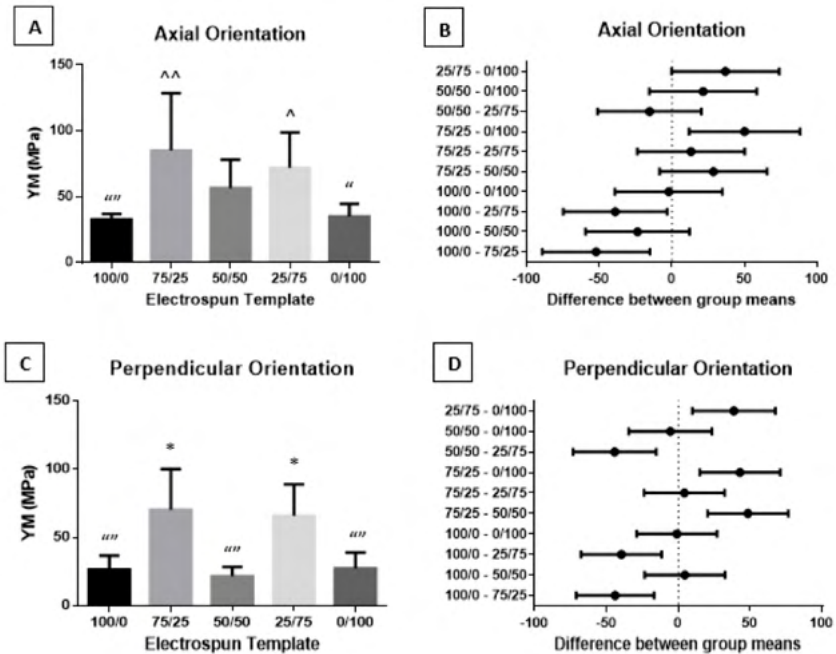


Figure 3. YM histograms with 95% confidence intervals (Tukey's) for (A and C) axial and (B and D) perpendicular oriented punches. "" indicates significant difference from 75/25 and 25/75. ^^ indicates significant difference from 100/0 and 0/100. ^ indicates significant difference from 100/0. "" indicates significant difference from 75/25. * indicates significant difference from all other templates ($p < 0.05$).

Figure 4 shows the histograms and 95% confidence intervals for the UTS of the PDO and FBG templates. The data suggest that UTS decreases with increasing FBG percentage for all electrospun templates, excluding PDO/FBG 100/0 when axially tested. Excluding the aforementioned template, the UTS for axial punches significantly decreased with increasing FBG incorporation. The perpendicular results showed that PDO/FBG templates with greater than 50% PDO were significantly stronger than all other templates.

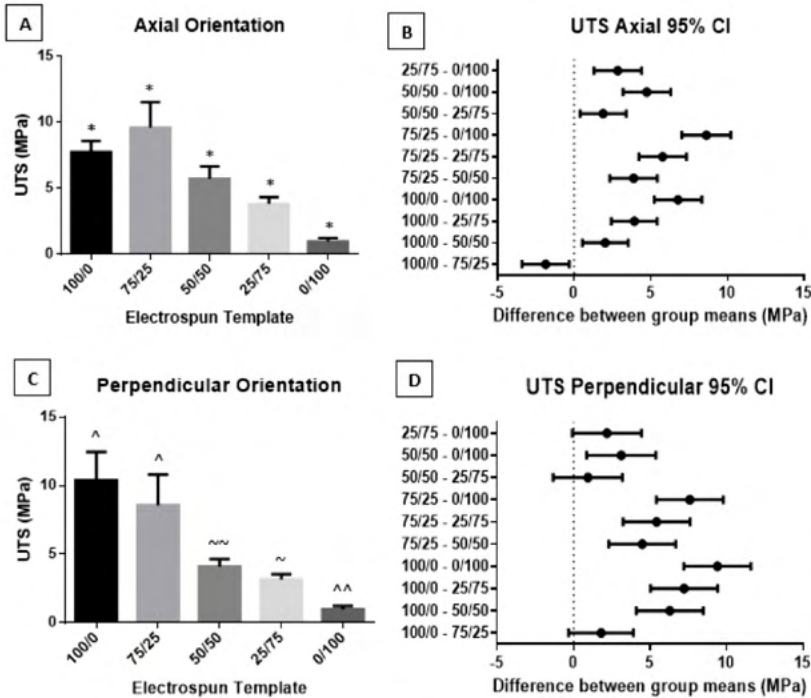


Figure 4. UTS histograms with 95% confidence intervals (Tukey's) for (A and C) axial and (B and D) perpendicular oriented punches. * indicates significant differences from all other templates. ^ indicates significant differences from 50/50, 25/75, and 0/100. ^^ indicates significant differences from 100/0, 75/25, and 0/100. ~ indicates significant differences from 100/0 and 75/25. ^^ indicates significant differences from 100/0, 75/25, and 50/50 ($p < 0.05$).

Figure 5 shows the histograms and 95% confidence intervals for the maximum strain of the PDO and FBG templates. The data shown in Figure 5 followed the general trend of decreasing maximum strain with increasing FBG incorporation. For the axial orientation templates, statistically significant differences were found in each comparison except 25/75 vs. 0/100, 50/50 vs. 25/75, and 75/25 vs. 50/50. Similarly, for the perpendicular orientation punches statistically significant differences were demonstrated in each comparison except 25/75 vs. 0/100 and 75/25 vs. 50/50.

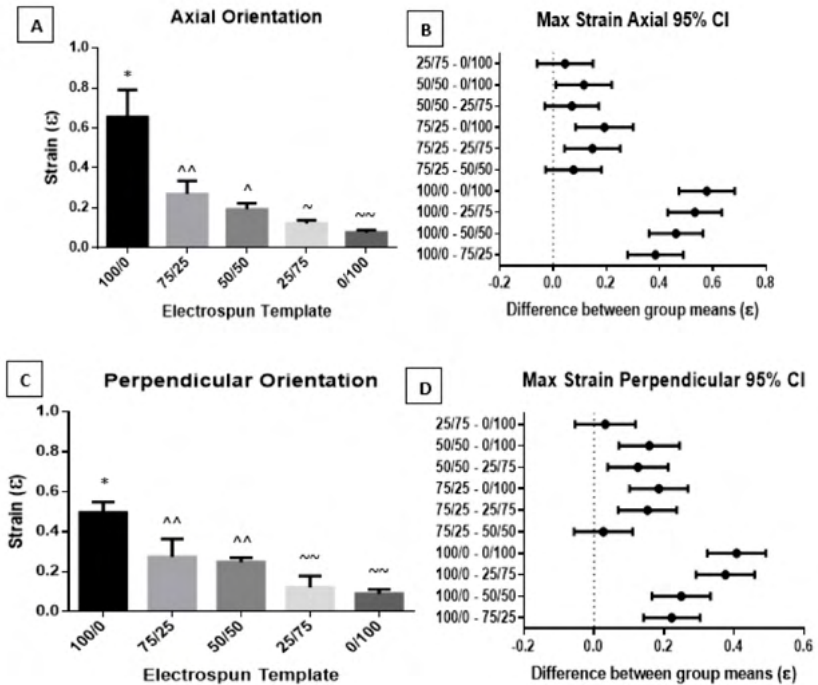


Figure 5. Maximum strain histograms with 95% confidence intervals (Tukey's) for (A and C) axial and (B and D) perpendicular oriented punches. * indicates a significant difference from all other templates. ^^ indicates a significant difference from 100/0, 25/75, and 0/100. ^ indicates a significant difference from 100/0 and 0/100. ~ indicates a significant difference from 100/0 and 75/25. ~~ indicates a significant difference from 100/0, 75/25, and 50/50 ($p < 0.05$).

Discussion

Conditions characterized by a lack of functional vascularization, such as PAD, may have blood flow restored to ischemic tissues via controlling the angiogenic abilities of MMP9 secretion from neutrophils. Since FBG has been shown to regulate the secretion of MMP9, we sought to incorporate this polymer into electrospun templates and stimulate the secretion of MMP9, thus inducing angiogenesis. Initially, our goal for the project was to fabricate electrospun templates for each vol/vol ratio of PDO and FBG with two different sizes of fibers in order to explore fiber diameter as another independent variable. After multiple repetitions of varying the concentration of PDO, the concentration of FBG, and the electrospinning parameters of the different solutions and still producing substandard templates (i.e. single solutions which yielded electrospun fibers of two extremely different diameters or templates which were composed of heavily beaded fibers), we focused on the successful fabrication of just one template per vol/vol ratio and evaluating the mechanical properties of these templates in comparison to one another.

The fiber diameter of the templates was a primary focus in the fabrication of these PDO/FBG templates. The PDO/FBG 100/0 template was electrospun at the lowest concentration possible with parameters refined to generate the smallest fibers possible from the Bezwada PDO. The smallest amount of FBG incorporation, just 25% by volume in PDO/FBG 75/25, yielded fibers which were smaller than those possible with electrospun PDO. Increasing FBG incorporation decreased the size of the fibers further until the PDO/FBG 0/100 template was fabricated. Electrospinning of this exclusively FBG solution produced fibers which were larger than those of both template 75/25 and template 50/50. This indicates that the mere combination of PDO and FBG may decrease the fiber size of their resultant electrospun templates. This change in template properties may be due to polymer chain entanglement in solution during the process of electrospinning or the degree of crystallinity of templates which contain both polymers.

Like the fiber size of the templates, the mechanical properties of each template varied with different degrees of FBG incorporation. The results for YM indicate that the stiffness of the electrospun material is influenced by percentage of FBG. YM was the greatest in the PDO/FBG 75/25 and 25/75 templates. This indicates an increase in rigidity when some intermediate amount of FBG is incorporated into a template between 0% and 50% and between 50% and 100%. Since no statistically significant difference was found in YM when comparing PDO/FBG templates of 100/0, 50/50, or 0/100, there is insufficient evidence to conclude that a combination of the polymers alone

increases the YM of electrospun PDO and FBG.

Trends in the data for both UTS and maximum strain indicate that mechanical strength decreases with increasing amounts of FBG in electrospun templates. With the exception of the axial PDO/FBG 100/0, all average values for UTS and strain decreased with an increase in percentage of FBG incorporation in the electrospun templates. Whereas this does indicate that electrospun PDO templates are more robust and durable with less FBG incorporation, it does not mean the templates composed of primarily FBG are inferior candidates for tissue regeneration. The UTS of the ECM of some tissues *in vivo*, such as the aorta, is 1.02 MPa [10]. This UTS is almost equivalent to that of the PDO/FBG 0/100 template (0.99 ± 0.28 MPa) which was fabricated from exclusively FBG. Therefore, the diminished strength of the FBG incorporated electrospun templates may make it the optimal electrospun material for certain tissue regeneration applications.

The UTS and maximum strain trends were similar to the trends in fiber diameter and indicate that the reduced fiber diameters decrease UTS and maximum strain. However, the fiber diameter of the PDO/FBG 0/100 template was significantly larger than the fiber diameter of PDO/FBG 25/75 template, yet the PDO/FBG 0/100 had the lowest UTS and maximum strain. Despite this elevated fiber diameter, the average UTS and maximum strain stayed consistent in their trends and reached their lowest point at PDO/FBG 0/100. This suggests that the decreases in UTS and maximum strain are due to percentage FBG incorporation instead of decreases in fiber diameter.

A potential concern regarding electrospun FBG is fiber diameter and the induced immune response. Our research has shown that high surface area to volume ratio increases the neutrophil response of NETosis on implanted PDO templates [12]. Since increasing the fiber diameter of electrospun FBG incorporated templates has heretofore been unsuccessful, an abundant inflammatory response may be problematic when neutrophils interact with FBG incorporated templates if we cannot electrospin larger diameter templates. However, since FBG is a natural polymer, it may inherently provoke less of an inflammatory response when electrospun than PDO even on high surface area to volume ratio templates. Therefore, the scaling down of the fiber diameter may be unnecessary for the successful fabrication of FBG incorporated electrospun templates.

If the templates are durable enough to be implanted without mechanical failure, can effectively facilitate angiogenesis, and do not significantly change in mechanical strength when hydrated, the templates may be suitable tissue regeneration templates for the treatment of PAD. Since each template was able to be handled through the cutting and testing process and demonstrated

mechanical characteristics greater than or equal to those of some decellularized ECM, the FBG incorporated templates should progress to the next stage of testing [11]. Future work on this project includes further electrospinning to fabricate FBG incorporated templates of larger fiber diameter and in vitro testing of these templates to verify and substantiate the claim that electrospun FBG upregulates the release of MMP9 from interacting neutrophils. Eventual research will test for the efficacy of this biomaterial in inducing robust angiogenesis.

Conclusion

This project has initiated the investigation into the effect that FBG incorporation has on electrospun PDO templates. Our research sought to create electrospun templates of five different concentrations of PDO and FBG and analyze the properties of each template. The project has given us sufficient evidence to refute our null-hypothesis and conclude that the incorporation of FBG into electrospun PDO templates does affect the mechanical properties of YM, UTS, and maximum strain. Increased FBG decreases the size of electrospun fibers and may decrease the possible range of fiber diameters which can be electrospun. Additionally, FBG incorporation influences YM of fabricated templates, and, in general, increasing the percentage of FBG in the electrospinning solution decreases the UTS and maximum strain of the template. This work holds significance in the field of guided tissue regeneration by demonstrating that different physical and mechanical properties of electrospun PDO may be tailored by the incorporation FBG. Future work will help in the determination if electrospun FBG will upregulate the secretion of MMP9 from neutrophils and spur angiogenesis, thereby increasing the efficacy of treatments for conditions such as PAD.

Acknowledgements

First, I would like to thank Dr. Bowlin for giving me the chance to work in his lab. He has been an outstanding mentor for me and has given me so many opportunities to excel in research over the last four years. I would also like to thank Allison Fetz for her continued assistance and patience with me as I learn new skills inside and outside of the lab. Additional thanks go out to each of my lab colleagues who have helped me with various issues associated with my research over the duration of this project and who have made the lab environment fun to work in. Research reported in this publication was supported by the National Institute of Biomedical Imaging and Bioengineering of the National Institutes of Health under Award Number R21EB024131 (GB). The content is solely the responsibility of the authors and does not necessarily represent the official views of the National Institutes of Health.

References

- [1] Y. Ostchega, R. Paulose-Ram, C.F. Dillon, Q. Gu, J.P. Hughes. Prevalence of Peripheral Arterial Disease and Risk Factors in Persons Aged 60 and Older: Data from the National Health and Nutrition Examination Survey 1999–2004, *Journal of the American Geriatrics Society* 55(4) (2007) 583-589.
- [2] M.J. Collins, X. Li, W. Lv, C. Yang, C.D. Protack, A. Muto, C.C. Jadlowiec, C. Shu, A. Dardik. Therapeutic Strategies to Combat Neointimal Hyperplasia in Vascular Grafts, *Expert Review of Cardiovascular Therapy* 10(5) (2012) 635-647.
- [3] M. Hong-De Wu, Q. Shi, Y. Onuki, Y. Kouchi, L.R. Sauvage. Histologic Observation of Continuity of Transmural Microvessels Between the Perigraft Vessels and Flow Surface Microostia in a Porous Vascular Prosthesis, *Annals of Vascular Surgery* 10(1) (1996) 11-15.
- [4] T. Pennel, D. Bezuidenhout, J. Koehne, N.H. Davies, P. Zilla. Transmural Capillary Ingrowth is Essential for Confluent Vascular Graft Healing, *Acta Biomaterialia* 65 (2018) 237-247.
- [5] F.J. Schoen. Interventional and Surgical Cardiovascular Pathology: Clinical Correlations and Basic Principles, *WB Saunders Company* 1989.
- [6] V.C. Ardi, T.A. Kupriyanova, E.I. Deryugina, J.P. Quigley. Human Neutrophils Uniquely Release TIMP-free MMP-9 to Provide a Potent Catalytic Stimulator of Angiogenesis, *Proceedings of the National Academy of Sciences* 104(51) (2007) 20262-20267.
- [7] V.C. Ardi, P.E. Van den Steen, G. Opdenakker, B. Schweighofer, E.I. Deryugina, J.P. Quigley. Neutrophil MMP-9 Proenzyme, Unencumbered by TIMP-1, Undergoes Efficient Activation In Vivo and Catalytically Induces Angiogenesis via a Basic Fibroblast Growth Factor (FGF-2)/FGFR-2 Pathway, *Journal of Biological Chemistry* 284(38) (2009) 25854-25866.
- [8] E.I. Deryugina, E. Zajac, A. Juncker-Jensen, T.A. Kupriyanova, L. Welter, J.P. Quigley. Tissue-infiltrating Neutrophils Constitute the Major In Vivo Source of Angiogenesis-inducing MMP-9 in the Tumor Microenvironment, *Neoplasia* 16(10) (2014) 771-788.
- [9] Rodriguez, I. (2010). *Mineralization Potential of Electrospun PDonHA- Fibrinogen Scaffolds Intended for Cleft Palate Repair* (dissertation).
- [10] Muiznieks, L. D., & Keeley, F. W. (2013). Molecular assembly and mechanical properties of the extracellular matrix: A fibrous protein perspective. *Biochimica Et Biophysica Acta (BBA) - Molecular Basis of Disease*, 1832(7), 866–875.
- [11] Beenakker, J.-W. M., Ashcroft, B. A., Lindeman, J. H., & Oosterkamp, T. H. (2012). Mechanical Properties of the Extracellular Matrix of the Aorta Studied by Enzymatic Treatments. *Biophysical Journal* 102(8), 1731–1737.

- [12] Fetz, A. E., Neeli, I., Rodriguez, I. A., Radic, M. Z., & Bowlin, G. L. (2017). Electrospun Template Architecture and Composition Regulate Neutrophil NETosis In Vitro and In Vivo. *Tissue Engineering Part A* 23(19-20), 1054–1063.

Amanda Campbell graduated *summa cum laude* with Honors in History and University Honors with Thesis designations in May 2020. She majored in history and African and African American studies and minored in English. She is the 2020 recipient of the Helen Hardin Honors College Director's Award and served as graduation marshal for the College of Arts and Sciences. Amanda has served the University as a Tiger Elite Ambassador and an Honors College Ambassador, and served on the executive board of the Honors Student Organization. She has presented research at the American Jewish Archives, the Library of Congress, and the University of Memphis.

Amanda Campbell

“The Chaplain of the New Left”: Reverend Richard Moon’s
Community of Influence and the 1968 Memphis
Sanitation Workers’ Strike

Faculty Sponsor

Dr. Aram Goudsouzian

Abstract

When 1300 sanitation workers went on strike in Memphis in 1968, many of the city's clergymen led the organizing effort that eventually settled the strike in the workers' favor. One of the only white clergymen to vocally support the strikers was Reverend Richard Moon, the Presbyterian chaplain of Memphis State University. Moon's meaningful relationships to other Memphis ministers and his connections to students through his role as the campus chaplain at MSU shaped his involvement in the sanitation strike, more than a Christian conviction or Presbyterian theology. He followed the lead of black ministers and distanced himself from white organizing efforts; he encouraged student involvement in the strike and championed continued student leadership after the strike was over. The Church, in fact, was shaped more by the activism of Moon and other socially-minded ministers than he was by any doctrine or theology.

At a Memphis city council meeting on March 5, 1968, Presbyterian minister Reverend Richard Moon read a Bible passage and shocked councilmember Gwen Awsumb. Awsumb later recalled:

The passage was from Jeremiah where the people tried to get their leaders to do something—whatever it was at the time. And the end of the long passage had something to do with the leaders being deaf and they could not hear the people say “We will burn his city down.” And he clamped the Bible closed, turned on his heel and went away... I was just horrified... for him to participate to this extent was appalling to me.¹

This meeting was three weeks into the sanitation workers’ strike that would be Martin Luther King, Jr.’s last civil rights campaign. The 1968 strike, which came after the Voting Rights and Civil Rights Acts, proclaimed to the nation that the movement was not complete. The strike would later become historically recognized for the “I Am A Man” placards carried by marchers. As Laurie Green explains, the slogan was “a claim to freedom” that “protested the supervisors’ paternalism.”² Many Memphis ministers, including Moon, were supportive of the striking workers. Moon raised money for strikers’ families, joined with the strikers in their daily marches from Clayborn Temple to City Hall, and negotiated with city officials on behalf of the strikers.³ By April 16, when the strike had ended, Moon had been maced, arrested, and had lost twenty-two pounds in a hunger strike.

The strike was not Moon’s first involvement with racial justice in Memphis, and he did not see it as the end of his role in the city. Moon’s meaningful relationships to other Memphis ministers and his connections to students through his role as the campus chaplain at Memphis State University shaped his involvement in the sanitation strike, more than a specific Christian conviction or Presbyterian theology. He followed the lead of black ministers and distanced himself from white organizing efforts; he encouraged student involvement in the strike and championed continued student leadership after the strike was over. The Presbyterian Church would be significantly shaped by the activism of Moon and other socially-minded ministers. Moon’s motivations for involvement in the Sanitation Strike grew from his connections to activist colleagues in the city and activist students at Memphis State far more than his connections to the Presbyterian denomination. His activism, however, made way for important changes in the denomination.

Moon was primed for involvement in civil rights when he arrived in Memphis in 1964 because of his earlier involvement in nonviolent campaigns in Louisville, Kentucky. He prioritized getting to know leaders of the black

community when he first moved to Memphis and read “Dr. Stewart’s study of the urban poor in Memphis” as a way of learning about the city.⁴ Memphis itself also had a long history of church-led activism. In 1947, Memphis’s National Association for the Advancement of Colored People (NAACP) chapter established a Church Department. In a letter to local ministers, the branch leaders stated, “We are well aware that from the very beginning, the NAACP has had the active assistance of thousands of church-people, including ministers, priests, rabbis, bishops, and heads of great religious organizations.”⁵ By the 1960s, the Memphis NAACP branch was supported by “sophisticated leaders with college degrees” including Maxine and Vasco Smith.⁶ Organizing was not new to young Memphians: Students at Lemoyne College requested a charter for a collegiate NAACP chapter in 1940.⁷ When the sanitation workers decided to strike, Moon and the Memphis religious community in general had experience in social justice campaigns. In Memphis in 1968, Moon was surrounded by activists.

Moon worked in several churches before his assignment as Presbyterian

¹ Joan Turner Beifuss, *At the River I Stand* (New York: Carlson’s Books, 1989), 156.

² Laurie B. Green, *Battling the Plantation Mentality: Memphis and the Black Freedom Struggle* (Chapel Hill: University of North Carolina Press, 2007), 253.

³ Michael Honey, *Going Down the Jericho Road: The Memphis Strike, Martin Luther King’s Last Campaign* (New York: W.W. Norton, 2007), 392.

⁴ Richard Moon, interview by Joan Beifuss, Judy Schulz, and Jerry Viar, 29 May 1968, recording and transcript, Mississippi Valley Collection, MSS 178, Container 19, Tape 55 and Container 23, Folder 180, page 6, Ned McWherter Library Special Collections, The University of Memphis, Memphis, Tennessee.

⁵ Sample Letter [September 1947], Box II: C185, Branch Files- Memphis, Tenn. IV, 1947-1950. National Association for the Advancement of Colored People Administrative Files, The Library of Congress Manuscript Division, Washington, D.C.

⁶ Honey, *Going Down the Jericho Road*, 30.

⁷ Letter, From Daisy E. Lampkin to Lucille Black, Box II: C185, Branch Files- Memphis, Tenn. I, 1940-1942. National Association for the Advancement of Colored People Administrative Files, The Library of Congress Manuscript Division, Washington, D.C.

chaplain at Memphis State University began in 1966. His first choice for ministerial appointment was a downtown church where he could engage in social work. He began his career as the pastor of Emmanuel Presbyterian, which he called “a purely white church,” where he started an after-school program for black elementary schoolers.⁸ This program upset many of the white congregants, and Moon took a position at Parkway Gardens Presbyterian where he pastored a black congregation on an interim basis before starting at Memphis State. Moon cultivated an important friendship with his Parkway Gardens successor, Reverend Ezekiel Bell, a young black minister and son of a sanitation worker. The two often marched side-by-side during the strike, and Moon “followed the leadership” of black ministers, including Bell, in joining the Committee on the Move for Equality (COME).⁹ COME was founded and headed by black ministers Reverend James Jordan of Beale Street Baptist Church and Reverend James Lawson of Centenary United Methodist Church. It formed during a meeting on February 23, 1968. After a march from City Hall that afternoon, the police had maced the strikers and their allies, including Moon, Bell, and other ministers. The group came to lead the organizing of the strike over the next eight weeks, holding strategy meetings every evening after the nightly mass meetings held for the strikers and their families. Moon served with COME throughout the strike and even called it a second job.¹⁰ Because Moon had intentionally patterned his ministry after Bell and others, he joined in the strike through COME.

Whereas Moon sought to closely follow the lead of black ministers, he intentionally distanced himself from most white ministers and characterized their actions as too moderate. Most white ministers were involved in the all-white Memphis Ministers Association (MMA), not COME. Moon viewed the MMA as too moderate, and he distrusted their resistance to integrate. There were many organizations involved in the sanitation strike. According to Michael Honey, this made it hard to unify the movement in Memphis. The NAACP, the MMA, and COME all pulled the movement in different directions.¹¹ Moon often remembered his involvement with the strike and with COME as being “the only white face in a sea of black.”¹² Reverend Malcolm Blackburn, a white minister who pastored the black congregation at Clayborn Temple was involved in COME throughout its operation as well. Blackburn sat permanently on the COME strategy committee, while Moon served only periodically.¹³ Nonetheless, Joan Turner Beifuss maintains that Moon bore the brunt of the white community’s resistance to white ministerial support of the strikers and that “his presence was always conscientiously reported on by the press.”¹⁴ Moon reported that he and his wife also received many threatening phone calls that attempted to intimidate him into ceasing his involvement with the strike.¹⁵

Moon distanced himself from the white ministers involved through the MMA. On April 5, 1968, the day after Dr. King was assassinated, the MMA had organized a prayer service at St. Mary's Episcopal Cathedral. It held a meeting after the service and decided to march to the mayor's office to express the ministers' continued commitment to a resolution of the strike. Moon was not, however, satisfied with this march. He recalled,

I all of a sudden found myself with my mouth open and saying to them, "Gentlemen, we have just heard the mayor say the same thing that he has been saying for the last eight weeks. He has not changed his mind. He is not going to change his mind...until the strike is over. And I'm going to stay without eating. Anyone who wants to join me, can." This was an emotional response to the situation. It wasn't so much a response to the mayor, as it was a response to the ministers.¹⁶

Moon lost twenty-two pounds over the next two weeks. His presence at City Hall was a daily act of insistent pressure during these weeks and a reporter remarked: "That was the first time I can really recall [Mayor Henry] Loeb showing real strain."¹⁷ He started eating again only after the mayor finally caved to the demands of the union and strikers. Moon admits that "it might have been a strategic error on my part" to inconvenience Loeb by occupying his office while asking to negotiate with him. To balance pressure and convenience, he urged those who wanted to join him to do so from their homes or a church, not to join him in his City Hall stakeout.¹⁸ Because of

⁸ Moon, interview by Beifuss et al, Folder 178, page 2-3.

⁹ Moon, interview by Beifuss et al, Folder 178, pages 22-23.

¹⁰ Moon, interview by Beifuss et al, Folder 179, page 4.

¹¹ Honey, *Going Down the Jericho Road*, 253.

¹² Moon, interview by Beifuss et al, Folder 178, page 31.

¹³ Malcolm Blackburn, interview by David Yellin and Anne Trotter, May 24, 1968, transcript, Mississippi Valley Collection, MSS 178, Container 23, Folder 77, page 2, Ned McWherter Library Special Collections, The University of Memphis, Memphis, Tennessee.

¹⁴ Beifuss, *At the River I Stand*, 181.

¹⁵ Moon, interview with Beifuss et al, Folder 179, page 18-19.

¹⁶ Richard Moon, interview by Joan Beifuss et al, Folder 180, page 4.

¹⁷ Beifuss, *At the River I Stand*, 322.

his distrust of white ministers' commitment to the cause, he was inspired to more radical acts, like the spontaneous hunger strike.

Moon's more immediate community—the students of Memphis State University—also contributed to the particular way he engaged with the strike in 1968. The sanitation strike was a watershed moment for student activists on Memphis State's campus because it was the first time black and white students worked together to affect change in their community.¹⁹ Black and white students tried to form an interracial student organization, the Student Alliance, in the fall of 1967, but the Student Government Association (SGA) denied the group a charter. The Black Student Association (BSA) had been organizing at the same time as the Student Alliance. Shortly after the Alliance failed, the BSA was granted its charter. The year 1968 was turbulent for college campuses across the country as the civil rights movement and anti-war protests reached a fever pitch, but Jeffery Turner argues that Southern activism looked different than activism at Ivy League institutions or in the burgeoning Free Speech Movement at University of California-Berkeley. Southern students organized differently because many of their institutions were dealing with the drama of integration throughout the 1950s and 1960s in ways that Northern schools were not.²⁰ Turner points out that white students in the South rarely had any interracial experiences before arriving at integrating campuses, and that the “many levels of closeness” necessitated by school integration gradually led to less resistance to integration and more embracing of racial activism among some students.²¹

Memphis State adheres to these larger trends of increased interracial activism. The strike was a crisis moment for both white activists, who supported the unions, and black activists, who highlighted the more explicitly racial elements of the strike.²² While the student newspaper, *Tiger Rag*, largely failed to claim a position on the strike until early March, an editorial praised students who were involved in campus marches in support of the strike on the front page of its March 8 issue. The same issue, however, also included a letter to the editor from a student who was “revolted” by the BSA's call to support the strike.²³ While MSU had one of the largest black populations of any southern, historically white university, the restrictions the administration placed on its black students robbed the university of genuine integration.²⁴ Even in this shift to greater interracial activism, most students were still suspicious of marches and demonstrations.

The Student Alliance was the first attempt at an integrated student organization since the Memphis State Eight arrived in 1959, with two notable exceptions: The Catholic Student Center and the Presbyterian Westminster House.²⁵ Moon inherited an integrated ministry from Reverend Gene Ether-

idge in 1966, and he was committed to supporting black and white student activists. Moon began working with Edwinna Harrel in September 1967 to start the Student Alliance until the SGA withheld its charter in March 1968.²⁶ He also aided the BSA, inviting the leaders to use the Westminster House as a printing press for their handbills and meeting announcements. Eddie Jenkins, one of the early organizers of the BSA called Moon's help throughout the 1967-1968 school year "invaluable."²⁷ Moon's connections to Jenkins and Harrel are indicative of his larger desire to connect with radical new left students on campus, who he claimed were all black. To Moon, the white activist students were not as engaged as white students at Berkeley and Columbia but he predicted that there would be many more radicals on MSU's campus in the future.²⁸ Moon's involvement with these new left students prompted his interviewer, Joan Beifuss to ask him,

¹⁸ Moon, interview by Joan Beifuss et al, Folder 180, page 7.

¹⁹ Jack Lorenzini, "Power Concedes Nothing Without a Demand': Student Activism at Memphis State University in the 1960s," Ph.D. dissertation (Memphis: University of Memphis, 2014), 143.

²⁰ Jeffrey A. Turner, *Sitting in and Speaking Out: Student Movements in the American South: 1960-1970* (Athens: University of Georgia Press, 2010), 280.

²¹ Turner, *Sitting in and Speaking Out*, 114.

²² Lorenzini, "Power Concedes Nothing Without a Demand," 146.

²³ *Tiger Rag*, "Campus Awakens," vol 31 (1967-1968), no. 33 (March 8, 1968), page 2, from Ned McWherter Library Special Collections, University of Memphis, Memphis, Tennessee.

²⁴ Lorenzini, "Power Concedes Nothing Without a Demand," 41.

²⁵ Lorenzini, "Power Concedes Nothing Without a Demand," 34, 24.

²⁶ Moon, interview by Beifuss et al, Folder 178, page 11.

²⁷ Eddie Jenkins, interview by Joan Beifuss and Walter Wade, January 7, 1969, transcript, Mississippi Valley Collection, MSS 178, Container 21, Folder 104, page 24, Ned McWherter Library Special Collections, The University of Memphis, Memphis, Tennessee.

²⁸ Moon, interview by Beifuss et al, Folder 178, 9-10.

“You are—besides serving as the chaplain of the Presbyterians—you are also chaplain of the New Left?” Moon laughed, but gave a serious answer: “I’ve never considered myself to be the chaplain of the Presbyterians, because there’s no way anymore to talk to students as Presbyterians... I’d like to take the name ‘Presbyterian’ off the board out front and put, ‘University pastor available.’”²⁹

As Moon became increasingly more involved in campus activism, he distanced his role from the theology and doctrine of the Presbyterian Church. He was not the chaplain of Presbyterian students, but of the university, and particularly the student activists. He made no excuses for his involvement with the BSA or the Student Alliance yet he was willing to give up ties on campus to his denomination by welcoming all students—not just Presbyterians. He recognized that for students at Memphis State, he was far more useful as an ally to their activism than as a preacher of a particular theology. He recognized that students in 1968 were no longer cleaving so closely to their denominations, but instead seeking practical guidance for interacting with the world, especially in the crisis moment of the strike. In this way, Moon’s involvement with student activism affected how the Presbyterian church appeared on campus. Moon’s ministry was more racially integrated, more activist, and more ecumenical than a traditional Presbyterian chaplaincy because of his relationships to students on campus. For his involvement in the strike, Moon’s activist organizing mattered more than his faith.

Shirletta Kinchen argues that the 1968 Sanitation Strike was the first activation of the Poor People’s Campaign and one of the civil rights movement’s first clashes between the church-led movement and new ideas from Black Power activists.³⁰ Young people in Memphis challenged the authority and methods of the clergy leaders of the strike. The BOP began to assert its influence more strongly during the strike. Though James Lawson included a few BOP members on the COME board, the group often felt ignored.³¹ The most storied clashing of old and new power in the nine-week strike was the march-turned-riot on March 28. This march was originally scheduled for March 22, but was snowed out. It was to be one of the largest because of the participation of Dr. King and other high-profile Southern Christian Leadership Conference (SCLC) leaders. The march devolved quickly as some marchers used the sticks that held their placards to smash windows.²² Dr. King blamed the violence on the BOP, though it was more likely the fault of poorly trained marshals and restlessness.³³ Around this time, rumors circulated that members of the BSA at MSU were plotting to assassinate Mayor Henry Loeb, and several student leaders of the BSA lost their downtown jobs as a result.³⁴ Rumors like this strained the relationship between BOP and COME.

Moon, however, offered no harsh words toward BOP or the Invaders, the militant arm, in recalling the drama of March 28, when he himself was teargassed. Instead, he called attention to the violence inflicted on children not only at the march, but at Hamilton High School that day, concluding “My assessment is that the police overreacted.”³⁵ He also “insisted that the marginalization of BOP in the strike strategy sessions led to the disturbance.”³⁶ BSA leader Ronald Ivy was marching with Moon and Reverend Ezekiel Bell when they were attacked by the police. Moon did not marginalize the youth activists. In fact, when asked about the future of the Memphis movement, Moon identified the BOP as key leaders: “they are the people doing the community organizing right now.”³⁸ Moon embraced his unofficial title, Chaplain of the New Left, with some vigor. It changed how he engaged with the strike. Rather than fearing the encroachment of young activists, he embraced the changes they brought.

Richard Moon’s relationships to his community of clergy friends and students influenced his involvement in the sanitation workers’ strike more than his relationship to the church. His involvement in the strike, however, did add to a trend among socially-involved ministers in influencing the church. The 1960s were a turning point in the white southern church. The civil rights movement offered a significant challenge and opportunity for

²⁹ Moon, interview by Beifuss et al, Folder 178, 10.

³⁰ Shirletta J. Kinchen, *Black Power in the Bluff City: African American Youth and Student Activism in Memphis, 1965-1975* (Knoxville: University of Tennessee Press, 2015), 3.

³¹ Anthony C. Siracusa, “Nonviolence, Black Power, and the Surveillance State in Memphis’s War on Poverty,” in *Black Struggles for Freedom in Memphis, Tennessee*, ed. Aram Goudsouzian and Charles W. McKinney, Jr. (Louisville: University Press of Kentucky, 2018), 292.

³² Siracusa, “Nonviolence, Black Power, and the Surveillance State in Memphis’s War on Poverty,” 285.

³³ Kinchen, *Black Power in the Bluff City*, 46-47.

³⁴ Lorenzini, “Power Concedes Nothing Without a Demand,” 155-56.

³⁵ Moon, interview by Beifuss et al, Folder 179, page 21.

³⁶ Kinchen, *Black Power in the Bluff City*, 65.

³⁷ Lorenzini, “Power Concedes Nothing Without a Demand,” 144.

³⁸ Moon, interview by Beifuss et al, Folder 180, page 13.

the Southern Baptist Church and the Methodist and Presbyterian Churches in the south, which had been historically defined by their support of slavery and segregation. These three churches had all split with their Northern counterparts before the Civil War and were each, to some extent, reconciling in the mid-20th century. This reconciliation involved a reordering of church priorities of which segregation was the keystone. Individuals affected great change in their churches during the civil rights movement.

In 1962, twenty-eight white Mississippi Methodist ministers published a statement titled “Born of Conviction” in support of school integration. The group published the statement after violence erupted on the University of Mississippi campus upon James Meredith’s integration of the school.³⁹ Their letter was perfectly aligned with the Methodist Church’s official stance on school integration, but the denomination had not yet been faced with an obvious opportunity to enforce this position, and many Mississippi Conference leaders strongly opposed the letter writers’ stance. These Mississippi leaders claimed that it was not the church’s place to offer an opinion on what they took to be a political matter, but as Joseph Reiff argues, the Born of Conviction ministers offered “a prophetic rejoinder” of spiritual and political matters with their letter.⁴⁰ By speaking out as ministers, they forced a political issue into a clerical collar and insisted their denomination deal with the issue of integration more explicitly. Their letter offered a challenge to the governing body of the Methodist Church and to their individual congregations. The denomination responded by supporting the ministers and offering them posts outside of the South. Many congregations pushed back, though, and nineteen of the twenty-eight signees left Mississippi by 1964.⁴¹ Reiff insists however, that the real story lies in the ministers that stayed with their congregations. Reverend Nick Nicholson, a progressive minister who did not sign the letter sought to help his congregation navigate issues of race by remaining in Mississippi, rather than departing the south.⁴² Many churches like Nicholson’s then went on to have meaningful conversations about race and faith.⁴³ These Mississippi Methodists, both those who signed and those who did not, worked to change the role of the Church from within.

In a similar way, religious activists in Memphis in 1964 and 1965 forced the hand of the Presbyterians by kneeling-in outside the Second Presbyterian Church each Sunday for months to challenge the church’s segregation policy. In the case of Second Presbyterian, the clergy and many congregants were in favor of allowing the interracial group of student kneelers into worship, but the controlling body of the church, the Session, was adamantly opposed. The clergy and the activists were in line with the denomination, whose official stance on integration had been supportive since 1954 when they were the

first white denomination in the South to support *Brown v. Board of Education*.⁴⁴ But, like the Methodists in 1962, they had yet to enforce this position. Stephen Haynes argues that the kneel-ins were the push the Church needed to fully support integration: “Segregation in individual congregations was generally not a denominational concern until the kneel-in era, when unwelcome visitors drew attention to exclusionary policies.”⁴⁵ The denomination was particularly pressured at this time because Second Presbyterian was scheduled to host the 1965 annual denomination meeting. After many other Presbyterian churches across the South condemned the actions of the Second Presbyterian Church, the governing body finally pulled the conference from Memphis, thereby effectively condemning the Second Presbyterian’s actions. In February 1965, the congregation voted to change the election process of elders in order to vote out the segregationist elders who had previously held lifetime appointments. A week later, eight elders resigned in protest, and the kneelers were welcomed into worship the following Sunday.⁴⁶ These activists, many of whom openly declared their own religious convictions as reasons for kneeling-in at Second Presbyterian, were prophetic voices that brought a shift in the way the Presbyterian Church understood its role in society.

Moon offered another prophetic voice just a few years later by getting involved with the sanitation strike as a minister. Though he did not speak about a Christian conviction when remembering his involvement in the strike, he was tied to the Presbyterian Church because of his identity as a minister. The denomination did not push him to march with the strikers. Yet, like the Born of Conviction ministers and the Second Presbyterian

³⁹ Joseph T. Reiff, *Born of Conviction: White Methodists and Mississippi’s Closed Society* (New York: Oxford University Press, 2016), 57.

⁴⁰ Reiff, *Born of Conviction*, 205.

⁴¹ Reiff, *Born of Conviction*, ix-x.

⁴² Reiff, *Born of Conviction*, 250.

⁴³ Reiff, *Born of Conviction*, 130.

⁴⁴ Stephen Haynes, *The Last Segregated Hour: The Memphis Kneel-ins and the Campaign for Southern Church Desegregation* (New York: Oxford University Press, 2012), 86.

⁴⁵ Haynes, *The Last Segregated Hour*, 91.

⁴⁶ Haynes, *The Last Segregated Hour*, 205.

kneelers, he offered a witness and a challenge. In 1983, the Southern branch of the Presbyterian Church re-merged with its northern counterpart to form the Presbyterian Church of the United States. This marked a shift in the denomination from one that openly supported slavery and segregation to one that could align itself with national ideals and embrace integration. It was the overt actions of ministers and other religious people engaged in causes of racial justice that forced the denomination to rethink its ideals and act out those new ideals in the world.

Two months after the sanitation workers had returned to work, Beifuss asked Reverend Moon if he planned to stay in Memphis. The Presbyterian minister had lived in Memphis only four years, but his experience in the strike was perhaps harrowing enough to suggest a dramatic change. And yet, the minister planned to stay in Memphis because he recognized that no other city was free of the struggles that Memphis faced in 1968: “no matter where you go nowadays—and I mean all over the world—you’re going to be faced with conflict and these kinds of human problems. So you might as well stay where you are and fight the battle where you are.”⁴⁷ His connections to black ministers and activist students kept him tethered to the city. These relationships inspired his involvement with COME and his positive response to student protestors. Moon’s activism, like others before him, affected change in the Church more than the Church affected changes in him. Rather than letting his Presbyterian chaplaincy inform his activism, Moon instead let his chaplaincy of the new left inform the Church.

⁴⁷ Moon, interview by Joan Beifuss et al, Folder 180, page 13.

Bibliography

- Beifuss, Joan Turner. *At the River I Stand*. New York: Carlson's Books, 1989.
- Eddie Jenkins, interview by Joan Beifuss and Walter Wade, 7 January 1969, transcript, Mississippi Valley Collection, MSS 178, Container 21, Folder 104, Ned McWherter Library Special Collections, The University of Memphis, Memphis Tennessee.
- Haynes, Stephen. *The Last Segregated Hour: The Memphis Kneel-Ins and the Campaign for Southern Church Desegregation*. New York: Oxford University Press, 2012.
- Lorenzini, Jack Brian. "Power Concedes Nothing Without a Demand': Student Activism at Memphis State University in the 1960s." Ph.D. dissertation. Memphis: University of Memphis, 2014.
- Malcolm Blackburn, interview by David Yellin and Anne Trotter, 24 May 1968, transcript, Mississippi Valley Collection, MSS 178, Container 23, Folders 76-77, Ned McWherter Library Special Collections, The University of Memphis, Memphis, Tennessee.
- Manuscript materials. Box II: C185, Branch Files- Memphis, Tennessee. National Association for the Advancement of Colored People Administrative Files, The Library of Congress Manuscript Division, Washington, D. C.
- Richard Moon, interview by Joan Beifuss, Judy Schulz, and Jerry Viar, 29 May 1968, recording and transcript, Mississippi Valley Collection, MSS 178, Container 19, Tapes 53-55 and Container 23, Folders 178-180, Ned McWherter Library Special Collections, The University of Memphis, Memphis, Tennessee.
- Reiff, Joseph. *Born of Conviction: White Methodists and Mississippi's Closed Society*. New York: Oxford University Press, 2016.
- Siracusa, Anthony. "Nonviolence, Black Power, and the Surveillance State in Memphis's War on Poverty." In *Black Struggles for Freedom in Memphis, Tennessee*, ed. Aram Goudsouzian and Charles W. McKinney, Jr. Louisville: University Press of Kentucky, 2018.

Tiger Rag, vol. 31 (1967-1968), no. 33 (8 March 1968) from Ned McWherter Library Special Collections, University of Memphis.

Turner, Jeffrey A. *Sitting in and Speaking Out: Student Movements in the American South 1960-1970*. Athens: University of Georgia Press, 2010.

Alexis K. Nelson graduated *magna cum laude* from the University of Memphis in May 2019 with a major in pre-health studies and a concentration in exercise, sport and movement sciences. She also earned the Undergraduate Research Scholar and University Honors with Thesis designations. Throughout her time at the University of Memphis, she has been in multiple research projects in the Musculoskeletal Analysis Laboratory under Dr. Douglas Powell and has presented her work at several regional and national conferences including the National Conference of Undergraduate Research, the Midsouth Biomechanics Conference, and the American College of Sports Medicine. Alexis did her internship in January under the supervision of Dr. Shalini Narayana in the Neuroclinic at Le Bonheur Children's Hospital. She will continue with the University of Memphis as a Graduate Research and Teaching Assistant in the Health Studies department to pursue a graduate degree in Health Studies. With her combined experience from Le Bonheur and the University of Memphis, she hopes to continue her education after the graduate degree to apply to a neuromechanics doctoral program to pursue a career in clinical research.

Alexis's paper received a *Quaesitum* best paper award.

Alexis Nelson

Effects of Stride Length on Knee Loading
in Simulated Obese Populations

Faculty Sponsor

Dr. Douglas Powell

Abstract

Walking is part of our daily activities. Increasing body mass potentially increases biomechanical mal-adaptations including reduced step length (SL), and increases joint loading (JRF). The purpose of this study was to determine if acutely added mass (AM) or SL change knee JRFs during walking. Hypotheses included: AM will alter SL, reduced SLs will increase JRFs, and AM increase JRFs. Fourteen participants performed eight trials in four experimental conditions including two variations of SLs, and AM. 3D kinematics and ground reaction forces were collected simultaneously using an 8-camera motion capture system (240 Hz, Qualisys, Inc.) and force platforms (1200 Hz, AMTI, Inc.). Visual 3D was used to calculate joint angles, moments, powers and JRFs. Reduced SL had greater joint flexion angles, peak extension power, and JRFs than AM condition. It was concluded that reduced SLs are associated with greater JRFs while AM in isolation does not alter joint biomechanics.

Introduction

According to the National Institute of Diabetes, 70% of the United States population is overweight or obese ("Key Health Data About Tennessee," 2018). Tennessee itself has the sixth highest rate of obesity in the nation. Further, Memphis had an obesity rate of 33.8% in 2015 (Diseases, 2017; Ruiz, 2012). These statistics reveal that Memphis is one of the most obese cities in America ("Tennessee State Obesity Data, Rates and Trends," 2018). From 1990 to 2015, the obesity rate in Tennessee increased by 20% and continues to increase (Ruiz, 2012). As a nation, the prevalence of obesity is predicted to be 30-37% in men and 34-44% in women by the year of 2020 (Adams et al., 2006). Increasing obesity rates result in secondary increases in cardiovascular and musculoskeletal disorders which result in a concomitant increase in healthcare costs. Obesity-related medical expenses totaled an average of \$26 billion dollars per year in the United States from 2005 to 2011. Medical expenses are greater for obese individuals, who are estimated to pay an additional \$2,700 to \$3,600 per year compared to healthy individuals (Cawley & Meyerhoefer, 2012). As a country, state and city, we are collectively affected by obesity.

Obesity is a scale of excess weight that is associated with adverse health effects (Bessesen, 2008). A widely accepted way to assess excess weight is through a body mass index (BMI). BMI is calculated as the quotient of an individual's body mass divided by their height (in meters) squared (Haff & Triplett, 2016). BMI is used to categorize individuals as underweight (< 18 kg/m²), normal (18 kg/m² – 25 kg/m²), overweight (25 kg/m² – 30 kg/m²) or obese (>30 kg/m²). A positive correlation exists between BMI and mortality rates with greater BMI associated with a higher mortality rate (Adams et al., 2006). It is suggested that even modest increases in body weight have negative effects on lifespan (Figure 1), and that the serious negative effects of increasing body weight are not solely due to higher BMI values, but are the result of secondary effects of obesity including metabolic disorders, hyperlipidemia, hypertension, and diabetes (Gregg et al., 2005).

Though obesity has deleterious effects on cardiovascular and metabolic health, obesity is also known to lead to chronic musculoskeletal conditions such as osteoarthritis (Felson, Anderson, Naimark, Walker, & Meenan, 1988; Mohammed, Al-Numair, & Balakrishnan, 2015). Osteoarthritis (OA) is a progressive degenerative disorder of the articular cartilage around a joint: in this case, the knee. Twenty-seven million people in the United States have been diagnosed with OA, equating to more than 8% of the national population ("NIH fact Sheets – Osteoarthritis," 2018). OA accounts for an estimated \$10 billion in healthcare costs each year (Bliddal, 2008). Every 5kg

of weight gained increases the risk of osteoarthritis by 36% (Lementowski & Zelicof, 2008). Increasing body mass is associated with greater mechanical loading to the lower extremity. This mechanical loading is created through biomechanical maladaptations such as a reduced step length. Reduced step lengths equate to a greater step width and increased knee joint load.

Obese populations demonstrate aberrant gait biomechanics. Specifically, obese individuals walk with shorter step lengths and greater step widths compared to healthy individuals. A shorter step length is suggested to direct the forces of the system in a vertical direction, which may increase skeletal joint loading (DeVita & Hortobagyi, 2003; Westlake, Milner, Zhang, & Fitzhugh, 2013). A larger step width decreases peak knee joint moments and an increase in mediolateral ground reaction forces, causing abnormal motion and loading in the knee joint, and increasing the risk of musculo-skeletal insult and injury (Yocum, Weinhandl, Fairbrother, & Zhang, 2018). A knee joint moment is the rotational force applied to the joint. These two factors in combination (increased load and greater skeletal involvement) may underlie the higher rates of osteoarthritis in obese individuals exacerbating a sedentary lifestyle and furthering their obesity.

Mechanically, obesity affects multiple aspects of daily living (ADLs). To participate in ADLs, functional capacity has to be present with a low disability. Functional capacity for individuals overall decreases as BMI increases (Adams et al., 2006). Past research has also found a positive correlation between disability and obesity (Alley & Chang, 2007). Specifically, disability in this case will be defined by the increase in knee OA. The pathophysiologic process of knee OA has been identified biomechanically as an increase in knee-joint forces and knee-joint moments. Past research has examined this through changes in body mass (i.e. weight loss). Knee joint adduction moments have been related to an increase in compressive loads (Andriacchi, 1994), and weight loss has been found to reduce significant compressive knee-joint loads, or forces (Milner, Meardon, Hawkins, & Willson, 2018). Overall, obesity impedes movement, hindering the individual's ability to perform basic, daily activities. Many daily tasks require physical activity, which decreases BMI ratings, obesity, and mortality rates (Sui et al., 2007). A daily task that is available and physically demanding to most individuals is walking. A successful treatment many physicians prescribe to increase physical activity is to increase step goals for obese individuals. In order for obese individuals to increase physical activity per day, walking mechanics are important to examine. Doing so ensures that these individuals do not have secondary effects from an increase in walking prescription.

Though it is clear obesity results in altered gait biomechanics, the role of shorter step lengths on knee joint loading in obese individuals has not been established. Messier et al. (2005) reported that each pound of weight lost results in a four-fold reduction in knee joint load per step during daily activities. It has also been suggested that decreases in weight in combination with increased stride lengths result in substantial reductions in knee joint loading (DeVita, Rider, & Hortobagyi, 2016). In contrast, Milner et al. (2018) has suggested that a shorter stride length would reduce the vertical impulse applied to the knee joint, reducing the risk of developing OA. An important difference in these studies pertains to the population of interest. While Milner et al. (2018) focused on obese individuals at a single point in time, DeVita et al. (2016) performed an intervention study and evaluated gait biomechanics across multiple time points in a repeated measures design. The role of step length in knee joint loading has not been well established. There is a need to investigate the role of step length and increasing body mass on knee joint loading rates during gait. Therefore, the purpose of this study is to (a) determine if acutely added mass (weight vest) results in changes in step length during walking, (b) to determine if reduced step length independently (in the absence of added mass) increases knee joint loading, and (c) to determine if added mass results in an increase in knee joint loading. It was hypothesized that: (a) acutely added mass will result in differences in step length (b) reduced step lengths will result in an increase in joint loading, and (c) added mass will alter biomechanical variables and increase joint loading.

Methods

Participants

The location in which this experiment took place was the School of Health Studies Musculoskeletal Analysis Laboratory at the University of Memphis, Tennessee. Participants visited the Musculoskeletal Analysis Laboratory once for examination and testing. The session's duration lasted from 60 to 90 minutes. Prior to any warmup, measurements or testing, individuals were screened for inclusion in this study through the following mechanisms: providing written informed consent, completing a verbal training history to determine study eligibility, and completing a written Physical Activity Readiness Questionnaire (PAR-Q; Appendix A). For each session, testing occurred in the following order: (1) warm-up exercises, (2) placement of measurement sensors, and (3) completion of walking trials including four experimental conditions involving the interaction of two step length conditions and two added mass conditions.

Experimental Equipment

Anthropometric measurements included age, sex, height, and body mass. The following measurements were recorded using a stadiometer and scale. Following anthropometric measurements, retro-reflective markers were placed bilaterally on the participant's lower extremity including the trunk, pelvis, thigh, shank and feet to measure individual segment motion during walking trials (step length x added mass) using a 9-camera motion capture system (240 Hz, Qualisys AB, Goteburg, Sweden). A pair of force platforms were used to record ground reaction forces (GRFs; 1200 Hz, AMTI Inc., Watertown, MA, USA).

Experimental Protocol

All walking trials required the participants to perform eight over-ground walking trials across a 20-meter walkway in each of four experimental conditions. Experimental conditions include the interaction of two step lengths (natural and constrained, 0.68 m) and two weighting conditions (unloaded and loaded) at the participants preferred walking speed. The constrained step length of 0.68 m was selected based on previously published data for obese individuals walking at a self-selected speed (Devita et al., 2016). The self-selected walking velocity was characterized as the pace at which the participant would normally walk during daily activities. The natural step length condition allowed participants to walk with their chosen step lengths while the constrained step length condition required participants to walk with a step length of 0.68 m as outlined on the laboratory floor using masking tape. The unloaded weighted condition was characterized as the participant walking without additional load added onto the participant's body mass. The added mass condition entailed the participants performing the walking trial with an added load of 20% body mass in weighted plates; the plates were placed into a vest worn around the participant's chest. To ensure each participant qualified as "obese" in the added mass conditions, a BMI calculation was performed with the added load to identify if each participant's new BMI exceeded 30 kg/m² to classify them in the obese category.

A successful walking trial was characterized by the participant walking across the runway at the prescribed velocity and having the foot of interest fully supported by the force platform in the center of the walkway. Participants completed eight successful walking trials per condition totaling 32 walking trials with 60- to 90-second periods of rest between trials to avoid fatigue. Participants wore their active shoe of choice to perform the movements.

Data Analysis

Data captured from the three-dimensional motion capture system were labeled and exported to c3d file. Visual3D (C-Motion, Bethesda, MD, USA) was used to calculate knee joint angle, moment, and power time-series, as well as the knee joint reaction force time-series. Custom software (MatLab, Mathworks, MA, USA) was used to calculate discrete biomechanical variables during the stance phase of gait, including peak knee flexion, knee joint range of motion, peak knee extension moments and powers, and peak positive knee joint reaction force.

Statistics

Five 2 x 2 (load by step length) repeated measures analyses of variance were used to assess the interaction of mass and step length on the following biomechanical variables: peak knee flexion angles, knee joint range of motion, peak knee extension moments, peak knee extension powers and peak knee joint reaction forces. In the presence of a significant interaction or significant main effect, post-hoc paired sample t-tests were used to determine the source of significance. Significance was set at $p < 0.05$.

Results

Table 1 presents the biomechanical variables of interest for each experimental condition including: peak knee flexion angle, knee joint range of motions, peak knee extension moments and powers and peak positive knee joint reaction forces. In Figure 1, no mass by step length interaction was observed for peak knee flexion angles ($p = 0.524$). The constrained step length was associated with greater peak knee flexion angles than the preferred step lengths ($p = 0.043$). Post-hoc t-tests revealed that peak knee flexion angles were greater in the constrained compared to preferred conditions for added mass ($p = 0.03$), but not the unloaded condition ($p = 0.08$). No effect of mass was observed for peak knee flexion angles ($p = 0.578$). In contrast to peak knee flexion angles, no mass-by-step length interaction was observed for knee joint range of motion in Figure 2 ($p = 0.571$). Further, no main effect of step length ($p = 0.299$) or mass ($p = 0.585$) was observed for knee joint range of motion.

Variable	Body Mass			Added Mass		
	Preferred SL	Constrained SL	p-value	Preferred SL	Constrained SL	p-value
Peak Knee Flexion Angle (deg)	-36.0±12.9	-40.5±7.7	0.04	39.0±10.5	-41.4±7.7	0.52
Range of Motion (deg)	40.4±13.2	43.3±6.8	0.30	43.1±10.1	43.9±4.8	0.57
Peak Knee Extension Moment (Nm/kg)	2.9±2.3	2.3±0.8	0.15	2.4±0.7	2.3±0.9	0.31
Peak Knee Extension Power (W/kg)	6.1±4.2	4.6±1.0	0.04	5.7±1.8	4.8±1.0	0.61
Knee Joint Reaction Forces (N/kg)	7.1±2.0	6.1±1.1	0.02	6.9±2.3	5.4±3.1	0.75

Table 1. Biomechanical variables of interest for each experimental condition

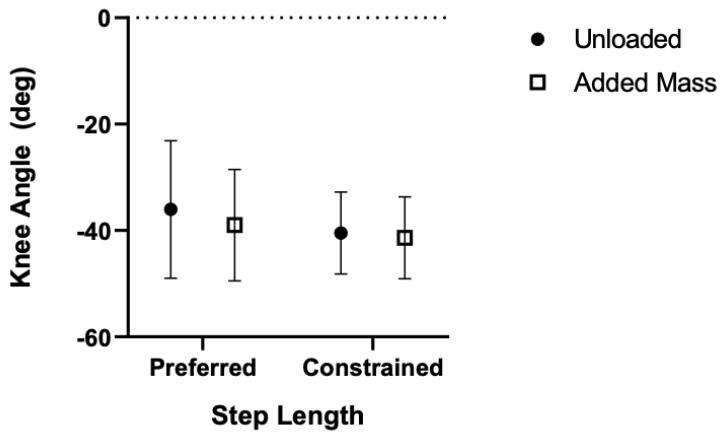


Figure 1. Peak knee flexion (deg) during level walking with increased mass and constrained step lengths. Constrained step length was associated with significant increases in peak knee flexion angles ($p = 0.040$). No changes were observed for added mass ($p = 0.520$).

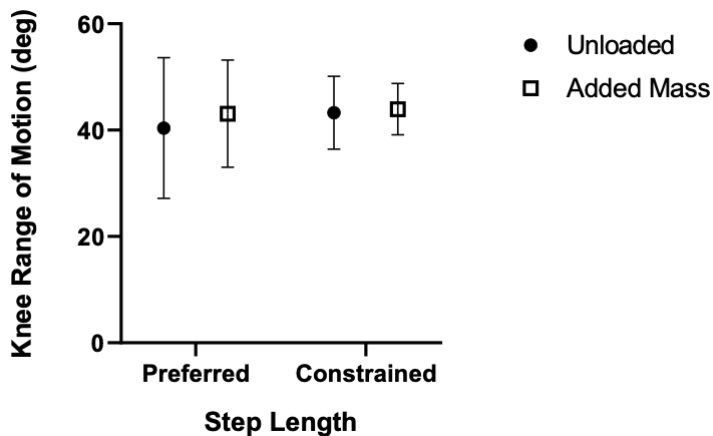


Figure 2. Peak knee range of motion (deg) during level walking with increased mass and constrained step lengths. No changes were observed for added mass ($p = 0.57$) or constrained step length ($p = 0.30$).

In Figure 3, no mass by step length interaction was observed for peak knee extension moment ($p = 0.306$). Further, no main effect of step length ($p = 0.153$) or mass ($p = 0.626$) was observed for peak knee extension moment. For peak knee extension power in Figure 4, no mass by step length interaction was observed ($p = 0.306$). However, a significant main effect of step length was observed ($p = 0.037$). Post-hoc t-tests revealed that peak knee extension power was greater in the constrained compared to preferred step length conditions for the added mass condition ($p = 0.007$) but not for the unloaded condition ($p = 0.09$).

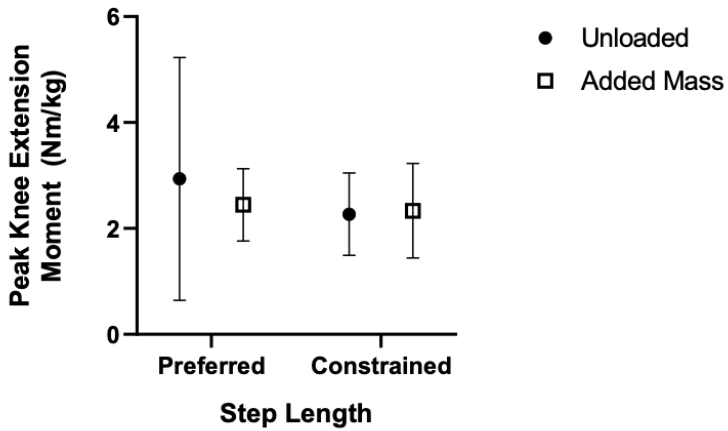


Figure 3. Peak Knee Extension Moment (Nm/kg) during level walking with increased mass and constrained step lengths. No changes were observed for added mass ($p = 0.31$) or constrained step length ($p = 0.15$).

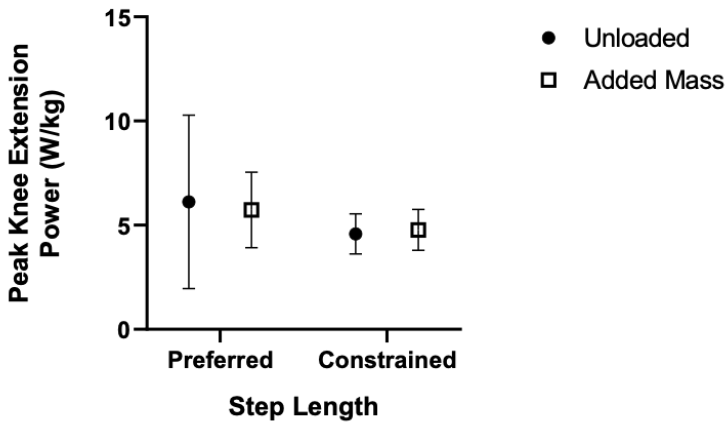


Figure 4. Peak Knee Extension Power (W/kg) during level walking with increased mass and constrained step lengths. Constrained step length was associated with significant increase in peak knee extension power ($p = 0.04$). No changes were observed for added mass ($p = 0.61$).

For knee joint reaction forces in Figure 5, no mass by step length interaction was observed ($p = 0.753$). A main effect of step length was observed ($p = 0.019$). Post-hoc analyses revealed greater knee joint reaction forces in the preferred compared to constrained step lengths in both unloaded ($p = 0.023$) and added mass conditions ($p = 0.048$). No main effect of mass on peak knee joint reaction forces was observed ($p = 0.918$).

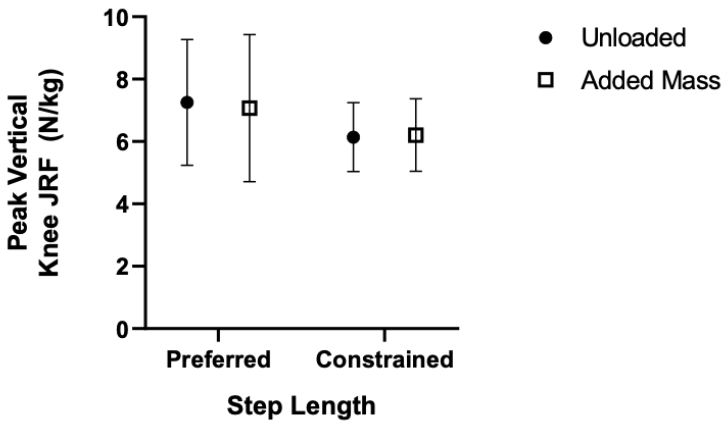


Figure 5. Peak Vertical Joint Reaction Forces (N/kg) during level walking with increased mass and constrained step lengths. Constrained step length was associated with greater knee joint reaction forces ($p = 0.02$). No changes were observed for added mass ($p = 0.75$).

Discussion

The purpose of this study was to determine if acutely added mass and/or step length would change knee joint loading during level walking. The major findings of the current study demonstrate that acutely added mass does not alter knee biomechanics; however, constraining step length alters both knee joint kinematics and kinetics. Specifically, constrained step lengths were associated with greater peak knee flexion angles as well as greater joint powers and joint reaction forces.

Current data revealed that acutely added load does not alter knee joint moments and powers during walking. These findings are in contrast with previously published research that demonstrated with added load at the knee during walking, the tasks relative to mass of the individual directly affected joint loads per step and reduced range of motion (Attwells, Birrell, Hooper,

& Mansfield, 2006; Milner et al., 2018). This difference in results can be explained as a chronic versus an acute response, as Messier et al.'s (2005) study was performed in six sessions over an 18-month long weight loss intervention for obese adults. Rather, acute responses to added load have been noted in numerous other studies (Attwells et al., 2006; Knapik, Harman, & Reynolds, 1996). Potential reasons for the differences could be that the added load was not sufficient to create an acute response in recreational athletes. Knapik et al. (1996) started to see significant results at 50% of body weight and up added onto their trained military professionals for kinematic and kinetic differences in walking. This could indicate that a higher stimulus was needed to evoke a difference in our participant population.

However, step length was a strong enough stimulus to evoke a response in knee joint flexion, power, and joint reaction forces. Our findings are supported by Milner et al. (2018), who found that shorter stride lengths reduce knee adduction joint loading. Our results mirror their findings by greater knee joint loads in the preferred step length (i.e., longer step length) compared to the constrained condition. However, our results analyzed different planes of motion compared to Milner et al. (2018) where we analyzed in the sagittal plane (knee flexion) instead of the frontal (knee adduction).

The mechanisms behind the increase in knee joint loading with a longer step length can be defined through kinematic and kinetic variables such as peak knee flexion, extension power, and extension moments. For peak knee flexion, the constrained step length increased under added load compared to the preferred step length condition. Our interpretation is that with an increase in load the subjects adapted to the load by increasing their muscular contribution by flexing the knee, therefore recruiting more muscles to attenuate load. However, this was not represented in the range of motion due to the unaltered state for the constrained added mass condition. This finding is contradicted by Attwells et al. (2006) who found that knee range of motion increases in conjunction to increased load, rather than the knee not changing in range of motion as the load increased. Since range of motion did not change, extension moments at the knee also did not change between conditions, and an increase in flexion was observed. Potentially, our participants walked with their knee more bent, providing a more athletic stance without reaching full extension in between walking phases.

Since there was an increase in peak knee flexion making a more crouched position, an increase of peak knee extension power was potentially due to the increase in force the muscles had to produce while maintaining this flexed position while walking. With the same distance and time the participant had to make a step, the increase in muscle force is a potential source of the increase

in peak knee extension power. While our findings suggest that an increase in muscular contribution to attenuate load helps preserve knee health, past research also states that an increase of load leads to an increase in muscular tension and knee injury (Attwells et al., 2006).

This study has two potential limitations. First, the added mass was applied to the chest region. In obese individuals, accumulative load is seen in alternative areas such as the thigh and lower abdominal regions. This could potentially alter kinematic variables in walking. As shown by Westlake et al. (2013), an increase in thigh circumference alters walking kinematics. If the load was distributed in other regions, such as the thigh, with altered kinematics, we could potentially alter walking kinetics. Another limitation could be that all of our subjects were athletes and not obese individuals. This could affect results since the participants were recreationally active and have an increased ability to adapt to stress unlike the population that this study simulated, obese adults. This was seen by Knapik et al. (1996) who found that foot soldiers did not have altered walking biomechanics until over fifty percent of their body weight was added to their weighted vest. Future studies should look at added load in alternate locations and with different populations to note if a simulated state shows accurate similarity between the two.

The current data demonstrate that increased step length (preferred step length condition) compared to the average preferred obese individuals' step length with or without added mass, decreases the load on the knee. Our findings add to past research that find an increase in stride length could help decrease the risk to skeletal structures by increasing the contributions to muscular components. This information can be applied clinically to individuals with a high risk of OA, such as older and obese populations, to make conscious decisions to increase stride length. However, more studies are needed to investigate simulated obese states to ensure a correlation between 'obese' and 'simulated' investigation data collection structures.

References

- Adams, K. F., Schatzkin, A., Harris, T. B., Kipnis, V., Mouw, T., Ballard-Barbash, R., . . . Leitzmann, M. F. (2006). Overweight, obesity, and mortality in a large prospective cohort of persons 50 to 71 years old. *N Engl J Med*, 355(8), 763-778. doi:10.1056/NEJMoa055643
- Alley, D. E., & Chang, V. W. (2007). The changing relationship of obesity and disability, 1988-2004. *JAMA*, 298(17), 2020-2027. doi:10.1001/jama.298.17.2020
- Andriacchi, T. P. (1994). Dynamics of knee malalignment. *Orthop Clin North Am*, 25(3), 395-403. Retrieved from <https://www.ncbi.nlm.nih.gov/pubmed/8028883>
- Attwells, R. L., Birrell, S. A., Hooper, R. H., & Mansfield, N. J. (2006). Influence of carrying heavy loads on soldiers' posture, movements and gait. *Ergonomics*, 49(14), 1527-1537. doi:10.1080/00140130600757237
- Bessesen, D. H. (2008). Update on obesity. *J Clin Endocrinol Metab*, 93(6), 2027-2034. doi:10.1210/jc.2008-0520
- Bliddal, H. (2008). Guidelines for the use of nonsurgical interventions in osteoarthritis management. *Expert Rev Clin Immunol*, 4(5), 583-590. doi:10.1586/1744666X.4.5.583
- Cawley, J., & Meyerhoefer, C. (2012). The medical care costs of obesity: an instrumental variables approach. *J Health Econ*, 31(1), 219-230. doi:10.1016/j.jhealeco.2011.10.003
- DeVita, P., & Hortobagyi, T. (2003). Obesity is not associated with increased knee joint torque and power during level walking. *J Biomech*, 36(9), 1355-1362. Retrieved from <https://www.ncbi.nlm.nih.gov/pubmed/12893044>
- DeVita, P., Rider, P., & Hortobagyi, T. (2016). Reductions in knee joint forces with weight loss are attenuated by gait adaptations in class III obesity. *Gait Posture*, 45, 25-30. doi:10.1016/j.gaitpost.2015.12.040
- Diseases, N. I. o. D. a. D. a. K. (2017). Overweight & Obesity Statistics. Retrieved from 222.niddk.nih.gov/health-statistics/overweight-obesity

- Felson, D. T., Anderson, J. J., Naimark, A., Walker, A. M., & Meenan, R. F. (1988). Obesity and knee osteoarthritis. The Framingham Study. *Ann Intern Med*, 109(1), 18-24. Retrieved from <https://www.ncbi.nlm.nih.gov/pubmed/3377350>
- Gregg, E. W., Cheng, Y. J., Cadwell, B. L., Imperatore, G., Williams, D. E., Flegal, K. M., . . . Williamson, D. F. (2005). Secular trends in cardiovascular disease risk factors according to body mass index in US adults. *JAMA*, 293(15), 1868-1874. doi:10.1001/jama.293.15.1868
- Haff, G., & Triplett, N. (2016). Nutrition Strategies for Maximizing Performance. In *Essentials of Strength and Conditioning* (4th ed., pp. 218-219). Champaign, IL: Human Kinetics.
- Key Health Data About Tennessee. (2018). Trust for America's Health. Retrieved from healthyamericans.org/states/?statid=TN
- Knapik, J., Harman, E., & Reynolds, K. (1996). Load carriage using packs: a review of physiological, biomechanical and medical aspects. *Appl Ergon*, 27(3), 207-216. Retrieved from <https://www.ncbi.nlm.nih.gov/pubmed/15677062>
- Lementowski, P. W., & Zelicof, S. B. (2008). Obesity and osteoarthritis. *Am J Orthop* (Belle Mead NJ), 37(3), 148-151. Retrieved from <https://www.ncbi.nlm.nih.gov/pubmed/18438470>
- Messier, S. P., Gutekunst, D. J., Davis, C., & DeVita, P. (2005). Weight loss reduces knee-joint loads in overweight and obese older adults with knee osteoarthritis. *Arthritis Rheum*, 52(7), 2026-2032. doi:10.1002/art.21139
- Milner, C. E., Meardon, S. A., Hawkins, J. L., & Willson, J. D. (2018). Walking velocity and step length adjustments affect knee joint contact forces in healthy weight and obese adults. *J Orthop Res*, 36(10), 2679-2686. doi:10.1002/jor.24031
- Mohammed, A., Al-Numair, K. S., & Balakrishnan, A. (2015). Docking studies on the interaction of flavonoids with fat mass and obesity associated protein. *Pak J Pharm Sci*, 28(5), 1647-1653. Retrieved from <https://www.ncbi.nlm.nih.gov/pubmed/26408884>
- NIH fact Sheets – Osteoarthritis. (2018). Retrieved from report.nih.gov/nihfactsheets/ViewFactSheet.aspx?csid=55

- Ruiz, R. (2012). America's Most Obese Cities. Retrieved from www.forbes.com/2007/11/14/health-obesity-cities-forbeslife-cx_rr_1114obese.html.
- Sui, X., LaMonte, M. J., Laditka, J. N., Hardin, J. W., Chase, N., Hooker, S. P., & Blair, S. N. (2007). Cardiorespiratory fitness and adiposity as mortality predictors in older adults. *JAMA*, 298(21), 2507-2516. doi:10.1001/jama.298.21.2507
- Tennessee State Obesity Data, Rates and Trends. (2018). Retrieved from stateofobesity.org/states/tn/
- Westlake, C. G., Milner, C. E., Zhang, S., & Fitzhugh, E. C. (2013). Do thigh circumference and mass changes alter knee biomechanics during walking? *Gait Posture*, 37(3), 359-362. doi:10.1016/j.gaitpost.2012.07.031
- Yocum, D., Weinhandl, J. T., Fairbrother, J. T., & Zhang, S. (2018). Wide step width reduces knee abduction moment of obese adults during stair negotiation. *J Biomech*, 75, 138-146. doi:10.1016/j.jbiomech.2018.05.002

Christian Brown is a senior physics and math major from Union University who participated in the Research Experience for Undergraduates at the University of Memphis in the summer of 2019. He worked under Dr. Francisco Muller Sanchez over a 10-week period. In the future, Christian plans to pursue a graduate degree in physics after completing his undergraduate degree.

Christian Brown

Physical Characteristics of the Nuclear Region of NGC 4388

Faculty Sponsor

Dr. Francisco Muller Sanchez

Abstract

Several observed relationships between black holes and galaxies show that growth of supermassive black holes relates to galaxy evolution. These relations can be addressed by studying feeding and feedback. The KONA survey observed the core region of the Seyfert 2 galaxy NGC 4388 in the near-IR spectrum (1.963-2.379 μm). The OSIRIS IFS produced a datacube of a 3.3" x 4.7" region containing the AGN. Gaussian curves were fitted to the peaks of Si VI, H₂ 1-0 S(1), and Br γ with QFitsView. QFitsView and Astropy were then used to produce, mask, and smooth the flux, velocity, and dispersion maps for the peaks. The Si VI and Br γ maps showed evidence of an outflow in the south, while H₂ 1-0 S(1) showed evidence of a warped disk, rotation, and behavior linked to the torus. Behavior of Si VI and Br γ in the north is likely linked to a ram pressure stripping event.

Introduction

The most powerful and luminous objects in the known universe, supermassive black holes (SMBH) reside at the center of galaxies and can measure up to billions of solar masses. Many observed relationships between black holes and their host galaxies indicate a close connection between the formation of the two (Heckman & Best 2014). Understanding the behavior and structure of the material in the central regions of Seyfert galaxies is undoubtedly critical to the understanding of the nature of these objects due to their incredible influence on the material. Certain phenomena such as inflows and outflows are especially important to discerning an accurate description of galactic nuclei and how the material in them interacts with the SMBH. This, in turn, would also shed light on the nature of the coevolution of galaxies and SMBHs.

The Keck OSIRIS Nearby AGN (KONA) survey (Müller-Sánchez et al.), which sought to study the nuclear kinematic structure of 40 nearby active galaxies through the Keck Telescope and OSIRIS near-infrared integral field spectrograph, was conducted with the goal of researching several of these Seyfert galaxies. NGC 4388 is one galaxy observed in this survey. It is a barred spiral galaxy that is almost edge on in its inclination ($i \approx 78^\circ$) (Veilleux et al.). It is a Seyfert 2 galaxy located in the Virgo Cluster (Phillips et al.) with a redshift $z = 0.00842$ (Lu et al.). It is near the center of the cluster and one of the brightest in the cluster with a magnitude of $M_r = -20.1$.

The galaxy has an active galactic nuclei (AGN) and shows evidence of a very extended emission line region (VEELR) that reaches to roughly 35 kpc to the northeast of the galactic plane (Yoshida et al.). This is possibly due to past interactions with other galaxies. Evidence of a ram pressure stripping event around 200 Myr ago that pulled material off of the galaxy adds credibility to this scenario (Vollmer et al.).

There is kinematic evidence for a misaligned nuclear disk near the core of the galaxy (Greene et al.). This disk in the central 1° is misaligned by 15° from the main disk of the galaxy. Additionally, there is a maser disk, or source of a high level of stimulated spectral line emission, on the sub-pc scale (Braatz et al.). The galaxy shows uniform rotation in the H_2 spectrum in the plane of the galaxy, but Bry and Si VI do not show this behavior (Greene et al.).

Observations and Methods

The KONA survey utilized the Keck observatory in Hawaii with the OSIRIS integrated field spectrometer (IFS) to observe NGC 4388 in the near-IR spectrum (1.963-2.379 μm). The observation was done on December 15,

2016, with a scale of 0.05 arcsec/pixel. A region of 66 x 94 pixels was observed. The observation was done under good atmospheric conditions with an airmass of 1.15. The collected data was stored in a .fits file datacube.

QFitsView was utilized to analyze the datacube. The emission peaks for Si VI, H₂ 1-0 S(1), and Br γ were identified for spectra at several different locations. Gaussian peaks were then fitted to these peaks. QFitsView was then used to automatically produce flux, velocity, and dispersion maps for these emissions centered on the wavelengths of these peaks at the central location. QFitsView produced flux maps based on the intensity of the peak at each pixel, velocity maps based the shift in wavelength of the center of the peak from the wavelength at the central position, and dispersion maps measured the full width at half maximum (FWHM) of the peak at each location. The starting parameters for Si VI were a center of 1.978187 μm and FWHM of 130 km/s for Si VI, 2.137739 μm and 230 km/s for H₂ 1-0 S(1), and 2.182589 μm and 190 km/s for Br γ .

The Astropy package in Python (Robitaille et al.) was then used to analyze the maps produced by QFitsView. Noise was filtered out by first removing pixels with unusually high or low values that did not fit into any physical structure. This was done by masking the maps with themselves in certain regions and choosing minimum and maximum values that were automatically replaced with a low value, 1 for velocity and dispersion maps and 0.01 for flux maps. A Gaussian smoothing function was applied to the maps and then another mask was applied using a smoothed continuum image to remove further noise in the extremes of the image. Flux maps were then normalized to the brightest pixel in each map. A rotational model was then produced for velocity maps with rotational motion. The model is in the form

$$V_{los} = \sqrt{\frac{R^2 GM}{(R^2 + A^2)^{\frac{3}{2}}}} \frac{\sin(i) \cos(\psi - \psi_0)}{\left(\cos^2(\psi - \psi_0) + \frac{\sin^2(\psi - \psi_0)}{\cos^2(i)}\right)^{\frac{3}{4}}}$$

where R is the radial coordinate, ψ is the angular coordinate, V_{los} is the velocity in the line of sight of the observer, G is the gravitational constant, i is the inclination, M is mass, A is the correspondent scale length to R , and ψ_0 is the angular tilt of the plane. The velocity maps were then subtracted from this model to create residuals.

Results

Location peak (x, y)	Flux	Height	Center	FWHM
(12, 60)				
Si VI	118.509	0.839419	1.448645	132.629
H ₂ 1-0 S(1)	399.924	1.70203	58.68266	220.738
Bry	120.078	1.02774	23.37855	109.761
(21, 60)				
Si VI	186.494	1.11297	-21.46072	157.417
H ₂ 1-0 S(1)	334.757	1.35027	71.83225	232.903
Bry	115.336	0.583478	4.66206	185.747
(28, 71)				
Si VI	172.653	1.11093	-13.7718	146
H ₂ 1-0 S(1)	142.555	0.473062	3.049578	283.094
Bry	158.197	0.481341	-11.88695	308.755
(33, 60)				
Si VI	2556.6	18.3413	0.00070061	130.948
H ₂ 1-0 S(1)	1089.83	4.34282	-5.151806	235.752
Bry	942.452	4.7224	0.07014403	187.484

Location peak (x, y)	Flux	Height	Center	FWHM
(36, 49)				
Si VI	527.624	1.98357	40.91657	249.888
H ₂ 1-0 S(1)	99.2693	0.419417	-8.000039	222.349
Bry	124.587	0.538189	48.8313	217.473
(41, 37)				
Si VI	260.25	0.799837	-63.60072	305.673
H ₂ 1-0 S(1)	68.0861	0.226325	-73.91846	282.614
Bry	164.192	0.315791	-74.13898	488.448
(45, 60)				
Si VI	1184.33	2.59361	-18.04886	428.98
H ₂ 1-0 S(1)	159.004	0.683473	-46.06937	218.552
Bry	120.058	0.431776	-13.00337	261.217
(54, 60)				
Si VI	1399.58	2.78901	-101.4793	471.429
H ₂ 1-0 S(1)	513.729	1.84718	-58.95029	261.273
Bry	90.5817	0.267641	-50.87357	3917.947

Table 1. Results from Gaussian fits of Si VI, H₂ 1-0 S(1), and Bry peaks at the given locations in velocity space. Each velocity space is centered on the wavelength of the peak at the central region.

Utilizing QFitsView, spectra were extracted from several regions of the galaxy. A diagram of this is shown in Figure 1. The following peaks were visible in the spectra: H₂ 1-0 S(3), Si VI, He I, H₂ 1-0 S(2), H₂ 1-0 S(1), Bry, Ca VIII, H₂ 1-0 S(0). The central spectra shows a slope near 0 with very prominent, narrow emission lines. Moving away from the center, the spectrum shows a more negative slope. The individual peaks of Si VI, H₂ 1-0 S(1), and Bry, were analyzed at these locations as well, with Gaussian curves being fitted to these peaks. The results are shown in Figures 2, 3, and 4, with the results of the Gaussian fits being shown in Table 1.

The Si VI peak broadens to the east and south sections of the map. It shows a tail of blueshift north of the AGN and slightly to the west. Slightly south of the core shows a redshifted behavior while further south shows blueshift.

H₂ 1-0 S(1) shows redshift to west and blueshift to the east. There is some visible broadening to the north and east portions of the map. The V/σ map has very low values, with a maximum of around 0.4, but does grow in magnitude towards the eastern and western extremes.

Bry shows strong broadening to the south and east as well as some redshift slightly south of the nucleus. Much of the behavior far from the core may be due to atmospheric noise.

Finally, QFitsView was used to produce flux, velocity, and dispersion maps by automatically analyzing the intensity, redshift, and full width at half maximum (FWHM) of the peak at each pixel in the observed region.

Once Astropy was utilized to mask and smooth the maps, and normalize the flux maps, they were plotted as images.

The Si VI flux map shows an extremely bright center with some spots of high intensity throughout the disk, but none of these show a flux higher than 0.16. The velocity map shows very little motion in the disk, but some slight blueshift north of the disk, and an area of noticeably high redshift to the south and very high blueshift further south and slightly east. The dispersion map shows an area of dispersion over 400 km/s south of the AGN as well as areas of lower dispersion to the northwest.

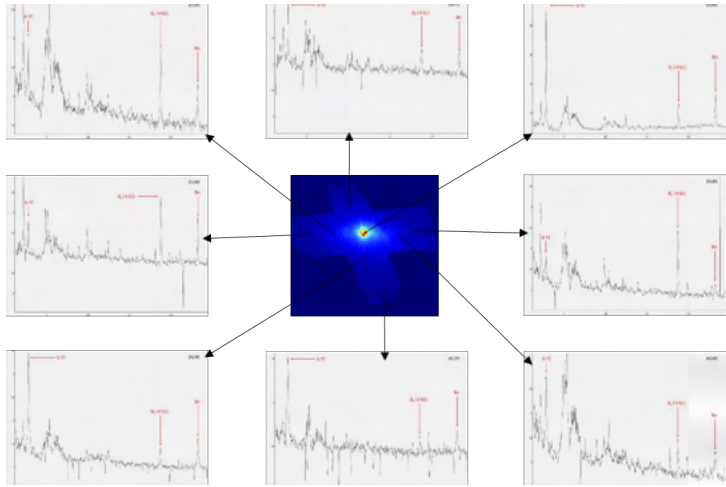


Figure 1. A continuum image of the galaxy (center), with spectra from the following positions (starting top right and going clockwise. Coordinates relative to center in form of (R.A., Dec.)): (0", 0"), (1.05", 0), (0.6", 1.05"), (-0.4, -1.15), (-0.15", -0.55), (-0.6", 0"), (-1.05", 0"), (0.25", 0.55"). Each spectrum shows the region (1.963-2.195 μ m) and was extracted from a region with a pixel radius of 3. The peaks for Si VI, H₂ 1-0 S(1), and Br γ are labeled on each spectrum.

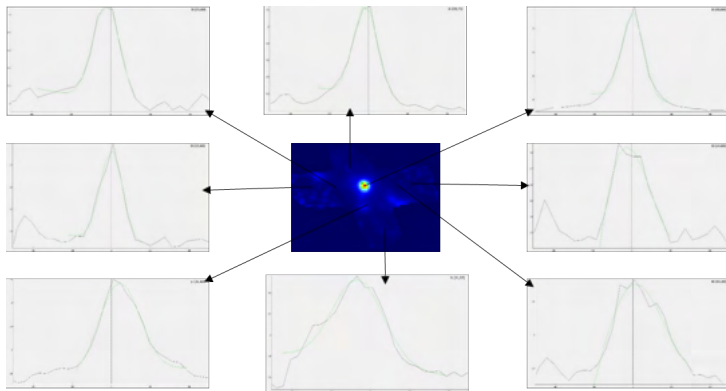


Figure 2. Same alignment as Figure 1 but showing the flux map for Si VI in the center and the spectrum peak for Si VI at each location. The spectra are in velocity space from -500 to 500 km/s, centered at 1.978187 μ m. A dotted line is shown on each spectrum to indicate this central position. Each peak is also shown with an approximate Gaussian fit.

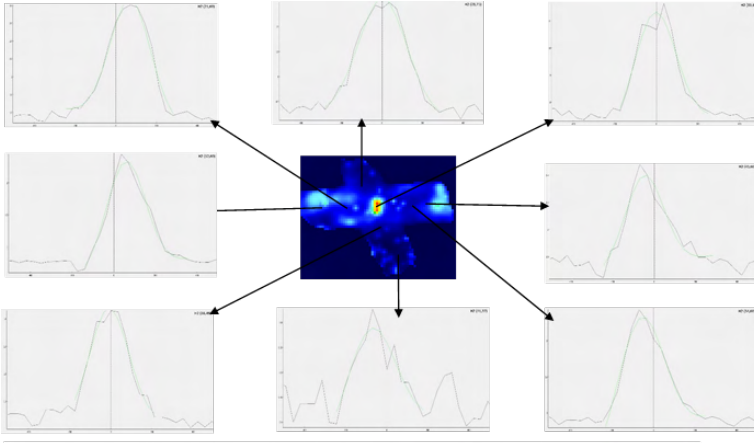


Figure 3. Same as Figure 2 but showing H_2 1-0 S(1) flux map and spectra peaks, centered at $2.137739 \mu m$.

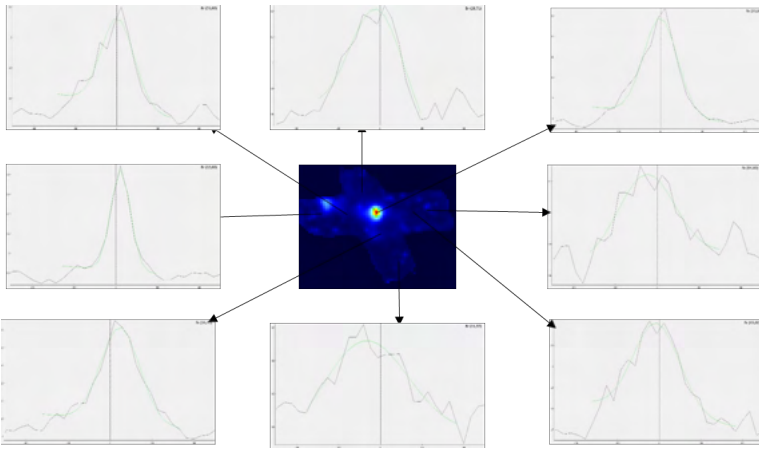


Figure 4. Same as Figure 2 but showing $Br\gamma$ flux map and spectra peaks, centered at $2.182589 \mu m$.

The H_2 1-0 S(1) flux map has a bright center, and areas of high flux within the disk both to the west and far east. The velocity map reveals a clear gradient in the disk from redshift in the west to blueshift in the east, along with some areas of slight blueshift to the far south. The dispersion map reveals spots of high dispersion scattered throughout the disk that seem to be spatially coincident with areas of low flux.

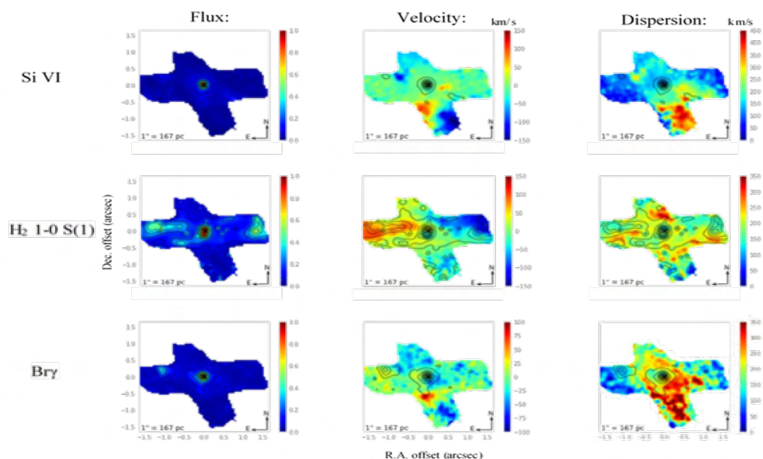


Figure 5. Flux, velocity, and FWHM dispersion maps for Si VI, H₂ 1-0 S(1), and Bry. All maps are plotted with the contours from that peak's flux map, with contours ranging from 0 to 1 on intervals of 0.1. A black x marks the estimated location of the AGN.

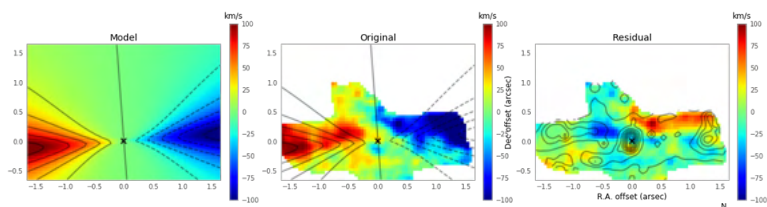


Figure 6. Shown are the model (left), H₂ 1-0 S(1) velocity map with contours of the model overlaid (center), and the residual with contours of H₂ 1-0 S(1) flux overlaid. The bottom section of the maps was cut to remove data that was not part of the rotational structure.

The velocity map shows similar structure to Si VI with relatively little activity in the disk, but a slight blueshift in the north, with an area of higher redshift to the south and high blueshift further southeast. The dispersion map has a ring-shaped structure of high dispersion surrounding the nucleus with extremely high dispersion in the south.

The Bry flux map has a bright center with another small area of high intensity to the west. The velocity and dispersion maps are very similar to those of Si VI but with a lower magnitude. There is also slightly more evidence of motion and dispersion within the galaxy plane.

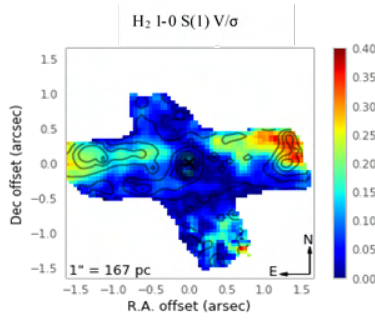


Figure 7. A map of the ratio of velocity and sigma for H₂ 1-0 S(1) overlaid with the same H₂ 1-0 S(1) flux contours as figure 5.

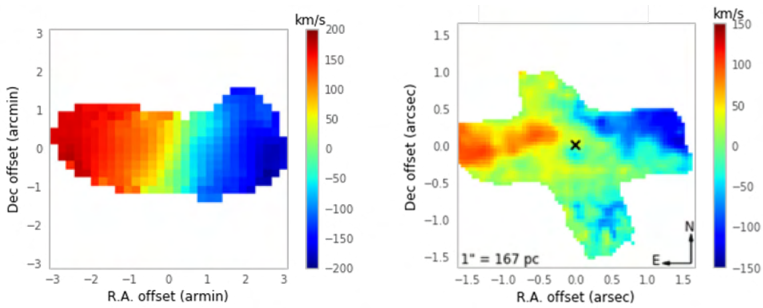


Figure 8. On the left is a velocity map from VIVA on the kiloparsec scale of NGC 4388. On the right is the KONA H₂ 1-0 S(1) velocity map on scale of 10's of parsecs. The angle of rotation for the inner area is measured to be around 82 degrees from south for the VIVA image and approximately 96 degrees from south on the KONA map. A black line has been added tracing the angle of rotation for each.

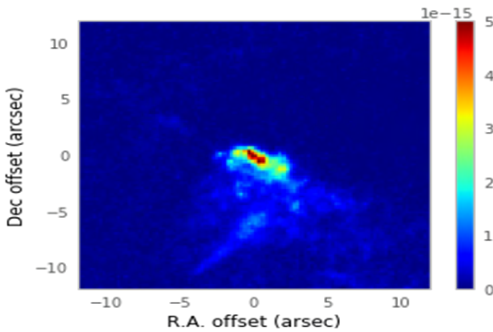


Figure 9. A Hubble Space Telescope image showing the OIII flux of NGC 4388. The ionization cone south of the nucleus is clearly visible.

A kinematic model in the form of

$$V_{los} = \sqrt{\frac{R^2 GM}{(R^2 + A^2)^{\frac{3}{2}}}} \frac{\sin(i) \cos(\psi - \psi_0)}{\left(\cos^2(\psi - \psi_0) + \frac{\sin^2(\psi - \psi_0)}{\cos^2(i)}\right)^{\frac{3}{4}}}$$

was created with values of $A = 300$ pc, $M = 2.5 \cdot 10^9 M$, and $i = 0.075$ radians. These values were estimated using a X2 minimization. The center of rotation is placed on the location of the AGN, and the maximum velocity within our domain is 107.5 km/s. The H_2 1-0 S(1) velocity map was then subtracted from this model to produce a residue. These results are shown in Figure 7.

Discussion

The position of the AGN was determined via level of intensity. Each continuum and flux map consistently showed the most luminous pixel in the center to be located at pixel (33, 60).

The H_2 1-0 S(1) velocity map shows strong evidence of rotation in the plane of the galaxy. This is consistent with observations done on larger scales, as well as stellar rotation (Greene et al.). However, this rotation is at a different angle from rotation at larger scales. Figure 8 shows an image from VIVA (Chung et al.) on the kiloparsec scale compared to one of our images and clearly shows an offset of around 14 degrees between the two images. This offset disk has been suggested by past observations (Greene et al.).

The V/σ map for H_2 1-0 S(1) shows relatively low values, indicating a thick disk. This combined with the aforementioned misaligned disk of rotation suggest it is aligned with the maser disk. Thus, the behavior of H_2 is associated with the torus.

The maps of Si VI and Bry show evidence for strong behavior south of the galactic plane. The dispersion for both is extremely high in this region, with Si VI having dispersion above 400 km/s at some spots. The velocities of both also show strong behavior in this region, with both having an area of high redshifted velocity and blueshifted in similar regions. Bry does show high areas of dispersion around the nucleus that Si VI does not, showing it may be more prevalent in the disk of the galaxy. These observations are consistent with results from observations on slightly larger scales (Greene et al.). The motion of Si VI and Bry indicate the ionized gas in the south of NGC 4388 is likely due to an outflow. Paired with the observations of a radio jet and ionized gas south of the galaxy (Falcke et al.), this indicates the presence of an outflow from the AGN. The ionization cone can be seen in Figure 9.

The H_2 1-0 S(1) velocity and dispersion maps, while weaker, also show some activity in the south with the velocity being blueshifted and dispersion showing spots of high activity. This could be evidence that some molecular gas is also involved in the outflow.

The northern section of the maps do not show as much activity as the southern part. This is due in part to some of the region being removed during the masking process due to noisy data. However, it still does show a slight blueshift in the Si VI and Bry velocity map. The dispersion maps for these two peaks also show some mild activity, while the H_2 1-0 S(1) dispersion map shows a spot of high activity in this region. Such behavior does not seem to be consistent with what is occurring in the south of the galaxy. A likely explanation for this is a ram pressure stripping event. It has already been shown that NGC 4388 likely went through such an event around 200 Myr

ago (Vollmer et al.). The effects of this event are likely tied to the behavior seen in the north of NGC 4388.

Conclusions

Data analysis of NGC 4388 revealed several things. The previously observed ionization cone and radio jet at the south of the galaxy is likely the result of an outflow from the AGN. This is most clearly seen in the dispersion and velocity maps of Si VI and Br γ , with some possible molecular gas also present as seen in the velocity and dispersion maps of H $_2$ 1-0 S(1). The H $_2$ 1-0 S(1) velocity map shows clear evidence of rotation within the disk of NGC 4388. However, this does not appear to be pure rotation. The angle of rotation does not line up with the angle seen from observations of the galaxy on larger scales. This is strong evidence for a warped disk in the inner region. The small values of H $_2$ 1-0 S(1) V/σ near the center suggest H $_2$ behavior is associated with the torus. Small blueshifted motion and low-level dispersion in the north of the galaxy are likely the result of NGC 4388 undergoing a ram pressure stripping event at some point in the past.

References

- Braatz, J. A. et al. "A Green Bank Telescope Search for Water Masers in Nearby Active Galactic Nuclei." *The Astrophysical Journal* 617.1 (2004): L29–L32. Crossref. Web.
- Chung, Aeree et al. "Erratum: 'VLA Imaging of Virgo Spirals in Atomic Gas (Viva). I. The Atlas and the HI Properties.'" *The Astronomical Journal* 139.6 (2010): 2716–2718. Crossref. Web.
- Greene, Jenny E. et al. "Circumnuclear Molecular Gas in Megamaser Disk Galaxies NGC 4388 and NGC 1194." *The Astrophysical Journal* 788.2 (2014): 145. Crossref. Web.
- Heckman, Timothy M. and Best, Philip N. "The Coevolution of Galaxies and Supermassive Black Holes: Insights from Surveys of the Contemporary Universe." *Annual Review of Astronomy and Astrophysics* 52.1 (2014): 589-660. Crossref. Web
- Falcke, Heino, Andrew S. Wilson, and Chris Simpson. "Hubble Space Telescope and VLA Observations of Seyfert 2 Galaxies: The Relationship Between Radio Ejecta and the Narrow-Line Region." *The Astrophysical Journal* 502.1 (1998): 199–217. Crossref. Web.
- Lu, N. Y., Hoffman, G. L., Groff, T., Roos, T., Lamphier, C. "H i 21 Centimeter Observations and I-Band CCD Surface Photometry of Spiral Galaxies behind the Virgo Cluster and toward Its Antipode." *Astrophysical Journal Supplement* v.88 (1993): 383-413. Crossref. Web.
- Müller-Sánchez, F. et al. "The Keck/OSIRIS Nearby AGN Survey (KONA). I. The Nuclear K-Band Properties of Nearby AGN." *The Astrophysical Journal* 858.1 (2018): 48. Crossref. Web.
- Phillips, M.M. and Malin, D.F. "NGC 4388: a Seyfert 2 galaxy in the Virgo cluster." *Mon. Not. R. Astr. Soc.* 199.4 (1982) 199, 905-913. Crossref. Web.
- Robitaille, T. P. et al. "Astropy: A community Python package for astronomy." *A&A* 558, A33 (2013): 1432-0746. Crossref. Web.

Veilleux, S., J. Bland-Hawthorn, and G. Cecil. "A Kinematic Link Between Boxy Bulges, Stellar Bars, and Nuclear Activity in NGC 3079 and NGC 4388." *The Astronomical Journal* 118.5 (1999): 2108–2122. Crossref. Web.

Vollmer, B. et al. "Two Uneven Sisters." *Astronomy & Astrophysics* 620 (2018): A108. Crossref. Web.

Yoshida, Michitoshi et al. "Discovery of a Very Extended Emission-Line Region Around the Seyfert 2 Galaxy NGC 4388." *The Astrophysical Journal* 567.1 (2002): 118–129. Crossref. Web.

Daniel Duong completed his B.S. in physics from the University of West Florida in August 2019. He was a member of the Society of Physics Students as well as the head of media for the Baptist Collegiate Ministries. Daniel was also involved in computation physics research under Dr. Christopher Varney. Over the summer of 2018, Daniel received an opportunity to conduct research under Dr. Firouzeh Sabri at the University of Memphis through the Research Experience for Undergraduates program funded by the National Science Foundation.

Daniel Duong
The Synthesis and Preparation of Upconverting and
Downconverting Phosphors for Sensing Applications

Faculty Sponsor
Dr. Firouzeh Sabri

Introduction

Thermometry has always been important for scientific and industrial applications. Its usage ranges from environment sensing and climate control to medical uses. Thermometry plays an important role in determining if a region of space is suitable to the application at hand, from habitable conditions and possible hazards to the usage of electronics. It helps determine how certain materials will behave, thus informing the best way to prepare accordingly.

Just as the applications of thermometry have a wide array, so are the types of thermometry, each with their respective strengths and weaknesses. One type of thermometry uses thermal expansion. A classic example of this would be the mercury thermometer. The mercury expands as it is heated, and the volume is then used to determine the temperature. While useful for a broad range of applications, a downside is that it must be in contact with the material itself. Other types of thermometry require a medium to travel through, are not highly accurate, or cannot detect a wide range of temperatures (Aryal, 2018). For the purposes of space exploration and settlement, these factors play a significant role in determining the type of thermometry used. As a result, phosphor thermometry is a strong contender to be the best way to deal with these issues.

Phosphor thermometry operates by using photoluminescence, thus avoiding all of the issues above. This occurs by shooting a short pulse laser at the phosphor, enabling the electrons to reach an excited state, and measuring the emissions from the electrons as they fall back to ground level (Aryal, 2018). This is why the phosphors are described as upconverting and downconverting. For the purposes of this experiment, the decay rate will be used to determine the temperature, as it is the most widely-used method, and a method which is compatible with a configuration which will be stated later (Allison et al, 2017). Phosphor thermometry does have one weakness, however. The phosphors are in powder form, which makes them difficult to handle.

Due to their small particle size, a variety of issues arise. They will easily cross contaminate with other materials, messing up measurements. In addition, their high surface charge causes them to adhere to most materials as well as cluster together, creating a non-uniform amount of the powder for sensing. Outside forces will cause the powder to disperse. In this form, the phosphor powders are hazardous, not only to people, but also to the environment, therefore necessitating Environmental Protection Agency regulations. Lastly, the phosphors are reusable, but not recoverable in this state, and can only be utilized on a limited number of surfaces (Rietema, 1991). Thus, the proposed

solution is to encapsulate the powders in Sylgard 184.

Sylgard 184 is classified under the family of polydimethylsiloxane (PDMS). PDMS is a common elastomer used for space exploration due to its insulating abilities, flexibility, non-flammability, and easy synthesis. Especially critical in this experiment is PDMS's characteristic of being inert (Fontenot et al, 2016). This allows it to be doped with different materials, enabling the creation of composites. By forming a composite with the phosphor powders, the phosphor itself becomes easier to handle and thus, more applicable. PDMS is also transparent in the visible spectrum, thereby not distorting the photoluminescence of the phosphor powders (Allison et al, 2017).

The purpose of this experiment is to create a method in which the phosphor powders can be reliably encapsulated without the loss of the powder. In addition, the identification of the best suited temperature dependent bandwidths will be identified. Finally, an investigation was made to see if the encapsulation process had any effect on the excitation or emission behavior of each compound.

Materials

Thirteen different phosphor powders were acquired for this research. Eight of the powders were acquired from Intelligent Materials, and the other five were acquired from the University of Louisiana, Lafayette. The powders acquired from Intelligent Materials were Yttrium, Lanthanum, Lanthanum/Gadolinium, 620 Nitrate, 630 Nitrate, Zinc Sulfide UV (Green), Bismuth, and Zinc Sulfide UV (Blue). From the University of Louisiana, Lafayette, three Europium Tetrakis powders and two Magnesium Tetrakis powders were acquired (Fontenot et al, 2012; 2015). Sylgard 184 was used as the encapsulation elastomer.

Procedures

The same general procedure was followed for the majority of the composites. First, Sylgard 184 and the curing agent were mixed at a ratio of ten to one to form PDMS. This ratio was predetermined by previous experiments. Following this, the sample was outgassed for four to five minutes. The PDMS was mixed with the phosphor powder at a ratio of twenty-two to one and mixed by hand thoroughly for three to four minutes. The sample was outgassed a second time for four to five minutes. Within the next three to four minutes, the mixture was poured into the dog bone mold and outgassed completely. Lastly, it was cured in an oven at 100 °C for an hour, cooled, and removed from the mold. Aside from this synthesis method, the Europium Tetrakis was

ground from crystals into a powder. As for Bismuth, an eighty-micrometer sieve was utilized to acquire a more homogeneous powder size.

To measure the photoluminescence of the powders, a 405-nanometer laser was first used to excite the electrons. A PDMS layer of 6.26-millimeter thickness was placed on top of the powders. The function generator was set with a square wave at a 1.5 millisecond pulse. A photomultiplier was placed to detect the luminescence of the powders. A variety of lenses were used in order to determine the temperature dependent bandwidths. The stage was connected to the temperature controller in order to vary the temperature of the powders. The powders were given five minutes to rise to the desired temperature if the temperature increment was five degrees Celsius, and eight minutes if the increment was ten degrees Celsius. The photomultiplier was then output into an oscilloscope in order to see the decay of the photoluminescence. From there, the decay rate of each of the powders at elevated temperatures were determined.

The exact same procedures were utilized to determine the decay rates of the composites. One exception is for the Zinc Sulfide UV (Green) for both the powder and composite form: a pulse length of 2.0 millisecond pulse length was utilized since it took the powders longer to reach a steady excited state. For the phosphors with the decay rates that were analyzable at room temperature, they were tested from room temperature to 200 degrees Celsius in five- or ten-degree increments.

Results

For the majority of the phosphor powders, they were successfully encapsulated into PDMS. Table 1 displays which materials were cured successfully and which were not. Other methods of curing were also tested on the Lanthanum/Gadolinium samples such as curing at 200 degrees Celsius and using UV curing. Unfortunately, neither of these methods worked. The composites remained liquid, indicating the powders were interfering with the curing chemical reaction. For the successfully cured samples, the physical characteristics of each composite varied and should be investigated at a later date.

Phosphor Powder	Successful Curing?
1: Yttrium	Yes
2: Lanthanum	Yes
3: Lanthanum/Gadolinium	No
4: 620 Nitrate	Yes
5: 630 Nitrate	Yes
6: Zinc Sulfide UV (Green)	Yes
7: Bismuth	No
8: Zinc Sulfide UV (Blue)	Yes
B: Europium Tetrakis #1	Yes
C: Europium Tetrakis #2	Yes
D: Europium Tetrakis #3	Yes
F: Magnesium Tetrakis #1	Yes
G: Magnesium Tetrakis #2	Yes

Table 1. Curing Composites

Next, the optimal wavelengths for each phosphor were observed and recorded. Table 2 shows which wavelength lens should be used for each phosphor.

Phosphor Powder	Optimal Wavelength
1: Yttrium	460 nm
2: Lanthanum	460 nm
3: Lanthanum/Gadolinium	460 nm
4: 620 Nitrate	650 nm
5: 630 Nitrate	650 nm
6: Zinc Sulfide UV (Green)	540 nm
7: Bismuth	540 nm
8: Zinc Sulfide UV (Blue)	460 nm
B: Europium Tetrakis #1	650 nm
C: Europium Tetrakis #2	650 nm
D: Europium Tetrakis #3	650 nm
F: Magnesium Tetrakis #1	460 nm
G: Magnesium Tetrakis #2	460 nm

Table 2. Powders and Composites Optimal Wavelength

The optimal wavelength was determined by selecting the most prevalent and analyzable decay rates. An example can be seen in Figure 1.

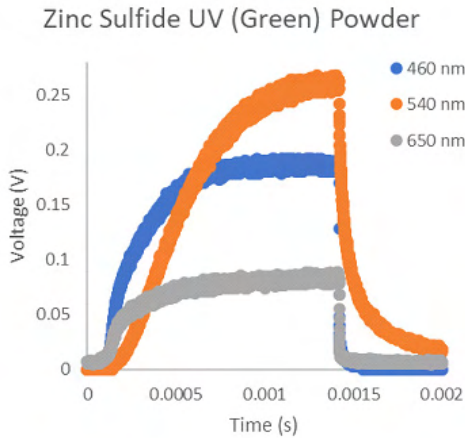


Figure 1. The decay rate for Zinc Sulfide UV (Green) Powder is shown above. It displays the amount of voltage against time.

From the figure above, it can be determined that the optimal wavelength for Zinc Sulfide UV (Green) is 540 nm due to the longer decay time. In addition, both the powders and the phosphors had the same optimal wavelengths. This is evident in Figure 2.

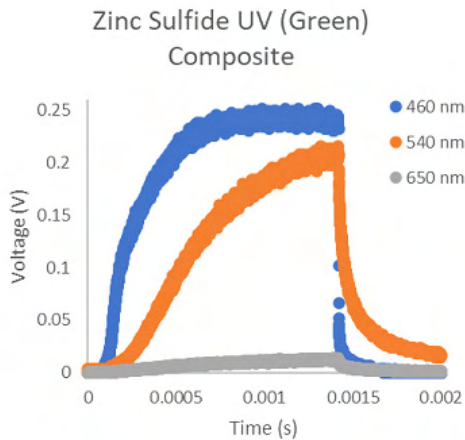


Figure 2. The decay rate for Zinc Sulfide UV (Green) Composite. It displays the amount of voltage against time.

Lastly, when setting up the decay behavior of the photo luminescence against the natural logarithm of the temperature, the same linear lines were evident between the powders and their respective composites. The standard data is seen in Figure 3.

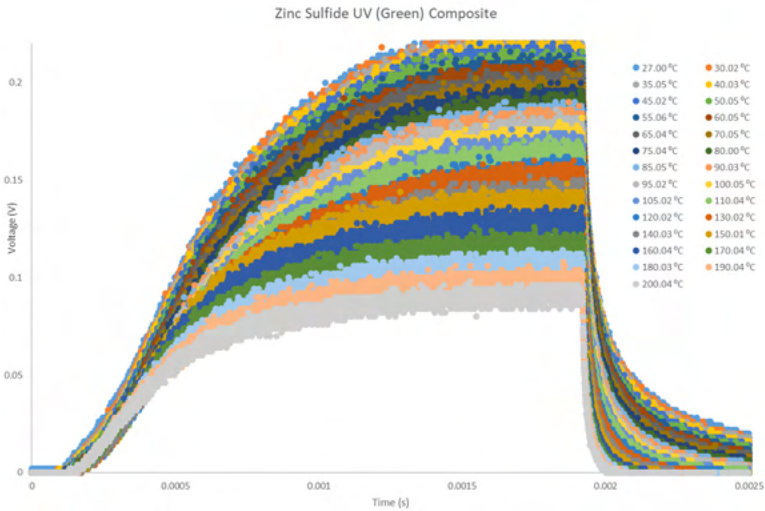


Figure 3. The decay rates for various elevated temperatures for Zinc Sulfide UV (Green) Composite using a 540-nanometer wavelength lens. A look at the data shows that higher temperatures are correlated with shorter decay rates.

When plotted in a log plot, the linearity of the correlation can be seen.

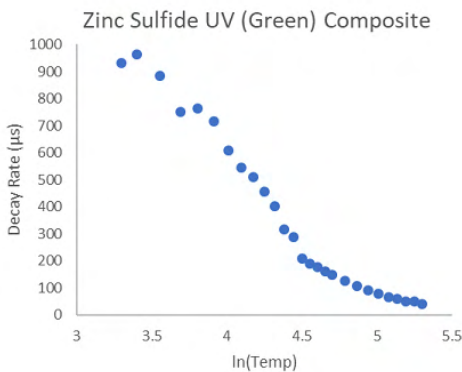


Figure 4. The decay rates plotted against the natural logarithm of the temperature. This is for the Zinc Sulfide UV (Green) Composite.

There also appears to be two separate linear sections in the correlation, which should be investigated at a further date. The Zinc powder and the Europium Tetrakis samples were also measured and a linear correlation is also seen. All of the other composites' decay rates were too short to measure at elevated temperatures.

Conclusion

The majority of the powders were successfully encapsulated by PDMS into composite form. In addition, the encapsulation process does not affect the readings on the decay rates. As a result, the benefits of the phosphor powders are retained while the weaknesses are eliminated. With the optimal wavelengths analyzed, the correct lens can be chosen to observe each phosphor powder.

As the composites have been analyzed, the phosphor samples can be used as a temperature sensing apparatus. The composites can be utilized where traditional methods of thermometry are lacking. Since taking readings is non-contact, accurate, and quick, this form of thermometry has many advantages, and one of the best utilizations is in space applications where conditions make temperature readings difficult.

In the future, it would be desirable to see lower temperatures explored. In addition, other characteristic tests of the composites would be useful, as while the effects of PDMS on the powders have been observed to an extent, the effects on the characteristics of PDMS has not. The potential of temperature flux has not been analyzed. It can be achieved by layering the different composites on top of each other and reading the different decay rates. Finally, encapsulation of the powders in other materials such as aerogels would be useful for future study.

References

- Allison, S. W., Baker, E. S., Lynch, K. J., & Sabri, F. (2017). In vivo X-Ray excited optical luminescence from phosphor-doped aerogel and Sylgard 184 composites. *Radiation Physics and Chemistry*, *135*, 88–93. doi: 10.1016/j.radphyschem.2017.01.045
- Fontenot, R. S., Bhat, K. N., Hollerman, W. A., Aggarwal, M. D., & Nguyen, K. M. (2012). Comparison of the triboluminescent yield and decay time for europium dibenzoylmethide triethylammonium synthesized using different solvents. *CrystEngComm*, *14*(4), 1382–1386. doi: 10.1039/c2ce06277a
- Fontenot, R. S., Owens, C. A., Bhat, K. N., Hollerman, W. A., & Aggarwal, M. D. (2015). Magnesium tetrakis dibenzoylmethide triethylammonium: A novel blue emitting phosphor. *Materials Letters*, *146*, 9–11. doi: 10.1016/j.matlet.2015.01.141
- Fontenot, R. S., Allison, S. W., Lynch, K. J., Hollerman, W. A., & Sabri, F. (2016). Mechanical, spectral, and luminescence properties of ZnS:Mn doped PDMS. *Journal of Luminescence*, *170*, 194–199. doi: 10.1016/j.jlumin.2015.10.047
- Rietema, K. (1991). *The Dynamics of Fine Powders*. Elsevier Applied Science.
- Aryal, M. (2018). Heat flux calculations of PDMS and silica aerogel through phosphor thermometry. [Master thesis, University of Memphis]

Jacob Parks is currently an undergraduate student double majoring in physics and mathematical sciences at the University of Memphis. After he completes his degree in spring 2021, he plans on going to law school to study patent law. One day, after law school, he hopes to start his own intellectual property law firm. In the summer of 2019, Jacob received a summer research fellowship from the Helen Hardin Honors College. He presented this paper at the Emerging Researchers National Conference in the spring of 2020 in Washington, D.C. When Jacob is not working on physics, he enjoys going to the gym, playing sports, and watching movies.

Jacob Parks

Mars Dust Adhesion: Characterizing Adhesion Behavior
of JSC Mars-1 Regolith on Aerogel Substrates

Faculty Sponsor

Dr. Firouzeh Sabri

Abstract

The adhesion of dust to critical spacecraft equipment poses a major challenge to planetary exploration. Regolith adhesion can cause issues that drastically reduce the length of missions and threaten the safety of astronauts. Regolith adhesion issues have been reported on both lunar and Mars missions, but Mars presents unique challenges due to triboelectrically charged dust suspended in its atmosphere. Mars regolith adhesion has not been studied extensively on aerogels, despite aerogel's rapidly growing number of space applications. The goal of this research was to understand the characteristics and mechanisms of regolith adhesion onto polyimide and polyurea aerogels under different surface charge conditions with Polydimethylsiloxane (PDMS) as a control. Results show that, in general, there is a strong correlation between higher magnitude surface charge and higher regolith accumulation and coverage.

Introduction

The adhesion characteristics of planetary regolith create a significant challenge for planetary exploration. Regolith adhesion, which is caused by Van der Waals and electrostatic forces, can cause major issues on spacecrafts [1]. These issues include reduced solar panel efficiency, damage to mechanical equipment, clogged air filters, and covered calibration targets [2]. These challenges have been reported on both Mars and lunar exploration missions [3]. However, Mars presents unique challenges because Mars' atmosphere contains suspended dust, which has been found to collect on spacecrafts at a rate of 0.28% per day [4]. Additionally, Mars experiences planet-wide dust storms which contribute to triboelectric charging of both Mars dust and spacecrafts, increasing adhesion [5].

One area of regolith adhesion research that is lacking is the characteristics of regolith adhesion onto various types of aerogels. Aerogels are a unique class of materials characterized by their extremely low density, porous structure, low thermal conductivity, and high specific surface area [6]. Because of these properties, aerogels are becoming an attractive material for use in space travel and planetary exploration. Aerogels have already been used in cryogenic fluid containment, thermal insulation on the Mars Rover, and high-velocity particle collection on NASA's *Stardust* [7]. Furthermore, new types of shape-memory aerogels could soon be used as self-deployable structures on spacecrafts [8]. Types of polyimide aerogels have also been considered for use as EDL systems, which will become more important as the size of Mars missions' payloads increase [9]. Thus, understanding dust adhesion to these materials can prevent problems when they are further implemented into planetary exploration. The goal of this research is to understand the mechanisms and causes of the adhesion of JSC Mars-1 simulant regolith onto polyurea-crosslinked and polyimide aerogels under various surface charge conditions, with PDMS as a control.

Experimental Procedures

Surface Potential Measurements

To understand the impact of electrostatic force on the surface of the materials being tested, surface potential measurements were taken using a Kelvin probe. The Kelvin probe used had a vibrating aperture which was 4.5 mm in diameter and was connected to a Trek Model 325 electrostatic voltmeter. Underneath the probe was a stage that allowed for manual x-y-z motion in increments of 1 mm. The probe was placed 1 mm above the sample as is recommended by the manufacturer to avoid fringe fields. Potential Mea-

measurements were taken by raster scanning in increments of 1 mm. From the potential readings, charge was calculated for each point using the equation.

$$Q = U \cdot \frac{\epsilon\epsilon_0 A}{d}$$

where Q is charge, U is potential, ϵ is the relative electric permittivity of air, ϵ_0 is the electric permittivity of vacuum, A is the area of the aperture, and d is the distance between the probe head and the sample.

Regolith Deposition Setup

Regolith deposition experiments were performed in an inverted set up under atmospheric conditions. Each sample was stored in a desiccator to control exposure to humidity prior to regolith deposition. The samples were sonicated in IPA to remove any dust particles on the surface of each sample. The baseline mass and surface charge of each sample was taken using an analytical balance and Kelvin probe, respectively. Samples were then put under one of three surface charge conditions: baseline, neutralized, or charged. These conditions were achieved by using static neutralizing and charging equipment on each sample. The samples in the neutralized condition were discharged using a Takk Ion-Edge model 400T static eliminator bar. The bar was in a fixed position and samples were placed at a distance of 0.5 cm from the bar, as suggested by the manufacturer. For the samples in the charged conditions, samples were first neutralized, then different amounts of charge were deposited onto their surfaces using a Takk 7081 charging bar. Again, the charging bar was fixed 0.5 cm above samples, as suggested by the manufacturer. After the surface charge conditions were placed on each sample, the samples underwent a controlled exposure to the regolith. Using tweezers, each sample was carefully lowered into a petri dish of JSC Mars-1 simulant regolith. The regolith had been treated in a vacuum oven at 105 °C for several days prior to the experiment to remove as much moisture from it as possible. The samples were removed from the regolith carefully so that only the top surface of each sample was exposed to the dust. The samples were shaken three times to remove any large, loose dust particles. The samples were then massed again and analyzed using optical microscopy.

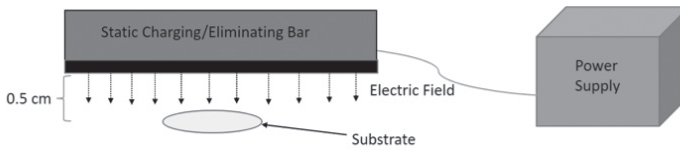


Figure 1. Experimental setup for charging/discharging

ImageJ

The regolith's area coverage on each sample was found from images obtained with a Unitron Examet-5 metallurgical microscope. Percent coverage was calculated through the software ImageJ, which uses thresholding to calculate area coverage. Thresholding is a technique which assigns number values to grayscale images. The software creates a cutoff: any pixel value below the cutoff becomes one category, and any pixel value above the cutoff becomes the other category. The user then must identify which pixel category represents the desired area coverage, and from that percentage the coverage on a substrate can be calculated. Coverage for each substrate was calculated as an average of threshold calculations from several individual images.

Results And Discussion

Surface Potential

Baseline surface potential measurements showed a wide range of potential on each substrate. The results of these measurements are shown in Figure 2. Both the polyurea aerogel and the JSC Mars-1 simulant regolith itself were found to have a weak positive surface potential, and, therefore, weak surface charge. Polyimide aerogels and PDMS both exhibited a high magnitude negative surface potential and charge.

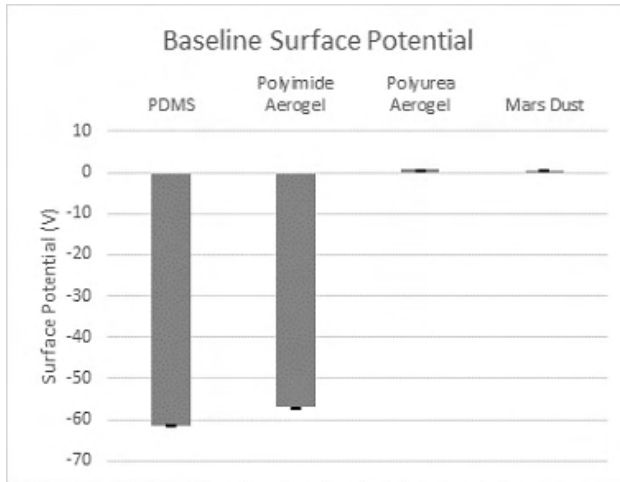
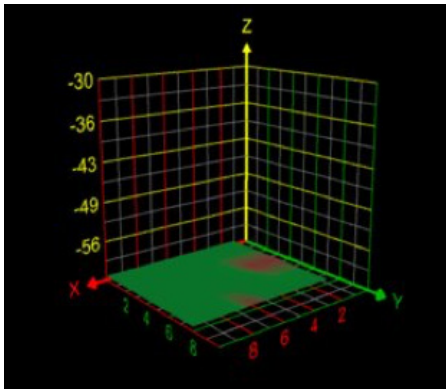
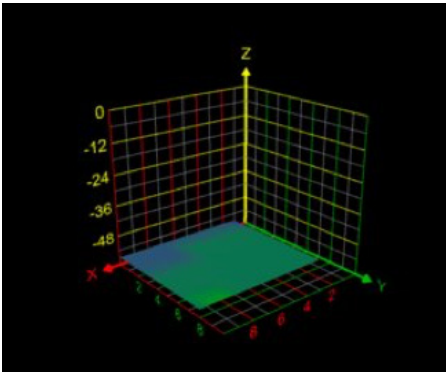


Figure 2. Average baseline surface potential for PDMS, polyimide aerogel, polyurea aerogel, and the Mars regolith.

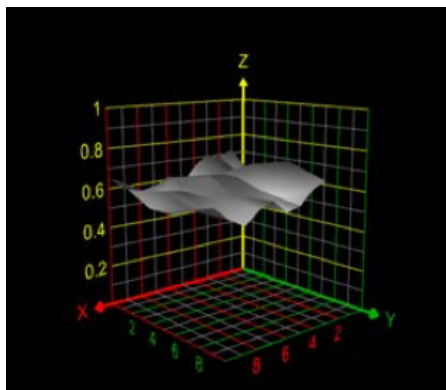
Furthermore, the PDMS and polyimide aerogels exhibited a more uniform potential distribution over the surface, shown in Figures 3a and 3b, respectively. The polyurea aerogel showed a more varied surface potential, with areas of higher and lower relative potential throughout the scanned area, as shown in Figure 3c.



(a)



(b)



(c)

Figure 3. Surface Potential Distribution for (a) PDMS (b) polyimide aerogel and (c) polyurea aerogel. The z-axis represents the surface potential in volts.

After electrostatic charging, the change in surface potential after neutralization was found for applied voltages from 1 to 10 kV. Each substrate exhibited similar properties when undergoing changes to surface charge. The samples experienced incrementally higher changes in surface potential with each step of applied voltage until a dielectric limit was reached, as shown in Figure 4. This dielectric limit occurred at 5 kV for PDMS, 6 kV for the polyimide aerogel, and 7kV for the polyurea aerogel. After this limit was reached, no more surface potential could be added to the surface, even with higher applied voltages.

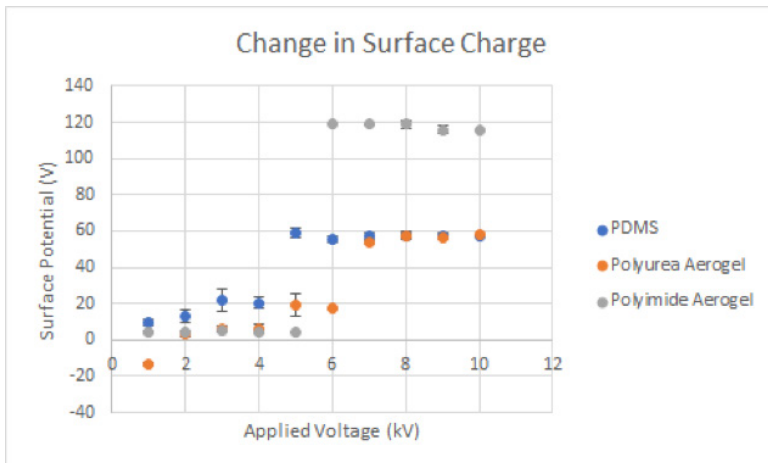


Figure 4. Change in surface charge for PDMS, Polyurea aerogels, and polyimide aerogels.

Gravimetric Analysis

After the dust was deposited onto each substrate using the inverted method, the masses were taken and compared to the baseline for each sample. The results of the gravimetric analysis of the samples at baseline surface charge are shown in Figure 5. At baseline surface charge, PDMS had the highest regolith accumulation, followed by the polyimide aerogel. The polyurea aerogel had the lowest accumulation (Fig. 5). This suggests that the higher the magnitude of surface charge, the higher the regolith accumulation. The regolith accumulation on the samples with 10, 15, and 20 kV of applied potential is also shown in Figure 5. For each sample, except for polyimide aerogel, the regolith accumulation was higher on the charged surfaces than the baseline samples. This is because applying voltage increases the surface potential, thus increasing accumulation.

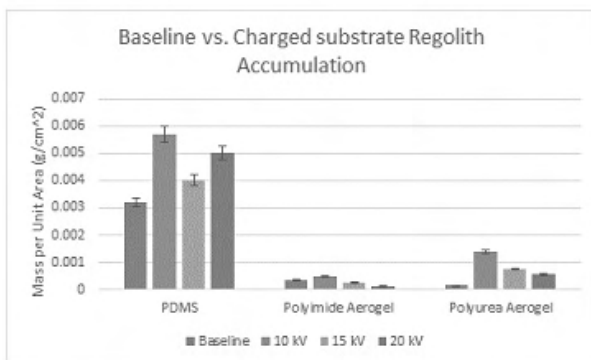


Figure 5. Regolith accumulation for each substrate at baseline, 10 kV, 15 kV, and 20 kV.

For each sample, the highest accumulation occurred at 10 kV. This is a direct result of the dielectric limit of each material being below 10 kV. For applied voltages higher than 10 kV, no additional surface potential was being added, so there was no additional regolith accumulation. The results shown in Figure 5 also suggest that the charge of the sample induces an opposite charge on the Mars regolith. Figure 2 shows that at baseline, Mars regolith has a weak positive surface potential. PDMS and polyimide aerogels at baseline have high negative surface potential, while polyurea aerogels have weak positive surface potential at baseline. PDMS and polyimide aerogels both exhibited a change in polarity with high applied voltages. This shows that the Mars regolith can take on both positive and negative charge, because there was adhesion to each substrate regardless of its surface charge polarity. The results of the gravimetric analysis of the neutralized samples are shown in Figure 6. For each neutralized sample, regolith accumulation was lower when compared to the baseline.

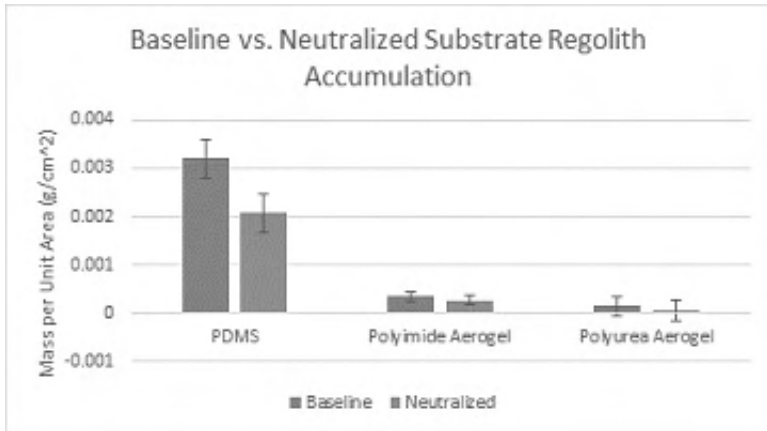


Figure 6. Regolith accumulation for each substrate at baseline and after neutralization.

These results again show that higher magnitude surface potential leads to higher regolith accumulation. This also confirms that other factors influence adhesion, because even with the low magnitude surface potential after neutralization, each substrate still accumulated regolith.

Optical Microscopy

The percentage of the substrate area covered by Mars regolith was calculated for each sample using ImageJ software. From this data, a clear relationship between higher surface charge and a higher concentration of dust adhering to the surface of each substrate can be seen. PDMS and polyimide aerogels exhibited the highest and most uniform coverage. The polyurea crosslinked aerogel, which had lower and less uniform charge, exhibited lower and less uniform coverage.

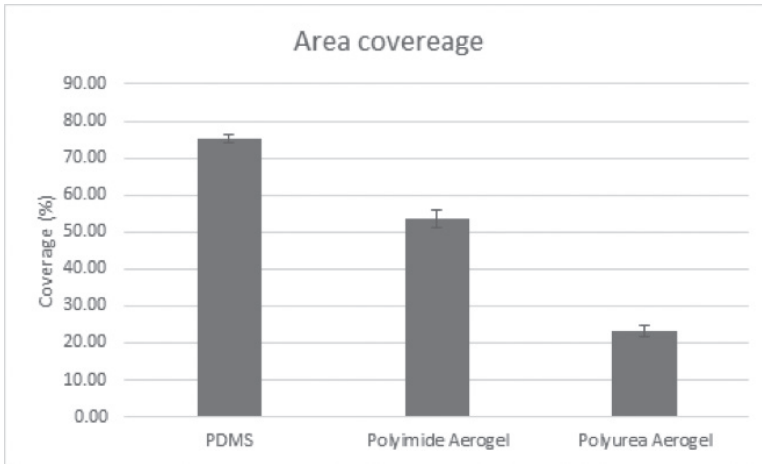


Figure 7. Areal coverage for each substrate at baseline surface potential.

The regolith coverage for the other surface potential conditions still needs to be explored. Another observation from optical microscope images was a towering effect which occurred on each substrate. The Mars regolith showed dust-dust adhesion as particles adhered to one another and stacked vertically on the substrate, as described by the schematic in Figure 8. Again, this shows evidence that the polarity of the Martian regolith can be influenced by the surface of the substrate as well as other regolith particles.

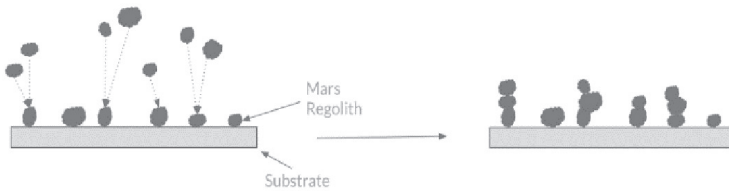


Figure 8. Schematic describing the towering effect

Conclusion

Adhesion characteristics of JSC Mars-1 simulant dust were explored through experimental methods. Experiments were performed on samples with a variety of surface charge conditions under atmospheric conditions in an inverted experimental setup. The effects of surface charge on adhesion behavior was very clear. Higher surface charge on PDMS and polyimide aerogels led to higher area coverage and more regolith adhesion by mass. Lower surface charge, consequently, led to lower coverage and regolith adhesion by mass. When voltage is applied onto the surface of a substrate, a dielectric limit is reached and surface potential no longer increases. This, in turn, keeps regolith adhesion from increasing infinitely as supplied voltage gets higher. Another characteristic of adhesion seen was the towering effect, which shows that there is dust-dust adhesion as well as adhesion between the dust and the substrate itself. This also shows that the samples and other regolith particles can change and induce charge in the Mars Regolith. Further exploration into the effects of low pressure, low humidity, different applied voltages, and temperature will need to be explored using the inverted experimental setup. Surface roughness measurements will also need to be taken before and after dust exposure to explore the relationship between adhesion behavior and surface roughness.

References

- [1] F. Sabri, T. Werhner, J. Hoskins, A. Schuerger, A. Hobbs, J. Barreto, D. Britt, and R. Duran, *Advances in Space Research* **41**, 118 (2008).
- [2] H. Perko, J. Nelson, and J. Green, *Proceedings of Engineering, Infrastructure, and Sciences*, 1 (2002).
- [3] T. Stubbs, R. Vondrak, and W. Farrell in: *Dust in Planetary Systems*, (NASA, Kauai, HI, 2005, pp. 239-243).
- [4] G. Landis and P. Jenkins, *Journal of Geophysical Research* **105**, 1855 (2000).
- [5] Z. Sternovsky, S. Robertson, A. Sickafoose, J. Colwell, and M. Horanyi, *Journal of Geophysical Research* **107**, 15 (2002).
- [6] A. Pierre and G. Pajonk, *Chem. Rev.* **102**, 4243 (2002).
- [7] S. Jones, *J Sol-Gel Sci Techn* **40**, 351 (2006).
- [8] W. Sokolowski and S. Tan, *Journal of Spacecraft and Rockets*, 1 (2007).
- [9] M. Meador, E. Malow, R. Silva, S. Wright, D. Quade, S. Vivod, H. Guo, J. Guo, and M. Cakmak, *ACS Appl. Mater. Interfaces*, **4(2)**, 536 (2012).

Jacob Seboly earned a B.S. in earth sciences and mathematics in Spring 2020. Jacob has been very involved in research at the Department of Earth Sciences, working under Dr. Esra Ozdenerol on public health and spatial analysis research related to topics including Lyme disease and COVID-19. He has also completed an honors thesis on tornado vulnerability in Tennessee and gave an award-winning presentation on his work at the 2019 MAGIC conference. Jacob also received the 2020 Sisco Outstanding Senior Award in Geography from the Department of Earth Sciences. After completing his bachelor's degree, Jacob plans to attend Mississippi State University to pursue a Master's degree in meteorology.

Jacob's paper received a *Quaesitum* best paper award.

Jacob Seboly

Assessing Tornado Vulnerability in Tennessee through
Tornado Incidence and Societal Exposure

Faculty Sponsor

Dr. Esra Ozdenerol

Abstract

Tornadoes are the deadliest type of natural disaster in Tennessee, and detailed analysis of tornado vulnerability in Tennessee is necessary to improve preparedness. This study defines tornado incidence as the likelihood of a particular location to experience tornadoes, and societal exposure as the ability of a particular community to cope with and recover from tornado disasters. Tornado incidence and societal exposure are combined to estimate overall tornado vulnerability across the state on a county-by-county basis. Tornado count data are used to assess tornado incidence. Regression analysis indicates that out of a selection of social vulnerability indices from previous literature, The Center for Disease Control and Prevention's SVI index best predicts tornado fatalities, so it is used to estimate societal exposure. The study found that tornado vulnerability generally decreases from southwest to northeast across the state with Hardeman, Haywood, Lake, and Lauderdale counties identified as most vulnerable.

Introduction

Tornadoes represent the deadliest category of natural disaster in Tennessee. From 1950 to 2017, tornadoes inflicted 347 deaths, 4,500 injuries, and \$1.8 billion in property damage in Tennessee (NCEI, 2019). These statistics indicate that there is much room for improvement for tornado preparedness in Tennessee. A detailed assessment of tornado vulnerability on a county-by-county basis across Tennessee will likely be a valuable tool for decision-makers who seek to improve preparedness in the state.

This study uses a conceptual model adapted from Dixon and Moore (2012) which defines tornado vulnerability as a function of climatological conditions (tornado incidence) and socioeconomic conditions (societal exposure). Tornado incidence represents the frequency and strength of tornadoes affecting a particular community. It will be calculated using data on the geographic location and Fujita Scale rating of historical tornadoes. Societal exposure represents the ability of a particular community to cope with and recover from natural disasters including tornadoes (Flanagan, Hallisey, Adams, & Lavery, 2018). It will be assessed through the calculation of various social vulnerability indices. These indices incorporate socioeconomic variables such as income, education, and demographics and calculate a single value which represents the social vulnerability of a given location. Two social vulnerability indices have been designed for use with natural disasters (Flanagan et al., 2018), (Cutter, Boruff, & Shirley, 2003), but their effectiveness in predicting tornado impacts specifically has not been assessed. This study will provide a basic assessment of these two indices and their effectiveness in predicting tornado fatalities with the more effective index chosen to estimate societal exposure for this study.

Previous tornado studies in Tennessee have been performed; however, those studies focused on tornado incidence only (Brown, Ellis, & Bleakney, 2016), (Ozdenerol, 2004). The authors agreed that tornadoes are generally most common on the western side of the Tennessee and least common on the eastern side. However, it is important to also ascertain where the highest societal exposure to tornadoes lies. This study will build upon the previous studies by combining both tornado incidence and societal exposure to form a more well-rounded picture of tornado vulnerability in Tennessee.

Literature Review

Tornado Incidence in Tennessee

While Tennessee is not part of the traditional “Tornado Alley”, it is, according to recent research, one of the most tornado-prone states in the nation.

Notably, western Tennessee has suffered the highest rate of tornado-related fatalities in the United States since 1880 (Ashley, 2007). This region, along with much of the Southeast, is often referred to as “Dixie Alley” and is known for fast-moving tornadoes, nocturnal tornadoes, and tornadoes with high fatality rates (Ashley, 2007). Spatial analysis using kernel density estimation indicates that the area of highest tornado risk in the United States is not limited to traditional Tornado Alley but rather “extends roughly from Oklahoma to Tennessee and northwestern Georgia” (Coleman & Dixon, 2014, p. 366). Since this corridor encompasses western and middle Tennessee, these areas can be characterized as highly tornado-prone. Dixon et al. (2011) also noted that “Tornado Alley” should be extended to incorporate the southeastern United States including Tennessee. Also noteworthy is that Tennessee’s tornado count in its peak years eclipses that of the Plains states (Brown et al., 2016).

Additionally, the observed effect of climate change on the spatial distribution of tornadoes indicates that tornado risk in Tennessee may increase in the future. The Southeast, including Tennessee, experienced an increase in tornadic activity between 1984-2013 compared with 1950-1983 (Agee et al., 2016). Regression analysis also indicated a statistically significant upward trend in Southeast tornado counts (Moore, 2018). STP (Significant Tornado Parameter) values in the Southeast also demonstrated a statistically significant increase since 1979 (Gensini & Brooks, 2018). In all three of these studies, Tennessee was included within the Southeast region suggesting that the frequency of tornadoes in Tennessee is increasing. Since Tennessee is already one of the most tornado-prone states in the nation in terms of tornado counts and fatality counts, and tornado risk is expected to increase in the future, it is possible that Tennessee will become an epicenter for tornadic activity later in the 21st century and beyond.

Societal Exposure in Tennessee

Disproportionately high tornado fatality rates in Tennessee suggest that the state suffers significant societal exposure to tornadoes. From 1880 to 2007, an area of southwestern Tennessee near Memphis suffered the highest tornado fatality rate in the nation (Ashley, 2007). Several explanations for this high fatality rate have been proposed including high frequencies of nocturnal tornadoes (Brown et al., 2016) and off-season tornadoes (Brooks, Doswell, & Kay, 2003), the prevalence of mobile homes (Sutter & Simmons, 2010), and a lack of awareness and preparedness among residents (Ellis et al., 2018). Nocturnal tornadoes pose a greater threat to human life because they are difficult to see and because they strike while most of the population is asleep and unable to receive tornado warnings (Ashley, Krmeneč, & Schwantes,

2008). Fall and winter tornadoes are more dangerous because daylight is shorter during these seasons leading to more nocturnal tornadoes (Ashley et al., 2008) and because residents are less likely to be mentally aware of tornado risk (Brown et al., 2016). The danger that tornadoes pose to mobile homes is well documented. An individual is 10 to 20 times more likely to die from the same tornado in a mobile home than in a permanent home (Brooks & Doswell, 2001), (Simmons & Sutter, 2006). These factors, which have combined to produce Tennessee's high fatality rate, exemplify the state's high societal exposure to tornadoes. Tennessee's increasing tornado incidence rate and significant societal exposure to tornadoes underscore the importance of assessing tornado vulnerability patterns and improving preparedness throughout the state.

Methodology

Study Area

Tornado vulnerability was assessed on a county-by-county basis throughout Tennessee. Additionally, in order to make this study more useful for National Weather Service (NWS) operations, the study area was expanded to include additional counties from neighboring states such that the entirety of the NWS Memphis, Nashville, Morristown, and Huntsville forecast areas are covered. This resulted in the addition of ten Alabama counties, eleven Arkansas counties, twenty-two Mississippi counties, two Missouri counties, two North Carolina counties, and seven Virginia counties.

Tornado Incidence Data and Analysis

Tornado path data representing all reported tornadoes between 1950 and 2017 were obtained from the Storm Prediction Center. These data were used to determine tornado counts and incidence. F0/EF0 and F1/EF1 tornadoes were excluded because of reporting bias in urban areas (Anderson, Wikle, Zhou, & Royle, 2007). Weighted tornado counts were calculated according to the following scheme: F2/EF2 = 2 points, F3/EF3 = 3 points, F4/EF4 = 4 points, F5/EF5 = 5 points. This weighting scheme is adapted from the Texas study (Dixon & Moore, 2012). The distribution of tornado reports at the county level was noisy. Since the sample size of tornado events is rather small (less than 40 tornadoes per county), county-level tornado counts are likely influenced more by chance than by underlying tornado risk. To eliminate this issue, tornado incidence for each county was estimated using the tornado count within 50 miles of the county's centroid. This process increased the sample size for each county, resulting in a much smoother spatial distribution of tornado incidence.

Tornado fatality, injury, and property damage data were obtained from the NCEI Storm Events Database. The SPC tornado database has data for each tornado, but it is not divided on a county-by-county basis. Thus, the NCEI data was necessary to determine fatality, injury, and property damage totals per county.

Societal Exposure Data and Analysis

Societal exposure was estimated in this study through social vulnerability indices. Calculating a social vulnerability index is a well-established method of identifying which counties are best prepared to cope with and recover from a potential natural disaster. Two social vulnerability indices are relevant for the purposes of this study: the SVI and the SoVI. The SVI was designed by the Centers for Disease Control and Prevention (CDC) (Flanagan et al., 2018). It utilizes fifteen socioeconomic variables: per capita income, poverty, unemployment, education level, population age 65 or older, population age 17 or younger, disabled population, single-parent households, minority population, non-English-speaking population, multi-unit structures, mobile homes, crowded households, households with no vehicle, and population in group quarters (Flanagan et al., 2018). SVI values are calculated by summing the national percentile values of each of the fifteen variables for each respective county. Thus, the lowest possible score is 0 and the highest possible score is 15. In practice, the lowest values are generally around 6 while the highest values are around 12. Higher values signify greater vulnerability to disasters (Flanagan et al., 2018). The SoVI was originally designed by Susan L. Cutter, Bryan J. Boruff, & W. Lynn Shirley in 2003, with further updates following. This study utilizes the SoVI 2010-14, which is calculated using 29 variables. An additive model is used to combine the variables and the result is normalized, producing a Z-score. Negative values represent lesser vulnerability to disasters while positive values represent greater vulnerability (Cutter et al., 2003). These two indices were then evaluated based on their effectiveness in predicting tornado fatalities.

The SVI and SoVI indices were compared using regression modeling to estimate which index exhibits stronger correlation with tornado fatalities. A general empirical validation for these indices, accounting for all natural disaster types, had been performed by Bakkensen, Fox-Lent, Read, and Linkov (2017). The dataset for this study included all natural disasters in the Southeastern U.S. from 2000-2012. The results indicated that the SVI is a statistically significant predictor of disaster-related property damage and fatalities while the SoVI is a statistically significant predictor of property damage but not fatalities. Based on these results, it was hypothesized that the SVI would perform better, since, in the Bakkensen et al. study, it exhibited

statistically significant correlation with fatality counts while the SoVI did not.

A dataset of fatal tornado events was compiled using data from the NCEI Storm Events Database. All tornadoes within the study area between 1950 and 2017 which caused at least one fatality were selected. The resulting dataset contained 204 fatal tornado events. The NCEI Database provides tornado data on an event-by-event basis. Therefore, if multiple fatal tornadoes occurred in the same county on the same day, a separate entry is provided for each tornado. The date, time, county, population density of the county in the closest census, fatality count, and Fujita Scale rating of each fatal tornado event were recorded. Population density was determined by rounding the tornado year to the nearest decade and using the appropriate census. For example, a 1954 tornado would be paired with 1950 Census data while a 1955 tornado would be paired with 1960 Census data. All other storm-related data were obtained from the Storm Events Database. The 2014 SVI and 2010-2014 SoVI values for the appropriate county were also included in each tornado's entry. These data were obtained at the county level from the authors' websites. To estimate population density, census data from 1950-2010 at the county level were obtained from the National Historical GIS.

For this study, the negative binomial regression model from Bakkensen et al. (2017) was adapted with slight modifications. Negative binomial regression is the appropriate model for this type of analysis because fatalities represent count data and because fatality data is overdispersed (the variance is greater than the mean) and extremely right skewed. Underlying risk rate was omitted because that variable was mainly useful for dealing with a wide range of disasters over a large study area. Tornado Fujita rating was added to the model because it is an extremely significant factor in determining a tornado's impact. Thus, the explanatory variables used in this study are population density, tornado strength, and social vulnerability, represented by the SVI and SoVI. Values for the SVI and SoVI were both normalized. These modifications were necessary because the Bakkensen model incorporated all disaster types while this study incorporates only tornadoes.

The model equation was designed as follows:

$$F_{i,j,t} = \beta_0 + B_1 I_i + B_2 \ln(P_{i,t}) + B_3 F_j + \mu_{i,j,t}$$

$F_{i,j,t}$ represents fatality count of tornado j in county i in year t . I_i represents social vulnerability in county i . The normalized SVI and SoVI were used in this term. $P_{i,t}$ represents population density in county i in year t ,

in population per square mile. F_j represents the Fujita Scale rating of tornado j . $\mu_{i,j,t}$ represents the error term.

The model was run twice; once with the SVI as an explanatory variable and once with the SoVI as an explanatory variable. The correlation between social vulnerability index values and fatalities was noted for each run. Since the indices were both normalized, their coefficients (β_1) could also be compared. Several additional sensitivity tests were also performed. The model was run with 2014 population density (at the census tract level) replacing historical population density. This insured that the model was not significantly affected by tornadoes which passed through dense population centers. Census tract population estimates for 2014 were acquired from the Centers for Disease Control and Prevention. Finally, the model was also run with casualty counts (fatalities + injuries) replacing fatality counts to see if the results could also be applied to casualty counts.

The results of the regression models with respect to the SVI and SoVI, with the addition of several sensitivity tests, are displayed in the following tables.

Variable	Coefficient	Std. Error	Z-Score	Significant (p<0.05)?
SVI	0.14081	0.06143	0.011	Yes
Fujita Rating	0.61778	0.05833	<0.001	Yes
Population	0.13788	0.07513	0.033	Yes

Table 1. SVI vs. Fatalities Regression Model Results

Variable	Coefficient	Std. Error	Z-Score	Significant (p<0.05)?
SoVI	0.08182	0.06122	0.091	No
Fujita Rating	0.60955	0.05958	<0.001	Yes
Population	0.11092	0.07582	0.071	No

Table 2. SoVI vs. Fatalities Regression Model Results

Variable	Significant (p<0.05)?	Significant (p<0.05)?	Significant (p<0.05)?
	Historical Population	2014 Population	Casualties
SVI	Yes	Yes	No
SoVI	No	No	No

Table 3. Sensitivity Tests

The SVI exhibited a statistically significant positive correlation with fatality counts, while the SoVI did not. The SVI's coefficient was also higher, meaning that a one-point increase in the SVI corresponded to more fatalities than a one-point increase in the SoVI. When 2014 tract-level population density was substituted for historical county-level population density, the results did not change. The SVI had a statistically significant positive correlation with fatality counts, while the SoVI did not. Neither index had a statistically significant correlation with casualty counts. Because only the SVI had a statistically significant correlation with tornado fatalities, it was chosen for use in the societal exposure and tornado vulnerability calculations.

Tornado Vulnerability Calculations

This study used the same three calculation methods as Dixon & Moore (2012) to incorporate both tornado incidence and societal exposure into an overall

tornado vulnerability index. The CDC's Social Vulnerability Index (SVI) was used as the input variable for societal exposure since it outperformed the SoVI in predicting tornado fatalities. For each county, the tornado count (weighted, see section 3.2 for calculation) within 50 miles will be used as the input variable for tornado incidence. Percentiles and Z-scores for tornado incidence and societal exposure were calculated for each county.

Method 1 was designed to most effectively convey the unique combination of societal exposure and tornado incidence that each county experiences. For Method 1, the two input variables (societal exposure, tornado incidence) were not combined but instead classified separately. Each variable was categorized for each county as low (Z-score less than -1.00), moderate ($-1.00 < Z < +1.00$), or high ($Z > +1.00$). Since Method 1 preserves the distinction between societal exposure and tornado incidence, it is a useful tool for assessing the specific details of each county's situation. While a county with high tornado incidence and low societal exposure might be classified similarly to a county with low tornado incidence and high societal exposure by Methods 2 and 3, Method 1 preserves a distinction between the two counties.

Method 2 was designed to provide a balanced view of the combined effects of tornado incidence and societal exposure. For Method 2, the Z-scores of tornado incidence and societal exposure were added for each respective county. Method 2 is somewhat susceptible to statistical outliers and tends to emphasize counties with high societal exposure even if tornado incidence is low or nonexistent (Dixon & Moore, 2012).

Method 3 was designed to highlight the counties with high scores in both tornado incidence and societal exposure and minimize the impact of statistical outliers. Method 3 scores were calculated by multiplying the percentile scores of tornado incidence and societal exposure, resulting in a value between 0 (lowest) and 1 (highest). For Method 3, most counties receive scores close to 0, while the few counties with high values in both variables score closer to 1.

Results

Counties were classified according to their z-score of tornado vulnerability according to the following scheme: very low ($z < -1.50$), low ($-1.50 < z < -0.50$), moderate ($-0.50 < z < +0.50$), high ($+0.50 < z < +1.50$), and very high ($z > +1.50$). According to the calculations from Method 1 (see Figure 4), the highest tornado incidence is concentrated in north Alabama. Arkansas, Mississippi, and western and middle Tennessee were classified as experiencing moderate tornado incidence. East Tennessee and the Appalachian region enjoy the lowest tornado incidence. The highest values of societal

exposure are concentrated within the Mississippi River Delta, but there are also high societal exposure values in a few scattered counties outside the Delta. Poinsett County, Arkansas and Franklin County, Alabama were the only counties classified as “high” in both variables. Knox, Blount, and Washington Counties, in Tennessee and Washington County, Virginia were classified as “low” in both variables.

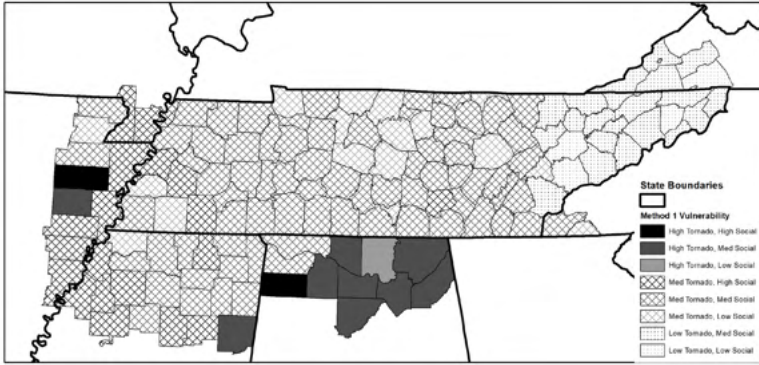


Figure 4. Method 1 Tornado Vulnerability

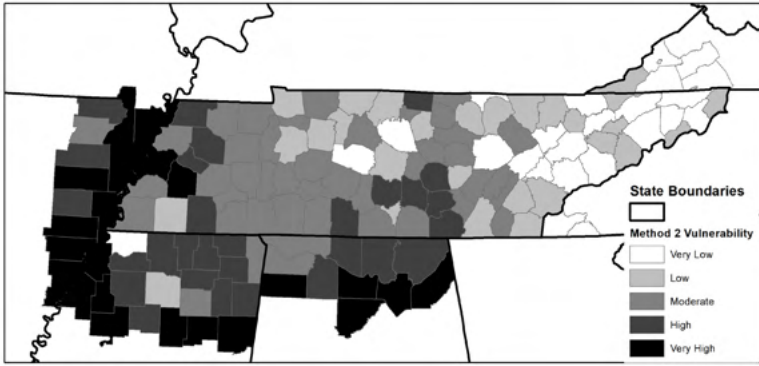


Figure 5. Method 2 Tornado Vulnerability

According to Method 2 (see Figure 5), the most tornado-vulnerable areas are along the southern and western periphery of the study area. Specifically, this area includes the Eastern Arkansas counties, the Mississippi Delta counties, and the counties in northern Mississippi and Alabama which comprise the southern edge of the study area. The Arkansas counties appear to be rated as vulnerable because of social factors, while the Mississippi and Alabama counties are rated as vulnerable because of their high tornado incidence. The county with the highest Method 2 vulnerability score is Marshall County, Alabama (+3.61). The least vulnerable area according to Method 2 is eastern Tennessee where tornadoes are comparatively rare. Societal exposure is also generally low in this area. The county with the lowest Method 2 vulnerability score is Williamson County, Tennessee (-3.47). Method 2 vulnerability scores for all counties in the study area are provided in Appendix A, Tables 4 and 5.

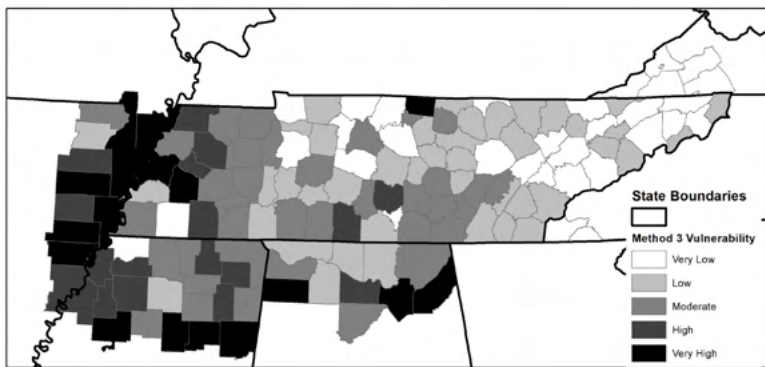


Figure 6. Method 3 Tornado Vulnerability

The southern and western periphery of the study area were also identified as the most tornado-vulnerable areas by Method 3 (Figure 6). However, Method 3 is designed to point out individual counties with high vulnerability in both variables rather than general areas. According to Method 3, the most vulnerable counties are Mississippi and Poinsett, AR; Dunklin, MO; Lake and Lauderdale, TN; Chickasaw, MS; and Franklin and Marshall, AL. Dunklin County, Missouri received the highest Method 3 vulnerability score (0.856). Williamson County, Tennessee and Russell County, Virginia tied for the lowest Method 3 vulnerability score (0.0).

DISCUSSION

SVI Comparison Implications

According to regression analysis on the two social vulnerability indices, the SVI was a more effective predictor of tornado fatalities in Tennessee than the SoVI. However, this result would not necessarily be applicable to other regions of the United States. Socioeconomic patterns and tornado seasonality patterns vary across the United States, so it is possible that the SoVI might outperform the SVI in other regions of the country. Further investigation is needed on this topic.

Fatalities and casualties were the only dependent variables modeled in this study. While the SVI predicted fatalities more effectively than the SoVI, there was no significant difference between the indices in predicting casualties. Therefore, no assumptions should be made about the correlation of the SVI and SoVI with other disaster impact variables such as property damage. Finally, the findings of this study should not be applied to vulnerability studies for other types of natural disasters. It is feasible that the SoVI would predict fatality counts for other types of disasters better than the SVI.

Possible Further Research

As mentioned in the literature review, the study of tornado vulnerability as a function of both tornado incidence and societal exposure is an undeveloped field of research. Currently, social vulnerability to tornadoes has only been assessed in Oklahoma, Texas, and Tennessee. Tornado vulnerability assessments which include socioeconomic variables need to be performed for the rest of the nation especially in the Great Plains, Midwest, and Southeast where tornado incidence is highest. The three methods used in this study and in Dixon & Moore (2012) to combine tornado incidence and societal exposure also must be tested, compared, and validated. Additional methods could also be proposed and validated.

This study included a basic assessment of the effectiveness of two social vulnerability indices, the SVI and SoVI, in predicting tornado fatalities. More widespread assessments of these indices are needed. It also remains unclear which index better predicts casualties and property damage. Further development of place-based weighted indices of social vulnerability would prove useful in this field as well.

Conclusion

This study assessed tornado vulnerability as a function of tornado incidence and societal exposure over an area including all of Tennessee and a selection

of counties from neighboring states. This area was designed to include all counties under the responsibility of the Memphis, Nashville, Huntsville, and Morristown offices of the National Weather Service.

The highest tornado incidence in the study area is concentrated in northern Alabama. Northern Mississippi, eastern Arkansas, and western Tennessee suffer moderate to high tornado incidence. Eastern Tennessee and southwestern Virginia have the lowest tornado incidence. Societal exposure is distributed more widely throughout the area, but notable regions included the Mississippi River Delta and isolated counties in Alabama, Mississippi, and Tennessee. The most tornado-vulnerable areas were identified to be northern Alabama, northern Mississippi, eastern Arkansas, and western Tennessee. The least vulnerable areas are eastern Tennessee and southwestern Virginia. Similar tornado vulnerability assessments are still needed across many areas of the United States.

Two social vulnerability indices, the SVI and SoVI, were compared for their effectiveness in predicting tornado fatalities within the study area. A negative binomial regression model was prepared with fatalities as the independent variable and population, social vulnerability, and tornado magnitude as the dependent variables. The SVI exhibited a statistically significant correlation with tornado fatalities while the SoVI did not. Further research on the appropriate use of social vulnerability indices in assessing tornado vulnerability is needed.

References

- Agee, E., Larson, J., Childs, S., & Marmo, A. (2016). Spatial Redistribution of U.S. Tornado Activity between 1954 and 2013. *Journal of Applied Meteorology & Climatology*, 55(8), 1681–1697. <https://doi.org/10.1175/JAMC-D-15-0342.1>
- Anderson, C. J., Wikle, C. K., Zhou, Q., & Royle, J. A. (2007). Population Influences on Tornado Reports in the United States. *Weather and Forecasting*, 22(3), 571–579. <https://doi.org/10.1175/WAF997.1>
- Ashley, W. S. (2007). Spatial and Temporal Analysis of Tornado Fatalities in the United States: 1880–2005. *Weather and Forecasting*, 22(6), 1214–1228. <https://doi.org/10.1175/2007WAF2007004.1>
- Ashley, W. S., Krmenc, A. J., & Schwantes, R. (2008). Vulnerability due to Nocturnal Tornadoes. *Weather and Forecasting*, 23(5), 795–807. <https://doi.org/10.1175/2008WAF2222132.1>
- Bakkensen, L. A., Fox-Lent, C., Read, L. K., & Linkov, I. (2017). Validating Resilience and Vulnerability Indices in the Context of Natural Disasters. *Risk Analysis*, 37(5), 982–1004. <https://doi.org/10.1111/risa.12677>
- Brooks, H. E., Doswell, C. A., & Kay, M. P. (2003). Climatological Estimates of Local Daily Tornado Probability for the United States. *Weather & Forecasting*, 18(4), 626–640. [https://doi.org/10.1175/1520-0434\(2003\)018<0626:CEOLDT>2.0.CO;2](https://doi.org/10.1175/1520-0434(2003)018<0626:CEOLDT>2.0.CO;2)
- Brooks, H. E., & Doswell III, C. A. (2001). Normalized Damage from Major Tornadoes in the United States: 1890–1999. *Weather & Forecasting*, 16(1), 168. [https://doi.org/10.1175/1520-0434\(2001\)016<0168:NDFMTI>2.0.CO;2](https://doi.org/10.1175/1520-0434(2001)016<0168:NDFMTI>2.0.CO;2)
- Brown, V. M., Ellis, K. N., & Bleakney, S. A. (2016). Tennessee Tornado Climate. *Southeastern Geographer*, 56(1), 118–133. <https://doi.org/10.1353/sgo.2016.0008>
- Coleman, T. A., & Dixon, P. G. (2014). An Objective Analysis of Tornado Risk in the United States. *Weather & Forecasting*, 29(2), 366–376. <https://doi.org/10.1175/WAF-D-13-00057.1>
- Cutter, S. L., Boruff, B. J., & Shirley, W. L. (2003). Social Vulnerability to Environmental Hazards. *Social Science Quarterly*, 84(2), 242.

- Dixon, D. P., Mercer, A. E., Choi, J., & Allen, J. S. (2011). TORNADO RISK ANALYSIS: Is Dixie Alley an Extension of Tornado Alley? *Bulletin of the American Meteorological Society*, 92(4), 433.
- Dixon, R. W., & Moore, T. W. (2012). Tornado Vulnerability in Texas. *Weather, Climate, and Society*, 4(1), 59–68. <https://doi.org/10.1175/WCAS-D-11-00004.1>
- Ellis, K. N., Mason, L. R., Gassert, K. N., Elsner, J. B., & Fricker, T. (2018). Public perception of climatological tornado risk in Tennessee, USA. *International Journal Of Biometeorology*, 62(9), 1557–1566. <https://doi.org/10.1007/s00484-018-1547-x>
- Flanagan, B. E., Hallisey, E. J., Adams, E., & Lavery, A. (2018). Measuring Community Vulnerability to Natural and Anthropogenic Hazards: The Centers for Disease Control and Prevention's Social Vulnerability Index. *Journal of Environmental Health*, (10), 34.
- Gensini, V. A., & Brooks, H. E. (2018). Spatial trends in United States tornado frequency. *Npj Climate and Atmospheric Science*, (1), 1. <https://doi.org/10.1038/s41612-018-0048-2>
- Hout, E. M., Yuan, M., McIntosh, J., & Weaver, C. (2010). *Spatial Analysis of Tornado Vulnerability Trends in Oklahoma and Northern Texas*. Presented at the 25th Conference on Severe and Local Storms, Denver, CO.
- Moore, T. W. (2018). Annual and seasonal tornado trends in the contiguous United States and its regions. *International Journal of Climatology*, (3), 1582. <https://doi.org/10.1002/joc.5285>
- National Centers for Environmental Information. (2019, May). NCEI Storm Events Database. NCEI Storm Events Database. <https://www.ncdc.noaa.gov/stormevents/>
- Ozdenerol, E. (2004). *Tornado Hazards in Tennessee: Understanding Vulnerability to Tornadoes in Tennessee*.
- Simmons, K. M., & Sutter, D. (2006). Direct Estimation of the Cost Effectiveness of Tornado Shelters. *Risk Analysis: An International Journal*, 26(4), 945–954. <https://doi.org/10.1111/j.1539-6924.2006.00790.x>
- Sutter, D., & Simmons, K. M. (2010). Tornado fatalities and mobile homes in the United States. *Natural Hazards*, (1), 125. <https://doi.org/10.1007/s11069-009-9416-x>

Jeremy Walker graduated in spring 2020 from Weber State University. He earned his degree *magna cum laude* with departmental honors in physics. In the summer of 2019, he conducted research at the University of Memphis in the Research Experience for Undergraduates program funded by the National Science Foundation. Jeremy has done two research projects in computational physics and presented one project at the American Physical Society's Four Corners meeting in 2018. He has been accepted to a master's program in applied physics at the University of Oregon.

Jeremy Walker

A Molecular Dynamics Study of Lipid Membranes
Cushioned by Polymer Brushes

Faculty Sponsor

Dr. Mohammed Lardji

Abstract

We present a numerical study of self-assembled lipid membranes, that are cushioned by polymer brushes, using molecular dynamics simulations of a coarse-grained implicit solvent model.

Introduction

Lipid bilayers are a crucial component of life. When a group of lipids is exposed to water, the hydrophobic groups turn toward each other while the hydrophilic groups turn toward the water. These bilayers make up the ever-important lipid membrane of cells. The lipid membrane acts as a barrier between the inner and outer parts of the cell, provides structural integrity for the cell, and supports numerous large transmembrane proteins needed for proper cellular function. Without lipid membranes, cells would spill out of their bounds and not even simple single celled organisms could survive.

Prior studies have employed a variety of techniques to study the function, structure, and dynamics of lipid bilayers. At the most basic level, substrate supported studies can be done (McCabe, 2013; Andersson, 2016; Deverall, 2005). In these experiments, the membrane is placed directly on a substrate with a water layer cushion that is a few nanometers thick. This limits the motion of the membrane in the direction perpendicular to the substrate and is an especially poor way to study transmembrane proteins because they are too large and often denature with excessive contact with the substrate due to their protrusion below the bilayer (McCabe, 2013). To overcome these obstacles, an additional layer of polymer can be added below the membrane to act as a cushion. This polymer supported model allows transmembrane proteins to sink into the polymer and as such, they are less likely to denature. One type of polymer support is a polymer brush, which is formed by chemically tethering polymer chains to a substrate and introducing a membrane on the free ends. In this computational study, we will simulate a polymer brush support because it mimics the cytoskeleton of the cell and as such, is a better model to study biological processes. We aim to study the mutual effects of the membrane and the polymer brush interactions and to increase the theoretical understanding of this model for use in future experiments.

Model And Computational Method

A coarse-grained implicit-solvent model was used (Revalee, 2008; Laraji, 2016), in which a lipid molecule is coarse-grained into a semi-flexible chain composed of one head (h) bead and two tail (t) beads. The potential energy of the lipid bilayer has three contributions:

$$U(\{r_i\}) = \sum_{(i,j)} U_0^{\alpha,\alpha_j}(r_{ij}) + \sum_{(i,j)} U_{\text{bond}}(r_{ij}) + \sum_{(i,j,k)} U_{\text{bend}}(\vec{r}_i, \vec{r}_j, \vec{r}_k), \quad (1)$$

where \vec{r}_i describes the coordinates of bead i , $r_{ij} = |\vec{r}_i - \vec{r}_j|$, and $\alpha_i (= h \text{ or } t)$ is the type of bead i . In Eq. (1), $U_0^{\alpha\beta}$ is a soft two-body potential, between beads of types α and β and separated by a distance r , and is a piece-wise function given by (Laradji, 2016),

$$U_0^{\alpha\beta}(r) = \begin{cases} (U_{\text{max}}^{\alpha\beta} - U_{\text{min}}^{\alpha\beta}) \frac{(r_m - r)^2}{r_m^2} + U_{\text{min}}^{\alpha\beta} & \text{if } r \leq r_m \\ -2U_{\text{min}}^{\alpha\beta} \frac{(r_c - r)^3}{(r_c - r_m)^3} + 3U_{\text{min}}^{\alpha\beta} \frac{(r_c - r)^2}{(r_c - r_m)^3} & \text{if } r_c < r < r_m \\ 0 & \text{if } r > r_c, \end{cases} \quad (2)$$

where $U_{\text{max}}^{\alpha\beta} > 0$ and $U_{\text{min}}^{\alpha\beta} \leq 0$ for any pair (α, β) . $U_{\text{min}}^{\alpha\beta} = 0$ implies a fully repulsive interaction between beads α and β , and $U_{\text{min}}^{\alpha\beta} < 0$ implies a short-range attraction between the two beads. The self-assembly of the lipids into thermodynamically stable bilayers is ensured by choosing $U_{\text{min}}^{hh} = U_{\text{min}}^{ht} = 0$ and a sufficiently negative value of U_{min}^{tt} (Laradji, 2016).

In Eq. (1), U_{bond} ensures connectivity between beads that belong to the same lipid chain and is given by

$$U_{\text{bond}}(r) = \frac{k_{\text{bond}}}{2} (r - a_b)^2, \quad (3)$$

where k_{bond} is the bond stiffness coefficient and a_b is the preferred bond length. Finally, U_{bend} in Eq. (1) is a three-body potential that provides bending stiffness to the lipid chains and is given by

$$U_{\text{bend}}(\vec{r}_{i-1}, \vec{r}_i, \vec{r}_{i+1}) = \frac{k_{\text{bend}}}{2} \left(\cos\varphi_0 - \frac{\vec{r}_{i,i-1} \cdot \vec{r}_{i,i+1}}{r_{i,i-1} r_{i,i+1}} \right)^2 \quad (4)$$

where k_{bend} is the bending stiffness coefficient and φ_0 is the preferred splay angle of the lipid chain, taken to be 180° .

All beads are moved using a molecular dynamics scheme with a Langevin thermostat (Grest, 1986),

$$\dot{\vec{r}}_i(t) = \vec{v}_i(t) \quad (5)$$

$$m_i \dot{\vec{v}}_i(t) = -\nabla_i U(\{\vec{r}_i\}) - \Gamma \vec{v}_i(t) + \sigma \vec{\Xi}_i(t), \quad (6)$$

where m_i is the mass of bead i and Γ is a bead's friction coefficient. $\sigma \vec{\Xi}_i(t)$ is a random force with zero mean, and is uncorrelated for different particles, different times, and different components. Γ and σ are inter-related through the fluctuation-dissipation theorem leading to $\Gamma = \sigma^2 = 2k_B T$.

The simulations are performed in the NVT ensemble, where N is the total number of beads in the system. The model interaction parameters are given by,

$$\begin{aligned} U_{\max}^{hh} &= U_{\max}^{ht} = 100\epsilon, \\ U_{\max}^{tt} &= 200\epsilon, \\ U_{\min}^{hh} &= U_{\min}^{ht} = 0, \\ U_{\min}^{tt} &= -6\epsilon, \\ U_{\max}^{mm} &= xyz, \\ U_{\min}^{mm} &= 0, \\ U_{\max}^{mh} &= 1210\epsilon/r_m^2, \\ U_{\min}^{mt} &= 0, \\ U_{\min}^{mh} &= -\mathcal{E}, \\ k_{\text{bond}} &= 100\epsilon/r_m^2, \\ k_{\text{bend}} &= 100\epsilon, \\ r_c &= 2r_m, \\ a_b &= 0.7r_m. \end{aligned} \quad (7)$$

In Eq. (7), \mathcal{E} is the adhesion energy of a lipid head group per unit of area of the NP, and is henceforth used to define the *adhesion strength*.

All simulations are performed at $k_B T = 3.0\epsilon$, with a time step $\Delta t = 0.02\tau$, where $\tau = r_m(m/\epsilon)^{1/2}$. Eqs. (5) and (6) are integrated using the velocity-Verlet algorithm.

The bending modulus of the bare bilayer, with the interaction parameters given by Eq. (7), as extracted from the spectrum of the LM height fluctuations, is $\kappa \approx 30k_B T$ (Laradji, 2016), which is comparable to that of DPPC in the fluid phase (Nagle, 2015). The length scale, r_m , is estimated from comparing the value of the thickness of the LM $\sim 5r_m$, typical to phospholipid bilayer. We therefore estimate $r_m \approx 1$ nm. Hence, in the remainder of this article, all lengths are expressed in nanometers, and the adhesion strength, \mathcal{E} , is expressed in $k_B T / \text{nm}^2$.

Results

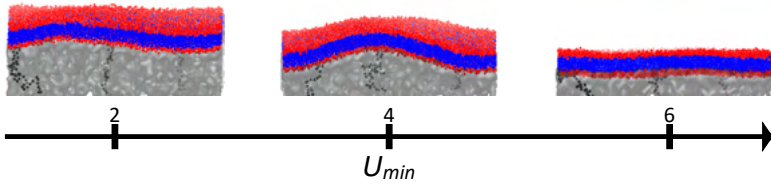


Figure 1. Typical configurations of the membrane for increasing \mathcal{E} . This system has a chain length $N = 50$, and a polymer brush grafting density $\sigma = 0.1$. Clearly, as \mathcal{E} is increased, the average height of both the membrane and the polymer brush decrease. Note that between $\mathcal{E} = 2$ and $\mathcal{E} = 4$, the membrane fluctuations increased. The opposite occurred for \mathcal{E} values past 4. Individual polymer chains have been highlighted to show how a typical chain behaves in the brush.

As shown in Fig. 1, the average height of the membrane and polymer brush decreases with increasing \mathcal{E} . Because of this compression, the density of the polymer layer is expected to increase. When a density profile is taken along the z -axis, the density of the polymer brush does indeed increase. However, this increase is largely localized near the membrane while the lower levels of the brush remain unchanged, as shown in Fig. 2. From this we conclude that a relatively highly dense layer of monomers forms directly under the bilayer. The increase in \mathcal{E} favors an increase in the amount of contact between the lipid head groups and the monomers, which can only be achieved by

having the membrane move closer to the substrate.

Density Profile Along z-axis For A Polymer Brush Supported Lipid Bilayer

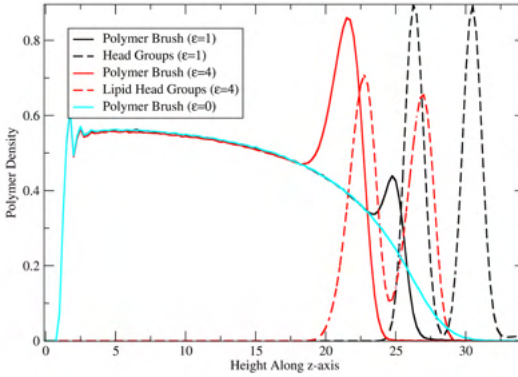


Figure 2. The density of the polymer brush is changed in the presence of a membrane. $\epsilon = 0$ corresponds to a polymer brush that does not interact attractively with a membrane. With attraction to the lipid heads in the membrane, the polymer brush density increases near the lipid heads. However, the density of the lower levels is relatively unchanged. Additionally, the shortening and widening of the peaks associated with the lipid head groups when $\epsilon = 4$ again imply the fluctuations of the membrane have increased as seen in Fig. 1. This data was collected from a system with $N = 50$ and $\sigma = 0.25$

Next, the bilayer's structure can first be characterized by the width of its fluctuations, $w = \sqrt{h^2 - \langle \bar{h} \rangle^2}$ where we define h as the height (z -coordinate) of a lipid head group in the top leaflet of the membrane. Fig. 3 and 4 demonstrate changes in the structure of the membrane caused by varying the grafting density or length of the polymer chains. There are three main features in Figs. 3 and 4. Namely, for very low ϵ , the membrane is not absorbed; followed by an abrupt decay in w at the absorption transition. For intermediate values of ϵ , there is an increase in the width, w . It then reaches a peak and then decreases for even higher ϵ . Because we expected a monotonic decrease in the fluctuations in the membrane, the intermediate increase of w vs. ϵ is puzzling and needs further investigation. In contrast, the decrease of w vs. ϵ for high ϵ is expected. The non-monotonous behavior of w vs. ϵ should be the result of some structural difference of the top layer of the polymer brush (vicinal to the bilayer).

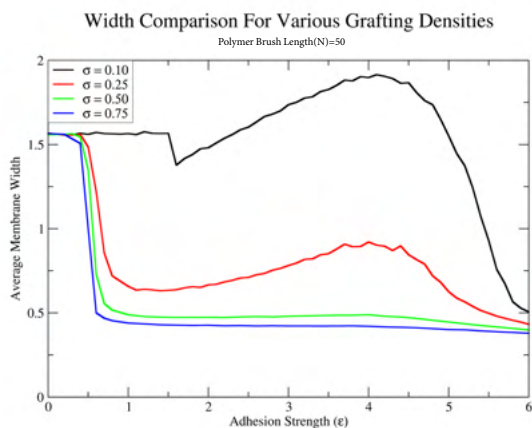


Figure 3. There is a systematic relationship between the width of w and the grafting density of the polymer brush, σ . For increasing σ , the membrane becomes more rigid and the membrane absorbs earlier for more dense systems. Surprisingly, for low density systems, the bilayer has more fluctuations than a free membrane. The non-monotonic behavior becomes less pronounced as σ is increased. This data was collected with $N = 50$.

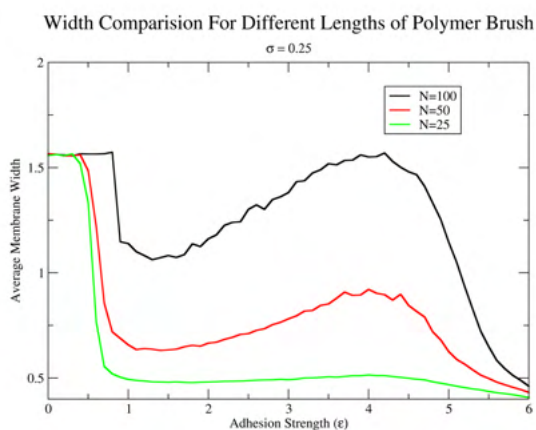


Figure 4. There is a systematic relationship between w and the number of monomers per polymer chain, N . For decreasing N , the membrane becomes more rigid and the membrane absorbs earlier for shorter systems.

The structure factor of a free membrane is given by,

$$S(q) = \frac{k_B T}{\gamma q^2 + \kappa q^4 + \dots} \quad (8)$$

where γ is the tension coefficient and κ is the bending modulus of the membrane. We can use this structure factor to further investigate how the membrane changes when absorbed onto a polymer brush. Transforming the structure factor to $1/q^2 S(q)$ vs. q^2 allows us to see the contributions of each term in the denominator. Figure 5 shows that for small wavevectors, $1/q^2 S(q)$ actually intercepts the y -axis at a finite value, which increases with increasing \mathcal{E} . This is expected as the absorption of the bilayer on the polymer brush leads to an energy cost resulting from vertical translation of the bilayer.

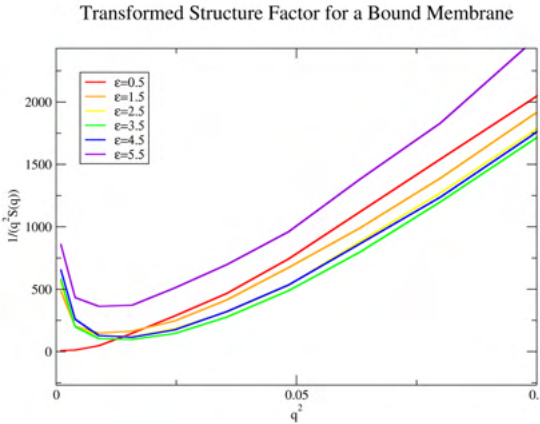


Figure 5. A plot of $1/q^2 S(q)$ vs. q^2 transformed from Eq.(8) Note that for an unbound membrane ($\mathcal{E} = 0.5$) the plot converges to zero as expected in the case of a tensionless membrane. However, when the bilayer is adsorbed on the brush, $1/q^2 S(q)$ increases rapidly as $q \rightarrow 0$. This indicates that due to binding, the bilayer has a preferred position along the z -axis, leading to the emergence of a mass term in the effective Hamiltonian of the bilayer. Interestingly, for small q (long wavelengths), $1/q^2 S(q)$ has a non-monotonic behavior, namely it decreases with increasing \mathcal{E} , then increases. This behavior mirrors that of w shown above.

Perpendicular Radius of Gyration For Various Grafting Densities

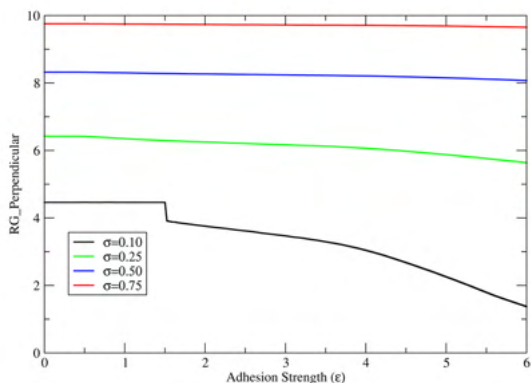


Figure 6. R_{\perp} monotonously decreases with increasing ϵ . This is expected since the monomers which are within the adhesion sublayer below the bilayer only weakly contribute to R_{\perp} , and the bilayer gets closer to the substrate as ϵ increases (hence R_{\perp} decreases with increasing ϵ). This is to say that the behavior of R_{\perp} is not surprising and not that interesting (in the sense that it does not help in understanding the non-monotonic behavior of w vs. ϵ).

Parallel Radius of Gyration for Various Grafting Densities

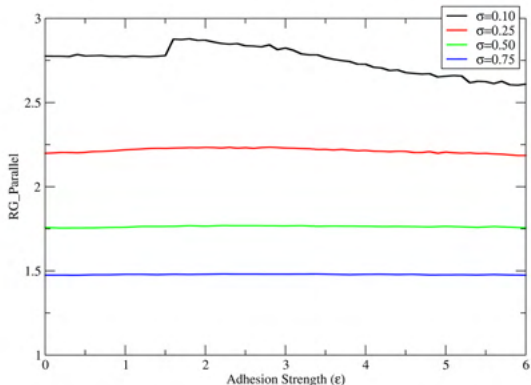


Figure 7. The radius of gyration acquired by summing the radius of gyration along both the x and y axes in quadrature. While the effect is small, there is a non-monotonic trend here that peaks around $\epsilon = 2$. This is due to the binding of the top monomers to the membrane.

In order to understand the non-monotonic behavior of w vs. \mathcal{E} , we observed the radius of gyration along the z -axis (R_{\perp}) and the xy -plane (R_{\parallel}) to provide more information about the structure of the polymer brush. As shown in Fig. 6, R_{\perp} was not useful in analyzing the non-monotonic behavior of interest. In contrast, Fig. 7 shows that R_{\parallel} has a more interesting non-monotonic behavior, though the change is very weak.

Next, we can look at the contact energy, E_{contact} that results from the interaction of monomers with lipid head groups. From Fig. 2, it is expected that E_{contact} will not depend on the length of the polymer chains, N .

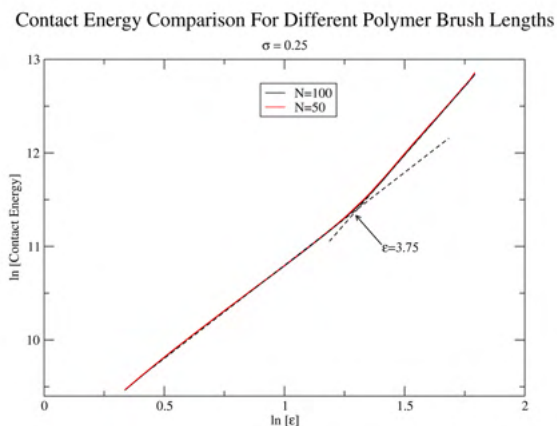


Figure 8. A ln-ln plot of the contact energy between the monomers in the polymer chain and the lipid head groups on the underside of the membrane. $N = 25$ and $N = 50$ chain lengths were used. The contact energy plots lay over top one another, showing that the lower levels of the polymer brush do not participate in the interaction with the membrane. E_{contact} steadily increases with \mathcal{E} . However, this increase becomes more pronounced for \mathcal{E} larger than 3.75. This corresponds closely to the peak seen in Figs. 3 and 4.

Figure 8 implies that the non-monotonic behavior of the fluctuations of the membrane is the result of different structural modes of the polymer brush. For low values of the interaction strength between the polymer monomers and the bilayer, the free energy of the system is dominated by the conformational entropy of the portion of the polymer in the vicinity of the bilayer rather than by interactions. The reverse occurs for high values of \mathcal{E} . The polymers conformational entropy is higher for low grafting densities than large ones. Hence, the effect above is expected to be stronger for low

values of σ . The non-monotonic behavior of w is indeed more pronounced for low values of σ , as shown in Fig 3.

Conclusions

Overall findings show clear mutual interactions between the lipid membrane and polymer brush. These effects vary with adhesion strength.

For intermediate adhesion strength ($\mathcal{E} \lesssim 4$), membrane fluctuations increase with adhesion strength. This trend is dominated by the polymer's conformational entropy. This effect is increased with increasing polymer length or decreasing grafting density.

For large adhesion strength ($\mathcal{E} \gtrsim 4$), the membrane fluctuations decrease with increasing adhesion strength. In this region the trend is dominated by the adhesion interaction between the membrane and the polymers.

The fluctuations of the membrane are reduced by either increasing the grafting density or decreasing the length of the polymer brush.

The greatest change in the polymer brush occurs near the membrane. The polymer brush becomes denser directly beneath the membrane as more monomers bind to it. This is evident in the peak occurring in the density profile near the membrane, the small change in the parallel radius of gyration, and the contact energy's independence of brush length. When supported by a polymer brush, the properties of lipid membranes change observably

Because of the clear changes in both the properties of the polymer brush and the lipid membrane, a slightly different model may be presented in the future to help preserve the properties of the lipid membrane in the presence of the brush. All the data here is presented with the assumption that the membrane was tensionless before its adhesion on the membrane. If this assumption is found to be false, the new model will need to change, so the membrane is tensionless in the beginning.

The theoretical understanding acquired from this study is meant to be a launching pad for future experimental work. Using the computational model described here, researchers can learn how their membranes will change if they use a polymer brush support without spending money and time producing the actual polymer brush. If the theoretical results match the desired conditions, an experiment can be conducted with more confidence.

References

- Andersson, J., & Köper, I. (2016). Tethered and Polymer Supported Bilayer Lipid Membranes: Structure and Function. *Membranes*, 6(2), 30. doi: 10.3390/membranes6020030
- Deverall, M., Gindl, E., Sinner, E.-K., Besir, H., Ruehe, J., Saxton, M., & Naumann, C. (2005). Membrane Lateral Mobility Obstructed by Polymer-Tethered Lipids Studied at the Single Molecule Level. *Biophysical Journal*, 88(3), 1875–1886. doi: 10.1529/biophysj.104.050559
- Grest, G. S., & Kremer, K. (1986). Molecular dynamics simulation for polymers in the presence of a heat bath. *Physical Review A*, 33(5), 3628–3631. doi: 10.1103/physreva.33.3628
- Laradji, M., & Kumar, P. B. S. (2016). Preface for the special issue “Biomembranes.” *International Journal of Advances in Engineering Sciences and Applied Mathematics*, 8(2), 87–87. doi: 10.1007/s12572-016-0167-0
- Mccabe, I. P., & Forstner, M. B. (2013). Polymer Supported Lipid Bilayers. *Open Journal of Biophysics*, 03(01), 59–69. doi: 10.4236/ojbiphy.2013.31a008
- Revalee, J. D., Laradji, M., & Kumar, P. B. S. (2008). Implicit-solvent mesoscale model based on soft-core potentials for self-assembled lipid membranes. *The Journal of Chemical Physics*, 128(3), 035102. doi: 10.1063/1.2825300

Aeona G. Seymour graduated *magna cum laude* from the University of Memphis in August of 2019 with a B.A. in political science and a minor in international relations. Before her senior year she chose to write this thesis on her targeted political science subfield: political psychology/behavior. Some of Aeona's interests include understanding why and how people vote, what shapes political & social identity, and how these identities in turn shape the world in which we live. Aeona's research conducted in the following paper won a second place award at the Student Research Forum at the University of Memphis and was accepted for presentation at the Midwest Political Science Association Conference. After spending some time in graduate school, Aeona now works at a law firm which specializes in subrogation and spends her free time practicing music.

Aeona Seymour

Who Do You Belong To?: Social Sorting Between
Gender and Partisan Identity Groups

Faculty Sponsor

Dr. Eric Groenendyk

Abstract

Individuals participate in social sorting when they align their various social identities with their partisan identity. While there exists significant research on the social sorting phenomenon, there is not much causal insight on the matter as it pertains to the American electorate. Where previous research correlates socio-economic status, geographical location, and generational replacement with social sorting, findings from this study indicate that social identity pressure to align gender and partisan identity in a 'correct' way causes weak partisans to participate in this phenomenon. Detecting social pressure as a cause of this phenomenon helps explain why social sorting occurs and raises questions about platforms which exert these pressures. This finding also highlights the role of perceptions in partisan identification, which suggests subjective factors, rather than logical and policy-based positions, play a significant role in the formation of partisan identity. Overall, this study enhances understandings of American political behavior.

Introduction

There exists a growing body of literature on the effects that social identification processes have on social groups within the American electorate. Tajfel and Turner's (1979) development of social identity theory allowed for growth in political psychology, specifically concerning how and why individuals group themselves. The social sorting phenomenon has emerged from social identity theory. Social sorting is the process by which individuals align their social identities with their partisan identities (Mason, 2016). This process is similar to the partisan sorting process— where individuals align their partisan identity with their ideological stance (Levendusky, 2010). However, social sorting will be the focus of this paper which will investigate how women's gender identity and partisan identities align. While much of the literature on social sorting is helpful in providing correlative explanations for this process, no research has provided causal evidence of the social sorting phenomenon. Where previous research has assumed more calculated factors such as policy preference to cause social sorting, this study analyzes social pressure as a potential cause of this occurrence. Social pressure is detected as a cause of social sorting in this study by using gender and partisan identity as variables dependent on these pressures. This finding indicates that individual perceptions of how social identities *should* intersect, promulgated by social pressures, lead members of the electorate to participate in social sorting.

Central to understanding social sorting is the concept of cross-pressures. This concept, first investigated by Berelson, Gaudet, and Lazarsfeld (1944) and Campbell et al. (1960), explains pressures individuals feel in response to concurrent prevailing social identities. These pressures stem from widespread perceptions of social identities which establish identity norms (Bicchieri, 2002). Perceptions of identity norms, in turn, influence how individuals feel they should simultaneously express their various identities (Miller et al., 1981; Bicchieri, 2002). Feeling cross-pressured in response to 'conflicting' identities decreases overall extremity of these identities among individuals and makes determining where they 'belong' more difficult (Miller et al, 1981). In other words, when individuals are internally divided between their own 'conflicting' identities, they are faced with the presumed responsibility to choose in favor of one identity or the other— a decision which, on a mass scale, leads to a more socially sorted electorate.

Decreased extremity in identity strength leads members of the electorate whose identities "cross-cut" to be more tolerable of individuals whose identities presumably conflict with their own and withhold less biases and feelings of negativity towards out-groups (Roccas and Brewer, 2002). Alternatively, individuals who have already sorted and aligned their identities tend

to be less tolerant of conflicting identities and withhold more biases than their non-sorted counterparts (Mason, 2014). On the one hand, arguments are made that this cross-pressured faction of the electorate will ease social tension, reduce judgments between groups, and lead to a more moderate electorate (Hillygus & Shields, 2008; Lavine, Johnston, & Steenbergen, 2012); whereas on the other hand, it is expected that individuals may begin to align their identities (to varying degrees) in response to these pressures and yield a more tense and divided electorate (Mason, 2016). When cross pressured individuals do sort into more cohesive groups, they begin to develop more biases and express less tolerance toward the ‘other’ side (Mason, 2016). This process causes bipolarity of American politics to intensify and could further polarize the electorate.

It is important to note the distinction between sorting and polarization, because while they are interconnected and mutually relevant, they are conceptually unique. Polarization differs from sorting as it occurs when members of the electorate take more extreme ideological and political stances (Levendusky, 2010). When the electorate becomes increasingly polarized, prevalence of moderate ideologies dissipates and ideological positions exist on a more bimodal spectrum (Levendusky, 2010). Where polarization exists primarily as a matter of ideological positions and intensity amongst partisans, sorting is a matter of how partisans align their various identities. While the distinction between polarization and sorting is clear, both remain inextricably linked to one another. Since both perpetuate an ‘us’ and ‘them’ mindset amongst individuals, these processes directly influence social identity and “motivate partisans to conform to defend the[ir] party’s positions” (Groenendyk, 2018, p. 166). Furthermore, it may be the case that social pressures play a significant role in polarization just as with social sorting, as both processes cause partisans to feel a need to ‘conform’ in one way or another.

Levendusky (2010) makes the point that polarization on the elite level contributes to sorting by publicly displaying which ideological viewpoints partisans should align with at the mass level. This results in simplification of elite cues to the electorate and more ideologically homogenous parties. Polarization and division on the elite level is presumed to cause ordinary voters, or those who hold more centrist positions, to feel as though there are only two options—to either be a conservative Republican or a liberal Democrat (Levendusky, 2010). Other research suggests that in addition to elite polarization increasing the divide between ideological poles, it also amplifies, “partisans’ potentially competing motives” (Groenendyk, 2018, p. 170). This amplification implies feelings of animosity towards out-groups do

not necessarily result in cohesion within groups (Groenendyk, 2018). This is important to note when considering the sorting process. While it would appear as though rise in intergroup disapproval and increased sorting would yield more cohesive in-groups, this may not be the case. Rather, the only thing perpetuating the facade of unity within partisans' own groups may be the stronger sense of disdain towards out-groups than one's own in-groups.

The nature of this division for individual group members varies depending on how impactful policy is on their partisan identity (Abramowitz, 2010). For instance, individuals who heavily consider policy positions to determine their partisan identity will feel politically divided (Abramowitz, 2010) whereas partisans who determine partisan identity primarily on identity matters will feel more socially divided. Furthermore, as members of the electorate who do not identify strongly with either partisan identity begin to sort more frequently, the bipolar nature of the American political system will intensify. As parties and their members increasingly shift further from the center, greater political and social intergroup divisions are likely to occur. When members of the electorate increasingly sort their partisan identities with their ideological positions, parties become, "more homogeneously liberal or conservative" (Levendusky, 2010, p. 9). As this process continues, members of the electorate are likely to feel pressure to sort between their cross-cutting identities and strengthen their aligned identities. Moreover, as partisan sorting takes place and ideologies increasingly align with certain parties, more specific collective understandings form around each party. These understandings include perceptions of which social identities 'should' correspond with each party. The social sorting phenomenon shows this leaves partisans feeling the need to sync their social identities with their partisan identity in a way that supports this collective perception.

Developments in literature on social identities and sorting has enhanced understandings of the gender gap, which Kaufmann explains as "male-female differences in party identification and voting behavior" (Kaufmann, 2006, p. 449). Gender identification has shown to carry significant weight in how partisans align their various social identities, including partisan identity (Kaufmann, 2004). Kaufmann explains that women as a whole identified more with the Democratic Party after President Lyndon B. Johnson took office, and that this gender-partisan identity alignment has incrementally increased over the years (Kaufmann, 2006). While the alignment between these two social identities has increased overall since the process began, its increase has not been entirely steady and has fluctuated along the way.

There are several factors which have been identified as contributors to the gender gap. Salience of policy issues, how individuals perceive political

elites (individually and collectively), and “changes in the distribution of political attitudes” are three reoccurring factors that appear to influence and deepen the gender gap in America (Chaney, Alvarez, & Nagler, 1998; Kaufmann & Petrocik, 1999; Kaufmann, 2006, p. 447). Kaufmann explains the mixture of policy positions and characteristics of elites who espouse these positions appear to significantly affect where partisans of differing genders direct their support (Kaufmann 2006). While these conclusions are not based upon causal evidence, voting and demographic trends do support this claim. Although policy positions and elite characteristics correlate with the widening of the gender gap, there must be certain fundamental aspects of each that cause this occurrence to take place. In other words, perhaps policy position and elite characteristics are not what cause the gender gap to widen, but rather the pressures people feel from their perceptions of both policy positions and elite characteristics.

Widespread perceptions of social identity groups are assumed to play a significant role in how individuals identify with groups. Huddy (2004) explains that social identities are generated through feelings of belonging to certain groups and are rooted in emotional connections to these groups. This subjective method of self-categorization allows for variance in strength, understanding, and feelings towards groups from person to person (Huddy et al., 2015). The assumption that perceptions significantly influence social group identification competes with Kaufmann’s suggestion that policy positions are the driving factors of partisan identification. Since perceptions are socially accumulated however, it appears logical that perceptions would significantly influence social identification processes—including partisan identification. Subjectivity of social identification makes the assumption that perceptions influence individuals’ social group identification seem firmer than the assumption that policy positions withhold the most influence. Just as social pressures from perceptions of policies and elite characteristics may contribute toward the widening gender gap, these pressures may also motivate individuals to participate in social sorting.

Findings from Tajfel and Turner (1979) explicitly emphasize individuals’ tendencies to self-categorize and differentiate their groups from others as a way to establish positive social identities (Huddy et al., 2015). While partisan identity is often viewed in comparison to social identities, Mason and Wronski (2018) clarify partisan identity itself is a social identity. This view is supported by the notion that the degree of an individual’s association with a particular party—or their partisan identity—is developed through “psychological attachment” to that political party (Huddy et al., 2015). Furthermore, it can be inferred one’s psychological attachments are

developed through social processes, making partisan identity just as much a social identity as gender identity or any other.

Understanding how individuals develop their partisan identity enhances comprehension of phenomena such as the widening gender gap and social sorting. Huddy et al., describe party identification as the most effective variable in understanding the dynamics of American political behavior. They also describe two separate mechanisms which explain party identification processes: instrumental and expressive partisanship. Instrumental partisanship suggests individual partisan identities are formed on party performance, ideological stance, and other crediting factors (Huddy et al., 2015), whereas expressive partisanship approaches the concept of partisanship entirely as an identity matter. Expressive partisanship views party identity as “strengthened by social affiliations to gender, religion, and ethnic or racial groups” (Huddy et al., 2015). Furthermore, expressive partisanship depicts party identity as something for individuals to be a part of and as something that is a part of individuals.

Assumptions that social pressures lead to sorting and widening identity gaps are supported by the expressive partisanship mechanism, whereas suggestions that policy preferences and elite positions influence these occurrences are supported by instrumental partisanship. When individuals’ party identification is influenced by policy preferences, logic and reasoning are the foundation of this identification. However, when party identification is influenced by social pressures, it is developed in a subjective manner. On the one hand, instrumental partisanship suggests parties and elites derive support from their abilities to effectively contribute toward goals that deal with policy positions, where on the other hand, expressive partisanship suggests that parties and elites gain support based on how individuals identify with and perceive each party. Although some individuals likely take an instrumental approach to partisanship, partisans who participate in social sorting and contribute to the widening gender gap are likely to take a more expressive approach and be influenced by social identity pressures because of the role that “psychological attachment” plays in social identification processes (Huddy et al., 2015).

Since perceptions play a significant role in social sorting, polarization, cross- pressures, and the gender gap—understanding how these perceptions are perpetuated plays an integral part in analyzing each occurrence. While modes of receiving information have evolved all throughout contemporary history, one method that has remained consistent is discussion. This said, the ways that individuals engage in discussion has evolved significantly—especially in more recent years with the rise of social media and the Internet.

While research on the impacts social media and online discourse have on society is limited, in part because of methodological restrictions, there is some research on the degree of influence social networking sites (SNSs) have on several aspects of social and political processes.

Zúñiga, Jung, and Valenzuela (2012) find that SNS use amongst individuals who seek information results in a “significant and positive impact on individuals’ activities aimed at engaging in civic and political action” (p. 329). This finding implies SNSs are, in a sense, gateways to facilitating political activity and inciting political and social engagement. Results from this research also reveal a connection between SNS usage for news with increased levels of social capital. Furthermore, this result suggests SNSs can play a role in communal development and can significantly increase bonds within social groups. While more research still needs to be conducted to better understand the dynamic role that Internet media resources play in social and political activity, Zúñiga, Jung, and Valenzuela have made substantial efforts in starting the conversation.

To better understand the current and future state of American politics and its actors, determining causes of both increasing division and alignment among social identity groups within the American electorate is important. Mason and Wronski (2018) point out that, “as social identities are increasingly associated with one party or the other, and as partisans increasingly identify with these party-associated groups, the American political divide grows more intractable” (p. 274). An intractable divide between social identity group alignments could considerably alter political structures within America resulting in civil discontent on social and political levels. By understanding what causes sorting and polarization, this growing divide can be better mitigated and prevented from becoming “intractable.” Finally, in addition to understanding the functions of these various socio-political occurrences, it becomes increasingly important that we also understand the factors which bring them to fruition. Considering the changing dynamics of communication in today’s world and the effects these changes have on public perceptions, this may be a good place to begin investigation.

Methodology Sample

The survey experiment created for this research was administered through Amazon's Mechanical Turk (M-Turk) and distributed among a sample of 388 people¹. While M-Turk subjects are often more representative of the general population than other platforms used for convenient sampling (Berinsky et al., 2012), the sample in this study is not representative of the target population. Berinsky et al., explain that subjects on M-Turk typically respond to stimuli in the same way as subjects used in research prior to M-Turk. Furthermore, the subject pool on M-Turk is not overused, so concerns about "habitual responding" are minor (Berinsky et al., 2012, p. 366). Since the study specifically analyzed alignment trends between women gender identity and American political parties, only individuals who identified as women and who are members of the American electorate were surveyed.

Experimental Design

This paper examines the relationship between social identity pressure and social identity alignment. To better understand this relationship, a survey experiment was designed and administered by use of Qualtrics and Amazon's Mechanical Turk (M-Turk). Various multiple choice and matrix table identity questions made up the contents of the survey experiment in addition to a single open-ended question following a graphic. Participants' partisan identities were assessed using the American National Election Studies (ANES) partisan identity scale at the beginning of the survey experiment and their partisan, gender, and feminist identities by a social identity (SID) scale at the end of the survey experiment². ANES partisan identity measures use a series of branching questions beginning with, "Generally speaking, do you usually think of yourself as a Republican, a Democrat, an Independent, or what?" and go on to determine strength of partisan identity by allowing participants to categorize themselves as either "strong" or "not very strong" members of their party. In the case where participants identify as "Independent" or "Other" the ANES scale helps determine whether participants consider themselves as "closer to the Republican or Democratic party." The SID scale

¹ M-Turk is a marketplace where researchers ("Requesters") can pay participants ("Workers") to take part in survey experiments

² The SID scale applied here was replicated from the scale used by Bankert, Huddy, & Rosema (2016) which was modeled on the Identification with a Psychological Group (IDPG) scale created by Mael and Tetrick (1992).

used in this study assessed the strength of individuals' social identities by determining the degree to which participants relate to statements about the social identities examined. The SID scale provides "Always", "Often", "Sometimes", or "Never" as possible responses to these statements³. In this survey experiment, five SID statements were used to determine the strength of participants' partisan, gender, and feminist social identities. These identities were measured using the same first four statements on the SID scale, but the fifth statement of each was different⁴.

The survey experiment randomly assigned participants into either the control or treatment group where they would view the control or treatment stimulus, respectively. Participants were asked to respond to an open-ended response statement after viewing either stimulus⁵. The stimuli for this research were in the form of an online social media discussion centered on voting as a woman in an "upcoming election". Social media discussion was selected as the format for the stimuli because social networking sites are often platforms where social identity pressures are exerted. Each stimulus pushed the idea that there are certain things women should do because of their gender identity as a woman. However, in the control stimulus it is pressed that women should vote because it is their womanly duty, whereas in the treatment stimulus participants are pressured to vote Democrat because it is their responsibility as a woman to do so. This pressure to align women's gender identity with Democrat partisan identity in the treatment stimulus was the only difference between the two stimuli, and phrasing was only minimally altered to accommodate this difference⁶. Partisan identity was tested before and after stimulus exposure to allow for observations of change.

³ The following statements were used to assess the degree of association with each social identity measured: (1) "When I speak about this [identity], I usually say 'we' instead of 'they'", (2) "I am interested in what other people think about this [identity]", (3) "When people criticize this [identity], it feels like a personal insult", and (4) "When I meet someone who supports this [identity], I feel connected with this person."

⁴ In measuring partisan identity "When I speak about this party, I refer to them as 'my party'" was the different statement used. In measuring gender identity, "When people praise women, it makes me feel good" was the different statement used. In measuring feminist identity, "I have a lot in common with other feminists" was the different statement used.

⁵ The open-ended response question stated "Explain how the discussion in the previous question made you feel."

Since the only difference between the two stimuli was social identity pressure to align gender and partisan identity, the only explanation for differing results between the two groups is social pressure⁷. The overall design of this survey experiment served to detect shifts in participants' identities as indication of social sorting.

Measures

Social pressure was targeted as the independent variable in the social sorting phenomenon and was exerted through a social media style discussion. The overall aim was to observe changes in participants' identity strength after their being exposed to social pressure to sort their identities. Data from the completed survey experiment was gathered and stored in Qualtrics. The data was then exported into Stata software so it could be analyzed. Several different tests were run to test my hypothesis that social pressure causes change in partisan identities. Republican and Democratic identifiers were tested separately. To assess the effect of stimulus exposure on partisan identity, participants' partisan identities were tested prior to exposure using the ANES partisan identity scale and after exposure using the SID scale. Data from the open-ended responses were coded into either positive or negative responses and compared between the control and treatment groups by partisan identity. Each response was individually coded as either a positive, negative, mixed, or neutral response. Positive, negative, and mixed responses were the responses considered in this process and mixed responses stood for both a positive and negative response. After all the data were collected, various regression analyses were run. These analyses detected shifts in partisan and gender identity strength and identified trends in positive and negative responses to the open-ended question between partisan groups.

Results

Social sorting is the process by which individuals align their various social identities. Since causal explanations of social sorting have been absent from the literature until now, findings in this study substantially aid current understandings of social sorting. This study sought not only to distinguish

⁶ These phrasing changes were not significant to the degree of having an effect on the stimulus' purpose.

⁷ Social pressure = independent variable; woman gender identity = dependent variable; partisan identity = dependent variable.

potential causes of this occurrence, but to also identify the role of sorting across gender and partisan social identity groups. Central to this research is the assumption that there are ‘correct’ and ‘incorrect’ ways for individuals to align their identities, which contributes toward the formation of identity norms. Identity norms can lead individuals to feel cross-pressured between their various social identities. This study demonstrates the role of cross-pressures and observes tendencies of gender and partisan identity group members to choose between their ‘conflicting’ identities and align in one direction or the other. Perceptions of how individuals ‘should’ identify give a certain validity to the assumption that ‘correct’ and ‘incorrect’ ways to identify exist. Furthermore, these perceptions deepen the prevalence of identity norms on a mass social level. Social pressures to conform in accordance with identity norms are emitted through social observance and interaction, which in turn leads to social sorting. The perceived ‘correct’ alignment of woman and Democrat social identities, which social pressures highlight, is used in this study to observe social sorting.

Identity Strength Before & After Stimulus Exposure

Results in Figures 1 and 2 were obtained by regression analysis of the collected data from both Democrat and Republican identifiers and display shifts in partisan identity strength of each party between control and treatment groups. The ANES identity scale labeled on the X-axis measures partisan

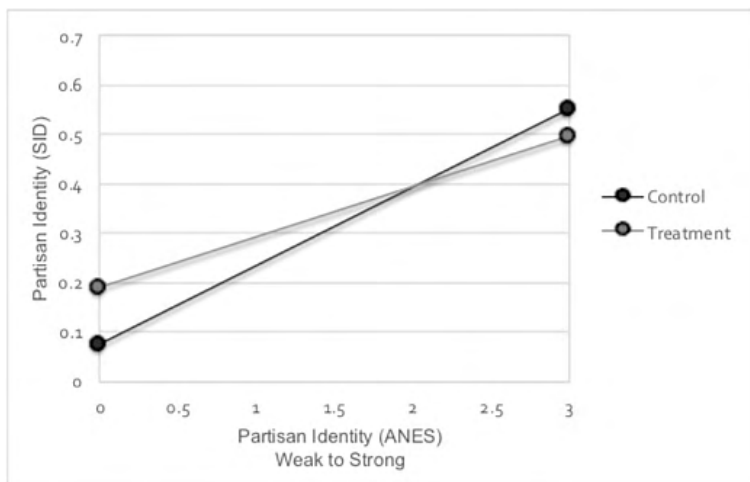


Figure 1. Strength of Democrat identity on ANES and social identity scale compared between control and treatment groups.

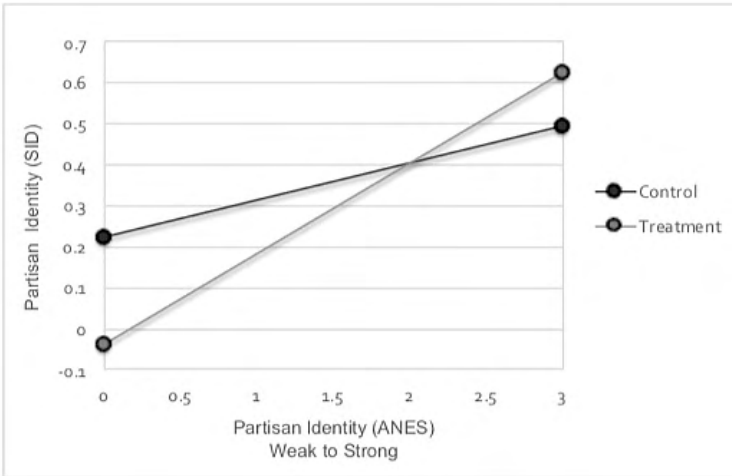


Figure 2. Strength of Republican identity on ANES and social identity scale compared between control and treatment groups.

identity from weak to strong, which was assessed prior to participants' exposure to either stimulus. The social identity scale on the Y-axis measures partisan identity strength of participants from weak to strong as well, but after exposure to either the control or treatment stimulus. Data in Figure 1 show no statistically significant shift in identity strength between the control and treatment groups, which only allows for inconclusive interpretations of these slight variations in strength. Data represented in Figure 2, on the other hand, shows a markedly different trend in response to stimulus exposure. Where Republicans in the control group did not experience any significant shifts in partisan identity strength, Republicans exposed to the treatment stimulus did experience significant shifts in partisan identity strength

While statistically insignificant, data in Figure 2 hint that strong identifying Republicans (on ANES scale) who were exposed to the treatment stimulus—which used social pressure to push the idea that it is a woman's duty to vote Democrat—may have increased their partisan identity strength towards even stronger Republicans on the social identity scale. Weak identifying Republicans (on ANES scale) who were exposed to the same treatment stimulus however, began identifying less as Republicans and shifted their partisan identity strength towards Democrat. While it cannot necessarily be said that weak Republicans who shifted towards Democrat now identify as Democrats, it can be said that these weak Republicans are participating in social sorting by directionally shifting their identity in accordance to

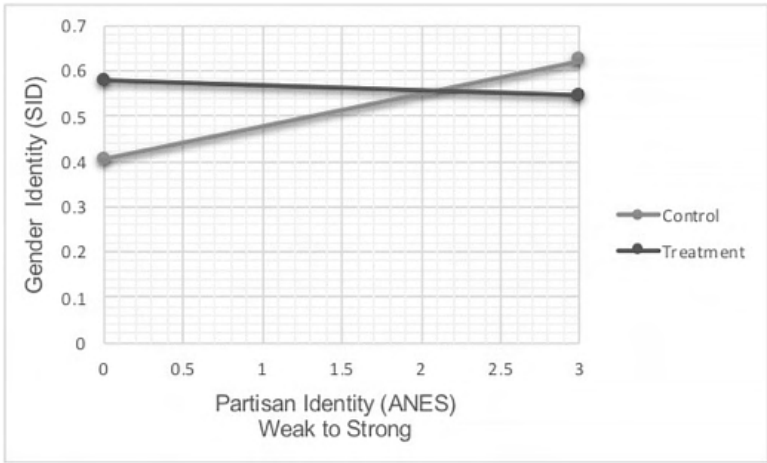


Figure 3. Strength of gender identity on social identity scale between control and treatment groups among Democrats.

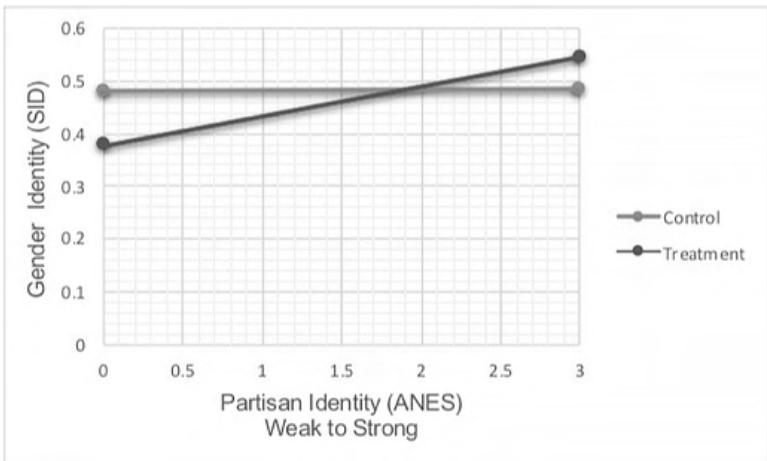


Figure 4. Strength of gender identity on social identity scale between control and treatment groups among Republicans.

the perceived ‘correct’ identity alignment. The same test was run between Democratic and Republican groups to detect potential trends of gender identity strength on the social identity scale in Figures 3 and 4, but there did not appear to be any significant shifts or trends in gender identity as a result of stimulus exposure for either. It was anticipated that strong Republicans

might shift their gender identity in response to the treatment stimulus, but this did not occur. Where significant shifts in gender identity were anticipated, only significant shifts in partisan identity occurred.

Trends in Social Identity Strength

The hypothesis that shifts would occur in identity strength of ‘misaligned’ participants after exposure to the treatment stimulus was confirmed by data of weak Republican identifiers in Figure 2. The data show a clear and significant shift in partisan identification among weak Republicans after exposure to the treatment stimulus. Since weak Republican identifiers shifted away from the Republican Party, it can be inferred that social identity pressure to align gender and Democrat identity was effective among these weak partisan women and acted as a catalyst in the social sorting process. This effect likely occurred because the ‘cross-cutting’ characteristics of participants’ identities (i.e. women’s gender identity and Republicans’ partisan identity) were highlighted by social identity pressure. Possession of cross-cutting identities thus made weak Republican identifiers consider the importance of these identities and motivated them to align in a way that would reduce cross-pressures. In other words, weak Republicans chose to identify less as Republicans because they viewed this as the acceptable and least conflicting way to socially identify.

On the other end of the Republican identity spectrum in Figure 2, the data display a slight increase in partisan identity strength amongst strong identifying Republicans after exposure to the treatment stimulus. Although this shift is statistically insignificant, it could show to be a more significant result with a larger sample size. This would indicate that social identity pressure leads strong partisan identifiers who do not conform to identity norms to resist the pressure and allow their identities to continue cross-cutting. Where weak partisans display susceptibility to sort in accordance to the identity norms, these results would indicate that strong partisans are not among those likely to participate in social sorting if the suggested identity alignment conflicts with their existing partisan identity.

Since the treatment stimulus pressured participants to vote Democrat because of their woman gender identity—and these participants already identified as Democratic women—the treatment results in Figure 1 were expected. Since social identity pressure pushed for alignment of woman and Democrat identity, this pressure likely further validated identities of participants who already met this alignment. Although statistically insignificant, it appears as though there was a slight increase in partisan identity strength of weak Democrats who were exposed to the treatment stimulus, and conversely,

an identity strength decrease among strong Democrats exposed to the same stimulus. While this slight variation could be attributed to random chance, a larger sample might show this shift to be significant.

Shifts in Figure 1, although insignificant in this data, would otherwise imply that when social pressure supports one's preexisting gender and partisan identity alignment, weak partisans may feel motivated to intensify their alignment whereas strong partisans may weaken their alignment. Interestingly, this would be the exact opposite result that occurs when social identity pressure advocates against individuals' preexisting identifications. If these results were significant, it would indicate that—in terms of partisan and gender identity—weak partisans are likely to sort and align in accordance with the pressure and strong partisans are likely to disengage with sorting and resist social identity pressures to align. In other words, where social identity pressure may contribute towards sorting in some cases, it may reverse the process in other cases. If data in Figure 1 for the treatment group and data in Figure 2 for strong identifiers in the treatment group do show to be significant in future research, this would indicate that social identity pressure only causes sorting when experienced by weak partisans. While only one significant shift was identified in the results in Figures 1 and 2, there were various statistically insignificant shifts that should be investigated further to help explain the current state of partisanship in America.

As shown in Table 1, gender identity strength data from both parties do not indicate any significant shifts after exposure to the treatment stimulus. Since the treatment suggested that women should be Democrats, it was expected that the gender identity strength of Republican women might shift in response to this pressure. But as seen in data from Figures 3 and 4 and Table 1, no shifts were detected. Since partisan identity has been noted in the literature as difficult to move, it was expected that strong identifying Republicans would cling to their partisan identity, and instead, identify less as a woman after treatment exposure. This would have indicated that gender identity is more susceptible to shift than partisan identity. However, Figure 2 suggests partisan identity is more susceptible to social identity pressure compared to gender identity. From this it can be inferred that when weak, unsorted partisans are pressured to align their partisan and gender social identities, gender identity will be more resistant to change, and partisan identity will shift in strength.

Likelihood of Positive or Negative Responses to Stimuli

In addition to observance of shifts in partisan and gender identity as a result of stimulus exposure, another test was run which assessed likelihood of participants having either a positive or negative response to the control or treatment stimulus. This section examines the mechanism underlying the effects observed in the previous section. The X-axis in Figure 5 measures partisan identity from strong Democrat to strong Republican and the Y-axis measures likelihood of having a positive response from unlikely to very likely. Data represented in Figure 5 show relatively consistent results between strong Democrats' to strong Republicans' likelihood of having a positive response to the control stimulus. There is only a slight decrease in respondents' likelihood of having a positive response as identities move closer to strong Republican. When exposed to the treatment stimulus, Democratic participants' likelihood of having a positive response remained quite high but significantly decreased as partisan identity moved closer toward strong Republican.

The X axis in Figure 6 also measures partisan identity from strong Democrat to strong Republican, but the Y axis measures respondents' likelihood of having a negative response. While the likelihood of participants having a negative response is steady across the spectrum of partisan identity for the control group—and remains quite low—the likelihood of participants having a negative response to the treatment stimulus shows clear trends. Where likelihood of strong Democrats having a negative response to the treatment stimulus only slightly increased, likelihood of strong Republicans having a negative response to the treatment stimulus shot up considerably. Overall, trends across Figures 5 and 6 show that Democrats are relatively steady in their positive and negative responses toward both the control and treatment stimulus, and that Democrats and Republicans reacted similarly towards the control stimulus. However, when responding to the treatment stimulus, Republicans were increasingly displeased as their partisan identity strengthened.

Figures 5 and 6 show consistencies between members of both parties' feelings towards the stimuli. It is not surprising that after exposure to the treatment stimulus, both the likelihood of having a positive response decreased and likelihood of having a negative response increased as participants' identities moved closer to strong Republican. Since the treatment stimulus implied that it is 'correct', or the identity norm, for women to be Democrats, the increased likelihood of Republicans' negative responses likely came from the perceived invalidation of their pre-existing identities (i.e. a Republican woman). Furthermore, it can be inferred that the increase in partisan identity strength among strong Republicans in Figure 2 may be

a result of their apparent resistance to the message in the treatment stimulus. Where strong Republican women do possess cross-cutting identities, they respond to cross-pressures differently than weak Republican women. On the one hand, weak Republican women appear to succumb to cross-pressure tensions and sort, whereas on the other hand, strong Republican women show an increased resistance to conform to identity norms and decreased likelihood to participate in social sorting.

Since the only difference between the stimuli is social identity pressure to align gender and partisan identity in the treatment stimulus, it is worth noting that both Democratic and Republican participants had similar likelihoods of responding positively or negatively to the control stimulus. While there was a slight decline in strong Republicans' likelihood of having a positive response after exposure to the control stimulus, this shift was statistically insignificant and could be attributed to random chance. Aside from this slight decrease in Republican positivity toward the control stimulus, the results in Figures 5 and 6 suggest that women across the partisan identity spectrum generally received the message in the control stimulus—that it is a woman's duty to vote—with equal amounts of positivity or negativity. This may be because voting is not viewed as an activity specific to women of one particular party over the other.

In considering voting, it could have been useful to test participants' likelihood to vote after exposure to the stimuli. Since the treatment stimulus suggested it is a woman's duty to vote as a Democrat, it would be interesting to see if Republican women's likelihood to vote shifted in response to this suggestion. Since Republican women resisted social identity pressure, it could be expected that these women may further express their resistance by either actively voting Republican in retaliation to the pressure or by choosing not to vote at all because of the idea pressed in the stimulus that it is wrong for women to vote Republican. While a shift in likelihood to vote may not affect the identities of partisans or social sorting, it could affect the actions partisans take in supporting their parties and considerably alter the state of American politics. According to these results, social identity pressures tend to be met with high to moderate positivity by individuals who already align in accordance with the pressures, and conversely, are met with increasing negativity by individuals whose identities cross-cut and go against the suggested identity alignment. Results in Figures 5 and 6 enhance understandings of how individuals across the partisan identity spectrum respond to specific social identity pressures. Furthermore, trends in this data provide further insight on the dynamics of social sorting, such as who participates in the occurrence and why.

Conclusion

Findings from this study show that social pressure influences weak partisans to participate in social sorting when their pre-existing social identities do not align with identity norms. These weak partisans aligned with women's gender identity norms to ease cross-pressure tensions between their partisan and gender identities. Identity norms and cross-pressure tensions were highlighted by social pressure in this study. While a larger sample should be tested to yield more significant results, it appears as though strong partisans with cross-cutting identities responded to this social pressure with resistance to sorting unlike weak partisans. Therefore, it can be said that weak partisans with cross-cutting identities are more likely to align with identity norms and sort as a result of social pressure than their strong partisan counterparts. Considering this, it becomes increasingly important to think about the modes by which these social identity pressures are transferred. Since social networking sites are common platforms where these pressures are transferred, the role these networks play on the composition of the electorate should not be understated. In addition to understanding the ways social sorting occurs, it is also important to consider the impacts of this phenomenon on the United States. Since social sorting affects how individuals identify and what actions are taken by members of the electorate, this phenomenon plays a significant role in American society and politics.

This study's demonstration of social identity pressure as a causal element of the social sorting phenomenon allows gaps to be filled in the literature on sorting. Where socioeconomic status, geographical location, and generational replacement are among factors correlated with widening the gender gap and increased sorting (Kaufmann, 2006; Bishop & Cushing, 2009; Putnam, 2000), research set forth in this paper identifies social identity pressure as a significant causal factor of social sorting. Since behavior of the American electorate determines the condition of America's republic, understanding the dynamics of these phenomena and their interconnectedness helps explain the existing state of American politics.

Resources

- Abramowitz, A. L. (2010). *The Disappearing Center: Engaged Citizens, Polarization, and American Democracy*. New Haven: Yale University Press.
- Bankert, A., Huddy, L., & Rosema, M. (2016). Measuring Partisanship as a Social Identity in Multi-Party Systems. *Political Behavior*, 39(1), 103-132.
- Berelson, B., Gaudet, H., & Lazarsfeld, P. F. (1944). *The People's Choice: How The Voter Makes Up His Mind in a Presidential Campaign*. Sloan & Pearce: New York.
- Berinsky, A. J., Huber, G. A., & Lenz, G. S. (2012). Evaluating Online Labor Markets for Experimental Research: Amazon.coms Mechanical Turk. *Political Analysis*, 20(03), 351-368.
- Bicchieri, C. (2002). Group Identity, Norms, and Communication in Social Dilemmas. *Rationality and Society*, 14(2), 192-228.
- Bishop, B., & Cushing, R. G. (2009). *The Big Sort: Why the Clustering of Like-Minded America is Tearing us Apart*. Boston: Mariner Books.
- Campbell, A., Converse, P. E., Miller, W. E., & Stokes, D. E. (1960). The American Voter. *Political Science Quarterly*, 75(4), 593.
- Chaney, C. K., Alvarez, R. M., & Nagler, J. (1998). Explaining the Gender Gap in U.S. Presidential Elections, 1980-1992. *Political Research Quarterly*, 51(2), 311-339.
- Groenendyk, E. (2018). Competing Motives in a Polarized Electorate: Political Responsiveness, Identity Defensiveness, and the Rise of Partisan Antipathy. *Political Psychology*, 39, 159-171.
- Hillygus, D. S., & Shields, T. G. (2009). *The Persuadable Voter: Wedge Issues in Presidential Campaigns*. Princeton, N.J: Princeton University Press.
- Huddy, L. (2004). Contrasting Theoretical Approaches to Intergroup Relations. *Political Psychology*, 25(6), 947-967.
- Huddy, L., Mason, L., & Aarøe, L. (2015). Expressive Partisanship: Campaign Involvement, Political Emotion, and Partisan Identity. *American Political Science Review*, 109(01), 1-17.

- Kaufmann, K. M. (2004). The Partisan Paradox: Religious Commitment and the Gender Gap in Party Identification. *Public Opinion Quarterly*, 68(4), 491-511.
- Kaufmann, K. M., & Petrocik, J. R. (1999). The Changing Politics of American Men: Understanding the Sources of the Gender Gap. *American Journal of Political Science*, 43(3), 864.
- Kaufmann, K. M. (2006). The Gender Gap. PS: *Political Science & Politics*, 39(03), 447-453.
- Lavine, H. G., Johnston, C. D., & Steenbergen, M. R. (2012). Ambivalent Partisans at the Polls. *The Ambivalent Partisan*, 153-180.
- Levendusky, M. (2010). *The Partisan Sort: How Liberals Became Democrats and Conservatives Became Republicans*. Chicago: University of Chicago Press.
- Mael, F. A., & Tetrick, L. E. (1992). Identifying Organizational Identification. *Educational and Psychological Measurement*, 52(4), 813-824.
- Mason, L. (2014). "I Disrespectfully Agree": The Differential Effects of Partisan Sorting on Social and Issue Polarization. *American Journal of Political Science*, 59(1), 128-145.
- Mason, L. (2016). A Cross-Cutting Calm. *Public Opinion Quarterly*, 80(S1), 351-377.
- Mason, L., & Wronski, J. (2018). One Tribe to Bind Them All: How Our Social Group Attachments Strengthen Partisanship. *Political Psychology*, 39, 257-277.
- Miller, A. H., Gurin, P., Gurin, G., & Malanchuk, O. (1981). Group Consciousness and Political Participation. *American Journal of Political Science*, 25(3), 494.
- Putnam, R. (2000). Bowling alone: The Collapse and Revival of American Community. *Choice Reviews Online*, 38(04).
- Roccas, S., & Brewer, M. B. (2002). Social Identity Complexity. *Personality and Social Psychology Review*, 6(2), 88-106.
- Tajfel, H., & Turner, J. (1979). An Integrative Theory of Intergroup Conflict. *Intergroup Relations: Essential Readings*, edited by Michael Hogg and Dominic Abrams, 94-109. New York: Psychology Press.

Zúñiga, H. G., Jung, N., & Valenzuela, S. (2012). Social Media Use for News and Individuals Social Capital, Civic Engagement and Political Participation. *Journal of Computer-Mediated Communication*, 17(3), 319-336.

Shelby A. Towers graduated from the University of Memphis in May of 2020 with a major in psychology. She graduated *summa cum laude* with Psychology Departmental Honors and University Honors with Thesis. Throughout her time at the University of Memphis, she has been involved in multiple neuroscience research projects under Dr. Deranda Lester and has presented her work at multiple conferences, including the 2019 Society for Neuroscience in Chicago, Illinois. She will attend the neuroscience doctoral program at the University of Texas at Austin beginning fall 2020. She hopes to continue her research focus on the neurobiological mechanisms behind psychological disorders.

Shelby's paper received a *Quaesitum* best paper award.

**Shelby Towers, Josiah Comstock, Nick Paige,
Price Dickson, and Deranda Lester**

Environmental Enrichment Alters Mesolimbic
Dopamine Release in Mice

Faculty Sponsor

Dr. Deranda Lester

Abstract

Social isolation in rodents is often used to model early life stress, increasing the occurrence of behaviors related to substance use disorder. Given that the rewarding properties of abused drugs are associated with increased dopamine release, the present study aimed to determine how various housing conditions affect dopamine functioning. Mice spent 10-12 weeks in one of three housing conditions: environmentally enriched (EE, including physical and social stimuli), socially enriched (SE, including only social stimuli), or isolation. *In vivo* fixed potential amperometry was used to quantify dopamine release in the nucleus accumbens before and after cocaine administration. Isolated mice showed an increased dopaminergic response to cocaine relative to both EE and SE mice. No differences were observed between EE and SE mice, suggesting social stimuli may be driving the protective effects of EE more so than physical stimuli. Identifying such factors may be important for prevention and treatment of substance use disorder.

Introduction

A survey from the National Institute on Drug Abuse (NIDA) in 2013 reported that approximately 24.6 million Americans 12 years or older used illicit drugs such as marijuana, cocaine, prescription drugs, hallucinogens, and heroin in a month span. According to Dr. Volkow, Director of NIDA, drug addiction is defined as “drug seeking that is compulsive, or difficult to control, despite harmful consequences.” However, some drugs are more addictive than others, and not everyone may become addicted to the same drug. Factors affecting the risk of addiction are both biological and environmental. Age of first exposure, genes, and preexisting mental disorders affect probability of becoming addicted to drugs as well as social pressure and relationships, feelings of stress and anxiety, and low cost and high availability of drugs (NIDA, 2018). Adolescents are at an even greater risk of abusing drugs relative to adults (Wagner & Anthony, 2002). Furthermore, adolescents who lack strong parental supervision and/or come from low socioeconomic status are even more likely to fall victim to drug addiction compared to adolescents with supportive, involved parental monitors from middle and/or upper socioeconomic statuses (Guo, Hawkins, Hill, & Abbott, 2001). Findings from animal studies further support that environmental factors such as reduced social and physical stimuli can have detrimental effects on the developing adolescent brain.

Rearing rodents in social isolation models an early life stressor; it has been shown to enhance the rewarding effects of drugs and increase the occurrence of behaviors related to psychological disorders such as depression and anxiety (Czoty, Gould, Gage, & Nader, 2017; Laviola, Hannan, Macri, Solinas, & Jaber, 2008; Yorgason et al., 2016). On the opposite spectrum, adding stimulating objects to cages such as toys with complex textures and running wheels create an enriched environment that mimics positive life experiences. Enriched environments (EE) reduce the occurrence of behaviors associated with substance use disorder, such as drug seeking, liking, and self-administration (Stairs, Prendergast, Bardo, 2011; Stairs & Bardo, 2009; Solinas, Chauvet, Thiriet, El Rawas, & Jaber, 2008). Furthermore, Nader et al. (2012) and Solinas et al. (2008) found that switching mice from standard group-housed conditions (aka social enrichment: SE) to EE cages for 30 days provides preventative effects against conditioned place preference for cocaine. Conditioned place preference is a common preclinical test for drug preference or liking. Thus, mice exposed to EE for more than 30 days displayed reduced cocaine preference or liking compared to SE mice. In the other direction, mice raised in EE and then switched to SE showed an increased cocaine preference compared to control (SE only) mice 7 and 30

days after the switch. Overall, the more time spent in EE the greater the positive effects regarding vulnerability to the rewarding effects of drugs.

As mentioned, EE generally consists of toys, climbing objects, running wheels, and cage mates. It is not fully understood whether one of these aspects of EE is more beneficial than others. Aarde, Miller, Creehan, Vanderwater, and Taffe (2015) and Cosgrove, Hunter, and Carroll, (2002) found that exposure to a running wheel led to an immediate decrease in self-administration of psychostimulants. Other studies indicate social interaction may be the driving force behind altered behaviors related to drug reinforcement (Gibson, Beckman, El-Maraghi, Marusich, & Bardo, 2011; Morse, Erwin, & Jones, 1993).

Reinforcing stimuli such as natural rewards and most drugs of abuse increase dopamine release in the mesolimbic dopamine pathway. This pathway originates in cell bodies in the ventral tegmental area (VTA) which project to and release dopamine in the nucleus accumbens (NAc) (Le Moal & Simon, 1991; Kalat, 2013). Previous studies regarding dopamine differences related to housing differences have not been consistent. For example, El Rawas et al. (2009) found similar drug-induced dopamine levels in the NAc of EE and SE, but Bardo et al. (1999) found increased drug-induced dopamine release in EE mice relative to SE mice. While some studies have found no differences in amphetamine-induced extracellular dopamine across EE, SE, and isolated rats using microdialysis (Meyer & Bardo, 2015), clear differences have been detected between isolated and SE rats using fast-scan cyclic voltammetry (Yorgason, Espana, Konstantopoulos, Weiner, & Jones, 2013). Differences are likely related to time spent in EE conditions, route of drug administration, and techniques used to measure dopamine.

The aim of the present study was to determine how these housing conditions alter mesolimbic dopamine transmission related to substance use disorder, in hopes of parsing the value of social and physical stimuli in protecting against the impact of isolation. In the present study, mice spent 10-12 weeks in one of the three housing conditions: EE, SE, and isolation. Following this time period, we used *in vivo* fixed-potential amperometry to quantify dopamine release before and after an injection of cocaine. Based on behavioral findings in previous studies, we hypothesized that mice in the isolated housing condition would have a greater dopaminergic response to cocaine relative to the mice in the SE and EE conditions, meaning we expected isolated mice to be more susceptible to the rewarding effects of

cocaine, thus providing a neurochemical basis for the protective ability of group and EE housing conditions towards behaviors related to drug reward.

Methods

These experiments have been approved by the Institutional Animal Care and Use Committee (IACUC) at the University of Memphis and were also aligned with those outlined in The Public Health and Service Policy on Humane Care and Use of Laboratory Animals (National Institutes of Health, 2015) and the Guidelines for the Care and Use of Mammals in Neuroscience and Behavioral Research (National Research Council 2003).

Subjects

Fifteen male C57Bl/6J mice were acquired from Jackson Laboratory (Bar Harbor, ME, USA) at 3 weeks of age. Upon arrival, mice were immediately and randomly separated into one of three housing conditions: EE ($n = 6$), SE ($n = 6$), or isolated ($n = 3$). Cages were kept in a temperature-controlled room ($21 \pm 1^\circ \text{C}$) with a 12:12 light-dark cycle (lights on at 0600). Food and water were available ad libitum.

Apparatus and Materials

In vivo fixed potential amperometry coupled with carbon fiber microelectrodes has been confirmed as a valid technique for real-time monitoring of stimulation-evoked NAc dopamine release (Forster & Blaha, 2003; Lester, Rogers, & Blaha, 2010). There are 3 amperometry set-ups in the Psychology building at the University of Memphis. An amperometry set-up consists of a large faraday cage to block electrical noise, a stereotaxic frame with electrode carriers (David Kopf Instruments, CA, USA), a programmable stimulator (Iso-Flex/Master-8; AMPI, Israel), and an electrometer to measure oxidation currents of dopamine (e-corder 401 and Picostat, eDAQ Inc., CO, USA) connected to a computer. All chemicals were purchased from Sigma-Aldrich. Standard operating procedures for urethane (U2500 Sigma-Aldrich), dopamine (H8502 Sigma-Aldrich), and cocaine (C5776 Sigma-Aldrich) were approved by the Environmental Health and Safety department at our university.

Procedures

Housing Conditions

Mice in the environmentally enriched (EE) housing condition were housed 3-5 per cage in large cages with running wheels, nesting materials, and

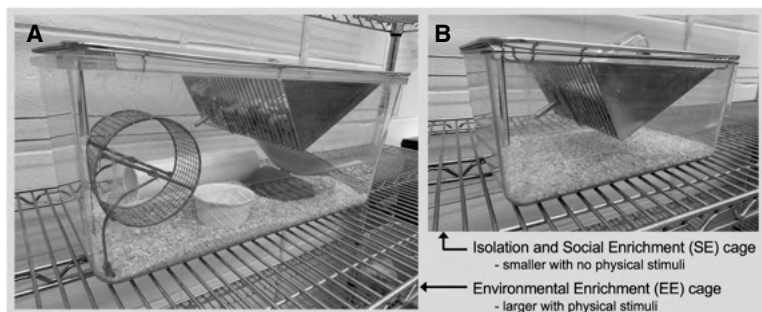


Figure 1. Experimental housing conditions. Mice in the environmentally enriched (EE) condition had access to running wheels, tunnels, and cage mates in a larger cage. Mice in the socially enriched (SE) and isolated conditions were in standard cages with no EE objects.

tunnels (Figure 1). EE items were obtained from Bio Serve. Mice in the SE condition were housed 3-5 per cage in standard cages without EE items. Mice in the isolated housing condition were housed individually in standard cages without EE items. Cages from all conditions were housed in the same room of the animal-care facility. Consequently, the isolated mice were housed without direct contact to social or physical stimuli, but auditory and visual social stimuli was present. Mice were housed in one of these conditions for 10-12 weeks.

Fixed Potential Amperometry

Mice were deeply anesthetized using two urethane i.p. injections totaling 1.5 g/kg. Foot and tail pinch and eye blink induced reflexes fifteen minutes after second injection guaranteed proper anesthetization. Mice were then placed under a stereotaxic frame that included a warming pad to ensure body temperature remained at $38 \pm 1^\circ \text{C}$. Stereotaxic carriers were used to guide all electrodes. A stimulating electrode (SNE-100 outer diam. 100 μm ; Rhodes Medical Co., CA, USA) was placed into the left VTA (coordinates in mm from bregma: AP -3.3, ML +0.3, and DV -4.0 from dura; Paxinos & Franklin, 2001). A carbon fiber dopamine recording electrode (7 μm o.d. and 500 μm long, Thornel Type P, Union Carbide, PA, USA) was positioned into the left NAc (coordinates in mm from bregma: AP +1.5, ML +1.0, and DV -4.0 from dura; Paxinos & Franklin, 2001). A silver-chloride reference and auxiliary electrode combination was placed in contact with the surface of the parietal cortex contralateral to the stimulating electrode (-3.0 mm from bregma) as shown in Figure 2. A fixed +8.0 V current was continuously applied to the recording electrode via an electrometer (ED401 e-corder 401 and

EA162 Picostat, eDAQ inc., Colorado Springs, CO). Changes in dopamine release in the NAc were monitored continuously in response to brief chains of electrical stimulation (20 pulses at 50 Hz every 30 sec for five minutes) applied to the VTA as a baseline recording. After five minutes, the mice received an i.p. injection of cocaine (10 mg/kg) to measure the dopaminergic system's transporter function and its psychostimulant response allowing us to examine the impact of housing conditions. Dopamine recordings continued 1-hour post cocaine injection.

In vitro electrode calibrations were performed after all experiments enabling dopamine oxidation currents (nAmp) to be converted to dopamine concentrations (μM). Each carbon fiber electrode was exposed to varying known dopamine concentrations (0.2, 0.4, 0.8, and 1.2 μM) via a flow injection system while recording oxidation current change (Dugast, Saud-Chagny, & Gonon, 1994).

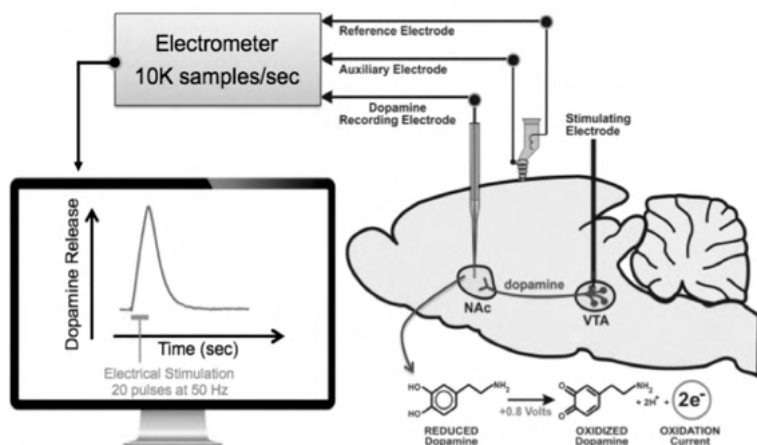


Figure 2. Experimental design. *In vivo* fixed potential amperometry with carbon fiber recording electrodes quantified nucleus accumbens (NAc) dopamine release evoked by stimulation of dopamine cell bodies within the ventral tegmental area (VTA).

Results

Baseline Dopamine Efflux

A one-way ANOVA was used to compare mean dopamine release before cocaine administration. There was a significant effect of housing on baseline dopamine release [$F(2, 19) = 4.16, p = .032$; Figure 3 and 4]. Post hoc com-

parisons using Tukey HSD test indicated that the mean dopamine release (in μM) for the EE condition ($M = 0.117$, $SD = 0.105$) was significantly lower than the isolated condition ($M = 0.280$, $SD = 0.130$; Figure 3). However, the SE condition ($M = 0.252$, $SD = 0.119$) did not significantly differ from the EE or isolated conditions.

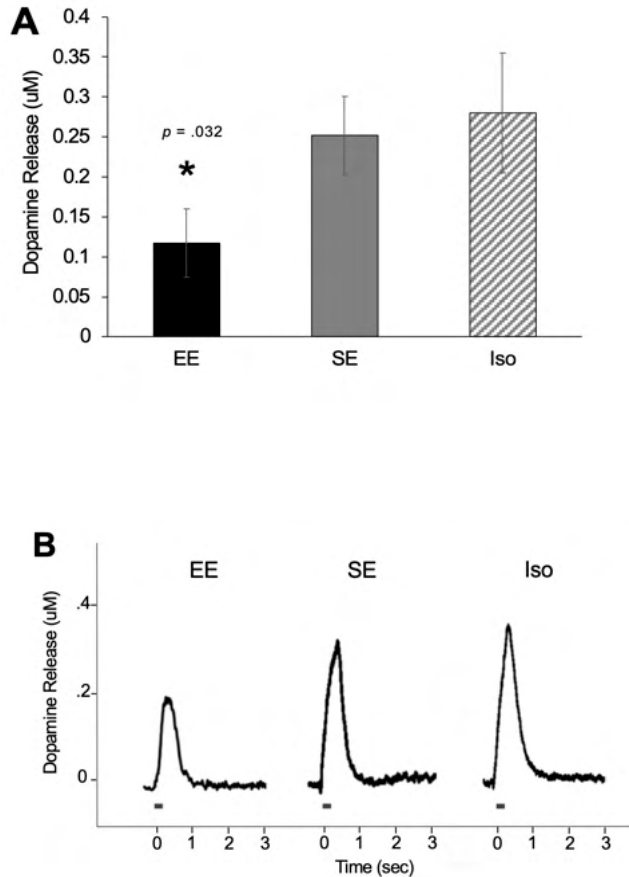


Figure 3. Baseline (pre-cocaine) dopamine release presented as (A) mean \pm SEM and (B) representative stimulation-evoked responses from each housing group. *Mice in the environmentally enriched (EE) condition had significantly reduced dopamine release relative to isolated mice.

Dopamine Efflux following Cocaine

Percent change in stimulation-evoked dopamine release following cocaine administration was compared in 10 min increments post injection. A two-way mixed ANOVA revealed a nearly significant effect of housing (between-subject IV) on dopamine release over time (the 60 min recording period, within-subject IV), $F(12, 72) = 1.835$, $p = 0.058$, $\eta^2 = 0.23$ (Figure 4). One-way ANOVAs showed a nearly significant difference in percent change in dopamine release between experimental groups at 10 min ($p = 0.059$)

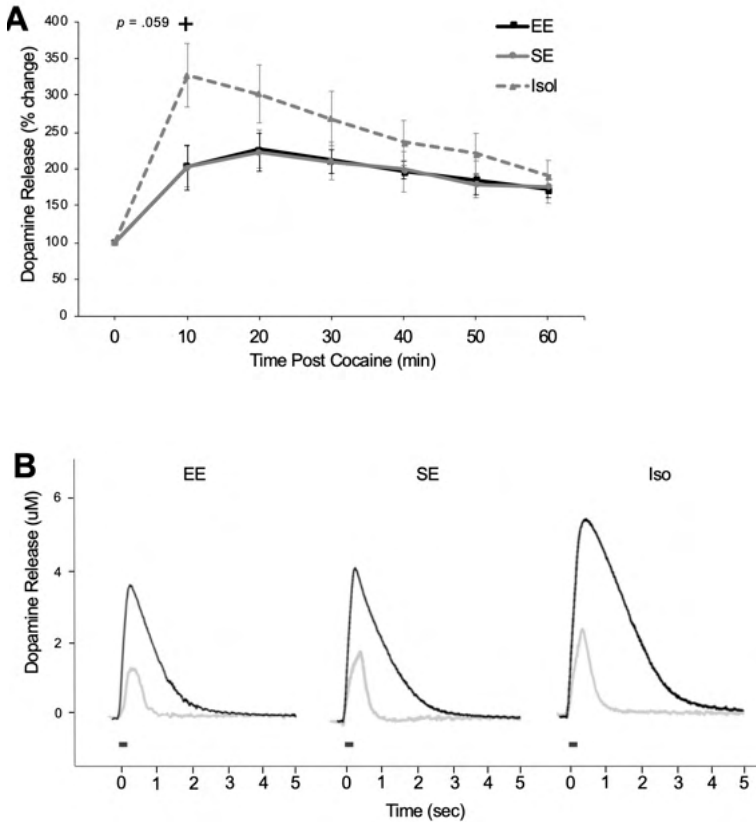


Figure 4. Dopamine release following cocaine administration presented as (A) mean \pm SEM and (B) representative stimulation-evoked responses from each housing group, with the light line depicting the pre-cocaine response and the black line depicting the response 10 min post cocaine. + There was a near significant effect of housing conditions on dopaminergic response to cocaine, indicating an increased response by the isolated mice compared to both EE and SE groups.

but no differences at any other time points. At the 10 min post-cocaine time point, Tukey's HSD post hoc analyses revealed a trend in the data in which the isolated mice had near significant increases in percent change dopamine release relative to EE ($p = 0.075$) and SE ($p = 0.071$).

Discussion

The rewarding effects of abused drugs are strongly associated with increased activity in the mesolimbic dopamine system (Le Moal & Simon, 1991). The purpose of the present study was to determine how housing conditions can alter NAc dopamine functioning and the response of this pathway to the well-known dopamine agonist cocaine. Mice were housed in either EE (physical and social stimuli), SE (social stimuli), or isolated (lacking both physical and social stimuli) conditions for 10-12 weeks prior to dopamine quantification using *in vivo* fixed potential amperometry.

Baseline dopamine release, as measured by the magnitude of the VTA stimulation-evoked response, was significantly lower in EE mice relative to isolated mice, with SE mice not differing from either of the other 2 groups. These findings suggest that the combination of the physical and social stimuli are more influential on the dopamine system relative to social stimuli alone, at least in mice. These effects may be species dependent. Recently, using a similar dopamine recording technique in brain slices, Karkhanis et al. (2018) found that isolated rats displayed increased stimulation-evoked dopamine release relative to group housed rats. Furthermore, exposure to chronic and intermittent social defeat stress also results in augmented stimulated dopamine release in rats (Deal et al., 2018). Social interaction is more rewarding for rats than mice, and social isolation has been shown to be more anxiety-provoking for rats than mice (see Ellenbroek & Youn, 2016).

Our results demonstrate that social interaction, or lack thereof, also impacts the response of this dopamine system to the psychostimulant cocaine. As expected, dopamine release was significantly increased following cocaine in mice from all housing groups. However, a strong trend in the data indicated that cocaine increased dopamine release to a greater degree in isolated mice relative to the enriched mice (both EE and SE) at 10 min post injection. At the time points following 10 min post injection, the cocaine-induced increases in dopamine release were similar in all experimental groups, but the observed increased dopaminergic response at the 10 min mark may have implications towards the rewarding effects of dopamine agonists. The sooner an increase in dopamine efflux occurs following a drug administration, the more rewarding potential that drug has (Volkow and Morales, 2015). Thus, these findings indicate cocaine may have greater reinforcing properties in

the isolated mice relative to the EE and SE groups.

EE mice had decreased dopamine release to begin with, but following cocaine, the findings showed the percent change in dopamine release did not differ from SE mice. Behavioral studies have shown that EE reduces responses to psychostimulants compared to isolation (Stairs, Prendergast, Bardo, 2011; Staires & Bardo, 2009; Solinas, Chauvet, Thiriet, El Rawas & Jaber, 2008). Regarding the isolated mice, these findings are consistent with the previously mentioned results on dopamine release post cocaine. Thus, while baseline (pre-cocaine) dopamine release was altered more by physical stimuli (EE group showing decreased release), the dopaminergic effect of cocaine was altered to a greater degree by social factors (isolated group showing increased response to cocaine). These findings provide neurochemical support for related behavioral studies.

The relative influence of physical and social stimuli on dopamine and drug reinforcement is not clear in the literature. While Gipson et al. (2011) indicate social interaction is the driving force behind altered behaviors related to drug reinforcement, others propose physical activity is important to reducing self-administration (Creehan, Vanderwater, & Taffe, 2015; Cosgrove, Hunter, & Carroll, 2002). Our findings are consistent with the former. No differences were observed between EE and SE groups post cocaine, indicating that social interaction may be the environmental stimuli providing the psychostimulant-related protective effect in both conditions.

There are numerous directions the present topic could be expanded for future research. Some of the most important include describing strain and sex differences. For example, DBA2J mice are another inbred strain commonly used in addiction studies and differ behaviorally from C57BL/6J mice (Voikar, Polus, Vasar, & Rauvala, 2005). They may be more susceptible to the effects of isolation. In addition, it is unknown whether female responses will match the male patterns. Adolescent social isolation has been shown to induce increased stress hormones and anxiety-related behaviors to a greater extent in male rats compared to females (Pisu et al., 2016).

In conclusion, the present findings extend our understanding of how the social and physical environment contributes to the development and functioning of the dopaminergic reward system and vulnerability to drug abuse. Further, we provide neurochemical support for behavioral studies showing isolated mice are more likely to self-administer cocaine. This information can help guide prevention and treatment programs for drug abuse. Ensuring positive environmental factors like social relationships and interactions may be beneficial additions to current therapies and prevention programs.

References

- Aarde, S. M., Miller, M. L., Creehan, K. M., Vanderwater, S. A., & Taffe, M. A. (2015). One day access to running wheel reduces self-administration of D -methamphetamine, MDMA, and methylone. *Drug and Alcohol Dependence*, *151*, 151-158. doi: 10.1016/j.drugalcdep.2015.03.016
- Bardo, M. T., Valone, J. M., Robinet, P. M., Shaw, W. B., & Dwoskin, L. P. (1999). Environmental enrichment enhances the stimulant effect of intravenous amphetamine: search for a cellular mechanism in the nucleus accumbens. *Psychobiology*, *27*, 292-299. doi: 10.1037/a0024682
- Cosgrove, K. P., Hunter, R. G., & Carroll, M. E., (2002). Wheel-running attenuates intravenous cocaine self-administration in rats: sex differences. *Pharmacology Biochemistry & Behavior*, *73*, 663-671.
- Creehan, K. M., Vanderwater, S. A., & Taffe, M. A. (2015). Intravenous self-administration of mephedrone, methylone, MDMA in female rats. *Neuropharmacology*, *92*, 90-97. Doi: 10.1016/j.neuropharm.2015.01.003
- Czoty, P. W., Gould, R. W., Gage, H. D., Nader, M. N. (2017). Effects of social reorganization on dopamine D2/D3 receptor availability and cocaine self-administration in male cynomolgus monkeys. *Psychopharmacology*, *234*, 2673-2682. doi: 10.1007/s00213-017-4658-x.
- Deal, A. L., Konstantopoulos, J. K., Weiner, J. L., & Budygin, E. A. (2018). Exploring the consequences of social defeat stress and intermittent ethanol drinking on dopamine dynamics in the rat nucleus accumbens. *Scientific Reports*, *8*, 332. doi: 10.1038/s41598-017-18706-y
- El Rawas, R., Thiriet, N., Lardeux, v., Jaber, M., & Solinas, M. (2009). Environmental enrichment decreases the rewarding but not the activating effects of heroin. *Psychopharmacology*, *203*, 561-570. doi:10.1007/s00213-008-1402-6
- Ellenbroek, B., & Youn, J. (2016). Rodent models in neuroscience research: is it a rat race?. *Disease Models & Mechanisms*, *9*, 1079-1087. doi: 10.1242/dmm.026120

- Forster, G. L. & Blaha, C. D. (2003). Pedunculopontine tegmental stimulation evokes striatal dopamine efflux by activation of acetylcholine and glutamate receptors in the midbrain and pons of the rat. *European Journal of Neuroscience*, *17*, 751-762.
- Gibson, C. D., Beckman, J. S., El-Maraghi, S., Marusich, J. A., & Bardo, M. T. (2011). Effect of environmental enrichment on escalation of cocaine self-administration in rats. *Psychopharmacology*, *214*, 557-566. doi:10.1007/s00213-010-2060-z.
- Guo, J., Hawkins, D., Hill, K., & Abbott, R. (2001). Childhood and adolescent predictors of alcohol abuse and dependence in young adulthood. *Journal of Studies on Alcohol*, *62*, 754-762.
- Kalat, J. (2013). *Biological Psychology* (11th Ed.). Wadworth, Cengage Learning.
- Karkhanis, A. N., Leach, A. C., Yorgason, J. T., Uneri, A., Barth, S., Niere, F., ... Jones, S. R. (2018). Chronic Social Stress during Peri-Adolescence Alters Presynaptic Dopamine Terminal Dynamics via Augmentation in Accumbal Dopamine Availability. *ACS Chemical Neuroscience*, *10*, 2033–2044. doi: 10.1021/acscchemneuro.8b00360
- Laviola G., Hannan, A. J., Macri, S., Solinas, M., & Jaber, M. (2008). Effects of enriched environment on animal models of neurodegenerative diseases and psychiatric disorders. *Neurobiology of Disease*, *31*, 159–168. doi: 10.1016/j.nbd.2008.05.001
- Le Moal, M. & Simon, H. (1991). Mesocorticolimbic dopaminergic network: Functional and regulatory roles. *Physiological Reviews*, *71*, 155-234. doi: 10.1152/physrev.1991.71.1.155
- Lester, D. B., Rogers, T. D., & Blaha, C. D. (2010). Acetylcholine-dopamine interactions in the pathophysiology and treatment of CNS disorders. *CNS Neuroscience & Therapeutics*, *16*, 132-162. doi: 10.1111/j.1755-5949.2010.00142.x
- Meyer, A. C. & Bardo, M. T. (2015). Amphetamine self-administration and dopamine function: assessment of gene×environment interactions in Lewis and Fischer 344 rats. *Psychopharmacology*, *232*, 2275-2285. Doi: 10.1007/s00213-014-3854-1.
- Morse, A. C., Erwin, V. G., & Jones, B. C. (1993). Strain and housing affect cocaine self-selection and open-field locomotor activity in mice. *Pharmacology, Biochemistry and Behavior*, *45*, 905–912.

- Nader, J., Claudia, C., El Rawas, R., Favot, L., Jaber, M., Thiriet, N., & Solinas, M. (2012). Loss of environmental enrichment increases vulnerability to cocaine addiction. *Neuropsychopharmacology*, *37*, 1579-1587. doi: 10.1038/npp.2012.2
- National Institute on Drug Abuse. (2013). Nationwide Trends. Retrieved from <https://www.drugabuse.gov/publications/drugfacts/nationwide-trends> on 2018, November 26.
- National Institute on Drug Abuse. (2018). Drugs, Brains, and Behavior: The Science of Addiction. Retrieved 11 Oct., 2018, from <https://www.drugabuse.gov/publications/drugs-brains-behavior-science-addiction>.
- National Institutes of Health. (2015) *Public Health Service Policy on Humane Care and Use of Laboratory Animals*. Bethesda, MD: Office of Laboratory Animal Welfare.
- National Research Council. (2003) *Guidelines For The Care And Use Of Mammals In Neuroscience And Behavioral Research*. Washington, DC: The National Academies Press. <https://doi.org/10.17226/10732>.
- Paxinos, G. & Franklin, K. B. (2001) *The Mouse Brain In Stereotaxic Coordinates* (2nd Ed.). San Diego, Academic Press.
- Pisu, M. G., Garau, A., Boero, G., Biggio, F., Pibiri, V., Dore, R., ... Serr, M. 2016. Sex differences in the outcome of juvenile social isolation on HPA axis function in rats. *Neuroscience*, *320*, 172-82. Doi: 10.1016/j.neuroscience.2016.02.009
- Solinas, M., Chauvet, C., Thiriet, N., El Rawas, R., & Jaber, M. (2008). Reversal of cocaine addiction by environmental enrichment. *Proceedings of the National Academy of Sciences*, *105*, 17145-17150. doi: 10.1073/pnas.0806889105
- Solinas, M., Thiriet, N., El Rawas, R., Lardeux, V., & Jaber, M. (2009). Environmental enrichment during early stages of life reduce the behavioral, neurochemical, and molecular effects of cocaine. *Neuropsychopharmacology*, *34*, 1102-1111. doi: 10.1038/npp.2008.51
- Stairs D. J. & Bardo, M. T. (2009). Neurobehavioral effects of environmental enrichment and drug abuse vulnerability. *Pharmacol Biochem Behav*, *92*, 377-382. doi: 10.1016/j.pbb.2009.01.016

- Stairs, D. J., Prendergast, M. A., & Bardo, M. T. (2011). Environmental-induced differences in corticosterone and glucocorticoid receptor blockade of amphetamine self-administration in rats. *Psychopharmacology*, *218*, 293-301. doi: 10.1007/s00213-011-2448-4
- Wagner F. & Anthony J. (2002). From first drug use to drug dependence: Developmental periods of risk for dependence upon marijuana, cocaine, and alcohol. *Neuropsychopharmacology*, *26*, 479–488. doi: 10.1016/S0893-133X(01)00367-0
- Vöikar, v., Polus, A., Vasar, E., & Rauvala, H. (2005). Long-term individual housing in C57Bl/6J and DBA/2 mice: assessment of behavioral consequences. *Genes, Brain, and Behavior*, *4*, 240-252. doi: 10.1111/j.1601-183x.2004.00106.x
- Volkow, N., & Morales, M. (2015). The Brain on Drugs: From Reward to Addiction. *Cell*, *162*, 712-725. Doi: <https://doi.org/10.1016/j.cell.2015.07.046>
- Yorgason, J. T., Calipari, E. S., Ferris, M. J., Karkhanis, A. N., Fordahl, S. C., Weiner, J. L., & Jones, S. R. (2016). Social isolation rearing increases dopamine uptake and psychostimulant potency in the striatum. *Neuropharmacology*, *101*, 471-479. doi: <https://doi.org/10.1016/j.neuropharm.2015.10.025>.
- Yorgason, J. T., Espana, R. A., Konstantopoulos, J. K., Weiner, J. L., & Jones, S. R. (2013) Enduring increases in anxiety-like behavior and rapid nucleus accumbens dopamine signaling in socially isolated rats. *European Journal of Neuroscience*, *37*, 1022-1031. Doi: 10.1111/ejn.12113.

Johnda Eliza Washington graduated *magna cum laude* from the University of Memphis in May 2019 with a double major in English and anthropology. She is a member of the anthropology, English, and University Honors programs and graduated with the distinction University Honors with Thesis after completing two honors theses. She also received the Undergraduate Research Scholar designation after presenting research for her anthropology thesis at multiple conferences, including the Society for Applied Anthropology Conference in Portland, OR in 2019. Johnda was a member of the University of Memphis Anthropology club for four years and she served as the club's president during her senior year. Johnda plans to continue her education by pursuing a graduate degree in medical anthropology after finishing a gap year.

Johnda Washington

Communication Across Cultural Boundaries Within
Memphis ESL Classrooms

Faculty Sponsor

Dr. Rebecca Adams

Abstract

This study looked at the ways that English as a Second Language (ESL) teachers in the city of Memphis navigate cultural differences between themselves and their students through intercultural communication. ESL teachers in Memphis schools encounter diverse populations and must be able to communicate with these students in a way that is effective and culturally sensitive. Two teachers and their classrooms were observed. One teacher taught in a mainstream ESL classroom and the other at an ESL magnet school. The magnet ESL teacher actively worked to encourage intercultural communication between students. She was also able to bridge the gap between herself and a large population of her students that were Hispanic because she herself was also Hispanic and fluent in Spanish. The mainstream teacher worked to create a classroom environment that provided adequate support for students and incorporated cultural content into lessons to foster intercultural communication and respect between students.

Introduction

ESL in Memphis

Memphis is an area with a history of diversity and immigration. That diversity is reflected within the classrooms of Memphis, where nearly 8,000 English Language Learning (ELL) students were enrolled in the 2015-2016 school year (NCES, 2018). Students within the English as a Second Language (ESL) classrooms of Memphis come from different cultural backgrounds than those of their English-speaking counterparts. The Shelby County School District, which merged with the Memphis City School District in 2011, has a duty to ensure a safe and effective learning environment for ELLs in its classrooms. Part of ensuring an effective and healthy learning environment for children who come from different backgrounds is having teachers who are willing to bridge the cultural gap between themselves and their students.

Memphis is home to nearly 653,000 people, the majority of which are African American (Data USA, 2017). There are 46,000 Hispanic people living in the city, and 37,000 Memphians speak Spanish as a primary language. The next most common language in Memphis is Vietnamese with 2,600 speakers. There is also a large population of people who speak a range of African languages in Memphis (Data USA, 2017). With such a large population of non-native English speakers in Memphis, the need for effective and culturally sensitive communication is evident (Zhang, 2017).

Tennessee has a large number of Hispanic immigrants. Most of these immigrants are located in the cities of Nashville, Memphis, and Chattanooga and their surrounding suburbs (Nagle, 2012). In the 2014-2015 school year, 3.7 percent of all students in Tennessee were ELLs, with the highest percentage of these being Hispanic students (NCES, 2017). This percentage grew to 4.1 percent in the following school year (NCES, 2018). This population has continued to grow in recent years as the population of immigrants in Tennessee has grown as well (Kebede and Bauman, 2017).

The Tennessee Department of Education states that it is “the responsibility of the educational system to ensure all [ELL] students are appropriately supported in their English language development and in their progress toward mastering the academic standards for each grade level and content area” (Tennessee Department of Education). While the importance of giving students adequate support is stressed here, the idea does not always play out so well when put into practice. The graduation rates of ELL students fall behind that of their counterparts in almost every state, including Tennessee. While 87.2% of all students in Tennessee graduate, only 73.0% of ELL students reach graduation (Sanchez, 2017). It is obvious that the system

in place for ESL education has flaws and needs to be improved. One of those flaws is a lack of teachers who are ready and able to take on the role of teaching English to a non-native speaker. In every year since 2005, the state of Tennessee has reported a shortage of ESL teachers (Sanchez, 2017). Teacher shortages lead to more densely packed classrooms and less comprehensive and individualized instruction. English Language Learners in Tennessee also have consistently lower averages on standardized tests that are regulated by the state, regardless of the subject that the test covers (OREA, 2012).

These gaps in performance by ELL students and native English-speaking students are due to several factors and happen nationwide. Within the city of Memphis recently, steps are being taken to help bridge this gap at the foundational level. Within most Memphis schools, newly immigrated students with no or very little understanding of English are only exposed to two classes of intense English language instruction before being placed in courses with native English speakers (Kebede and Bauman, 2017). This is not a model that benefits the children placed in these schools. It is clear from the research done on the topic that English learners need an average of three to five years to become socially, or orally fluent, and upwards of four to seven years to gain academic fluency. Expecting a student who has had less than half that amount of time to keep up with native level speakers is an impossible task. The system in place for school-aged immigrants entering Memphis is one that lacks empathy for their situation and seems to be set up against them from the start.

Within the Shelby County School District, there are 114,000 students, of these 7,600 are students who do not speak English as their first language. The number continues to grow. One of the most recent reactions to the continued inflow of ELL students into the schools of Memphis is a new magnet school for students who were born outside of the United States. Magnet schools are public schools which focus their curriculum around a theme, in this case English language learning. They are unique because they draw in students from across the entire school district (Magnet Schools of America). The ESL magnet school was spurred on in part by a complaint by the US Department of Education's Office of Civil Rights, which sought to investigate how the Shelby County School District behaves towards and communicates with English language learners. Memphis was among many school districts which discouraged school enrolment for minors who immigrated, preferring that they sought out a learning or tutoring center instead (Kebede and Bauman, 2017).

Literature Review

Culture

Culture is a broad term for the beliefs, values, and rituals shared by a group of people. Within the field of anthropology culture is often described as the beliefs, language, and traditions that bond a social group. It is important that we view these ideas with the respect that it is due and try to understand them as best we can.

To provide a strong foundation for language learning, ESL educators must provide cultural context to their language teaching (López-Rocha, 2016, p. 106). Language does not exist in a vacuum; it is tied heavily to culture. As López-Rocha points out, “oftentimes these hidden elements of culture are the ones responsible for culture shock and misunderstandings, potentially leading to stereotyping and even prejudice” (López-Rocha, 2016, p. 107). Providing appropriate cultural content in learning can be key to providing students with the tools to navigate these misunderstandings.

Intercultural Competence and Communication

Intercultural competence (IC) is a person’s ability to communicate effectively with people from another culture in their language (Thao, 2017; Byram, 1997). IC consists of five key components. They are knowledge, critical cultural awareness, openness, interpretive skills, and interaction skills (Byram, 1997; Thao, 2017). Intercultural communication is “situated communication between individuals or groups of different linguistic and cultural origins” (LanQua). Intercultural communication requires valuing and respecting the culture of people who are different from you while learning from each other, which makes it an essential part of language teaching. In the intercultural context, the emphasis is on the “mutual exchange of ideas and cultural norms” while in a cross-cultural setting one culture is often dominant and “all other cultures are compared or contrasted to the dominant culture” (Spring Institute, 2018). This imbalance is an important consideration within the context of ESL classrooms where the culture of English-speaking people is dominant.

Figure 1 explains the relationship of intercultural competence and intercultural communicative competence—the first is a facet of the other. ICC is the ability to navigate a cultural setting that is not your own while communicating in a language that is not your native language (Thao, 2017; Byram, 1997). Byram’s model of ICC builds upon intercultural competence. It includes intercultural competence, linguistic competence, sociolinguistic competence, and discourse competence (Thao, 2017; Byram, 1997;

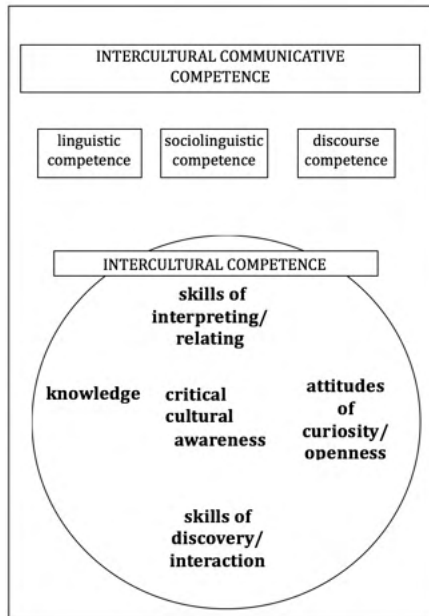


Figure 1. Intercultural Communicative Competence (ICC) (Byram, 1997).

López-Rocha, 2016). López-Rocha summarizes these points by stating,

A person who has developed ICC is able to build relationships while speaking in the foreign language; communicates effectively, taking into consideration his own and the other person’s viewpoint and needs; mediates interactions between people of different backgrounds, and strives to continue developing communicative skills” (López-Rocha, 2016, p. 107).

A key distinction between IC and ICC is that the communication involved in the former happens in one’s native language and the latter happens in a foreign language (Byram, 1997; López-Rocha, 2016). Those learning a language must develop ICC to navigate the cultural context in which their new language is embedded.

Intercultural Competence and ESL Learning

Students in ESL classrooms have the dual challenge of learning English and learning to navigate a cultural context that could be entirely unfamiliar to them. Having students gain intercultural communicative skills is as important as their language acquisition. Many ESL programs have adopted the idea

of total immersion and assimilation of students. This pragmatic approach has led to neglecting, and at times shaming, the home culture and language of the student. This push towards assimilation puts unneeded stress on the student and raises the anxiety levels of students.

These feelings affect how students navigate the classroom experience and are influenced by a variety of factors within the classroom environment. In a classroom environment where a student feels pressured to perform before they are ready, their anxiety level increases, which might lower self-confidence and motivation. A safe and low-stress classroom provides students with a zone where they feel comfortable and are able to face challenges and grow.

When teachers lack intercultural competence, they lack the ability to bridge the gap between themselves and students of other cultures (Thao, 2017). This means that the social and cultural needs of students might be overlooked and cause students unnecessary stress. Mastering cultural competency allows educators to meet the social, cultural, and linguistic needs of students in their classrooms in a way that is both respectful and beneficial to all involved. Intercultural competence is a valuable skill that should be taught to our educators. In a city as diverse as Memphis the need for culturally aware and respectful communication cannot be neglected.

Teachers of English must be culturally aware in order to provide students with the support they need while learning. They must cross the barriers of language as well as culture, which is not an easy feat. As Zhang points out, "Learning [a] foreign language is no longer about knowing how to use language for the purpose of speaking and reading, but about knowing how to communicate with people who have different cultural identities" (Zhang, 2017, p.229). Students of ESL learn to navigate the cultural setting that surrounds them, but it is less often that teachers are pushed to analyze and relate to the mix of cultural identities within their classrooms. Because ESL teachers are also in the midst of people from different cultures than their own, they must also understand how to communicate in this way. It is harder for teachers to help students navigate social interactions with people from other backgrounds if they do not see the students' points-of-view.

Classroom Environment as a Microcosm

Within our sociocultural context, English is the dominant language. It is hard to attend school, work, or settle into life in the US without some working knowledge of English. Because of the privileged position of English in the US and globally, English is often framed as the only important language, even if that means that students should give up their native language to

learn English.

Because culture is heavily tied to language, this belief can have detrimental effects on children from diverse backgrounds. Diverse areas like Memphis should lead the way towards a more interculturally aware and sensitive society. However, it does not appear that the southern United States is moving in that direction. Instead, “testing policies, new standards that marginalize multicultural learners, lack of resources, and local community values can constrain the ways in which linguistic difference and the teaching of language are approached by administrators, teachers, and students.” This leads to gaps in achievement like the lower graduation rates and test scores observed in the English language learner population (Fogle and Moser, 2017, p. 65).

This view of English as a lingua franca has effects that can be seen in teachers as well. Fogle and Moser (2017) interviewed teachers in the southern US who have experience working with English language learners. One of these teachers used this idea to ‘other’ students and praised teachers like herself who choose to work with them. ‘Othering’ or the creation of an us versus them mentality is one that exists outside of a society that values and seeks to understand cultural differences. This case is characteristic of many language teachers in the US and “represents a mainstream, monolingual position that emphasizes the role of the ESL teacher as a ‘good citizen’ and engages discourses of philanthropy rather than multilingualism” (Fogle and Moser, 2017, p. 72). The focus here is less on providing students with a knowledge of English that will help them to succeed and grow, and more on building teachers’ status and relationships to people outside of the classroom (Fogle and Moser, 2017). This process of othering students from different cultural backgrounds is common.

In cases such as this one in which “English language learners and immigrant families were constructed [by an ESL teacher] as in need of help, U.S. citizens, or monolingual English speakers, perhaps, were contrasted as ‘lucky’ and able to ‘help out’” (Fogle and Moser, 2017, p.72). There is a power imbalance between the culture that the student comes from and that which the teacher comes from. It is one in which one culture takes on the role of the dominant or superior and all other cultures are judged by their relationship to the dominant one (Spring Institute). As Zhang states, “competence in intercultural education is not an extra facet of teachers’ professional development but should become [an] integral part of that profession” (Zhang, 2017, p. 230). This means teachers should be acutely aware of their position within the classroom environment and how they relate to their students.

Most often in Memphis, ESL classrooms are not styled to be bilingual or transitional. They are pull-out ESL classes where students go to core classes with native-speaking peers and are pulled out from the classroom for intensive language lessons during the school day. Pull-out ESL allows students to get structured time with an ESL teacher, however, it does not provide enough support for most ELLs. The process of becoming socially then academically fluent in English is a long one that takes years to master and when students are limited to an hour or so of language instruction per day, they will struggle.

This is why new programs such as the ESL magnet school are seen as innovative and efficient ways of teaching students English. Students are given structured support throughout the day and taught the core curriculum by teachers who understand the challenges that their students are facing and have the experience, emotional intelligence, and intercultural competence to talk students through their challenges with language skills as well as course content. Unlike pull-out ESL programs, students are not pushed into classes with native speakers within a year of being introduced to English and expected to keep up.

Memphis is at the boundary of a major change in how it structures its ESL classrooms and how it treats students learning English. New programs, like those offered by the magnet school in this paper, focus on education for students who are newly immigrated to Memphis. Such programs are key to providing education that is intercultural and comprehensive. Students learning English as a second language are often left behind in classrooms where they are not adequately supported, and this shows in the statistics for ESL graduation rates and performance on standardized tests. Education that is truly fair to ESL students must give them support in a classroom that values their home language and culture. Intensive education that is based on mutual respect for other cultures and dedication to the success of students within the classroom is necessary for positive changes to occur within our ESL education system. These positive changes have never been more needed than now, because as immigrant populations within Memphis continue to grow, so will the English learning population.

Despite the unique importance of intercultural competence in Memphis schools, little is known about how educators in the area view or face this challenge within their classrooms. This gap in knowledge prevents school systems from providing educators with the information and tools they need to address the challenges of meeting their students' cultural needs alongside their language needs. It is important to understand the perceptions Memphis teachers have about culture in the classroom to work with teachers to provide students

with a classroom setting that meets their cultural as well as language needs. This paper will work to shed some light on this missing information.

Research Questions

1. What are Shelby County Schools ESL teacher's perceptions of the role of culture in language teaching?
2. How do Shelby County Schools ESL teachers enact intercultural communication in their classrooms?
3. Do teacher perceptions and enactment of cultural teaching differ between pull out ESL teachers in mainstream schools and teachers at an ESL magnet school?

Methods

Research Participants: Teachers

There were two teachers involved in this research. The first teaches at the ESL magnet school and has been teaching for nine years. She has been at her current position for two years. Before beginning this position she had been in a general education classroom. In her old position she frequently had ELL students in her classroom and saw the importance of ESL education.

The second teacher is located in a mainstream ESL classroom within Shelby County Schools. She has been teaching for 21 years and moved to the ESL classroom four years ago. She also had the experience of seeing many ESL students in her general education classroom. She saw the need for ESL teachers who cared about students and their success. When another teacher told her about the opportunity to get certified to teach ESL, she decided to go back to school.

Research Participants: Students

The students involved in this research come from many levels of English language proficiency. At the magnet school, the student population is comprised of children who have been in the United States for less than one calendar year. Most students become a part of the program because they are recommended or referred by local immigrant organizations. Typically, they lack foundational English proficiency when they come to the magnet school. The students come from many different cultures and speak many languages including Swahili, Arabic, French, Spanish, Tagalog, and Nepali. Spanish is the most common.

Research Participants: Researcher

The researcher on this project is an honors undergraduate student majoring in anthropology and English with a concentration in ESL. I have experience in conducting interviews, surveys, and focus groups through anthropological research internships. I have worked on teams of people with various cultural backgrounds both in the United States and abroad.

Observation

To understand Memphis ESL teachers' knowledge and perspectives on intercultural communicative competence and culture within the classroom it is important to observe classroom environments and talk with teachers. This project included semi-structured observations and interviews with teachers to determine how cultural teaching occurs in the specialist ESL school and in ESL classrooms in a mainstream school. A researcher reflection form was also used after observations and interviews to capture impressions and initial reactions to responses during the data collection.

Structured observations for this paper took place in Spring 2019 in two different locations, an ESL magnet school and a mainstream pull-out ESL classroom. The observations were conducted using an observation checklist that required the researcher to answer a series of standard questions, but also allowed for notes to be taken on classroom set-up, cultural content in lessons, student interest and attentiveness, as well as the way that the teacher communicates with students both verbally and nonverbally. Some questions were standard to the ESL practicum course and some were written for this project.

Observation Locations

The magnet school is open to high school students who have been in the country for less than one year. The school attempts to be a safe place where students feel comfortable speaking and developing. Teachers of every subject work alongside counselors and a bilingual cultural mentor to help students succeed.

The program incorporates science, math, social studies and language arts into courses that are taught by a teacher with ESL training. Students join the rest of their peer group for elective classes (Kebede and Bauman, 2017). Having ELL students separated from their native English-speaking peers is at times beneficial to ELL students; it creates a balance between teaching ELLs culture and language skills, and skills from other subjects. Combining subjects like science and math with language courses can provide students with the appropriate support and reduce their stress in the

classroom. During instruction at the magnet school, the teacher provides a translation of complex tasks in Spanish and repeats short phrases in Spanish after saying them in English. The majority of students in the classroom come from Spanish-speaking countries and speak Spanish as a first language.

The mainstream ESL classroom is divided into sections. There are whiteboards along two of the walls and they are filled with previous or on-going lessons along with charts and other helpful information. There are also areas with laptops and games, and a reading area with books for each reading level and subject. She says that most of the students who make up her classes are Hispanic, some are Asian, and one is Jamaican, but her “broken English” is what qualified her for the ESL program.

Observation Protocol

A total of 24 hours were spent observing the two classrooms and taking detailed notes. I observed the teacher at the ESL magnet school on three days for a total of nine hours and conducted two hour-long semi-structured interviews with the magnet ESL teacher. I observed the mainstream ESL classroom on three days for a total of fifteen hours and I conducted two hour-long semi-structured interviews with the mainstream ESL teacher. Before classroom observations took place, I talked with the teachers about my role in the classroom as the observer and discussed the data I would be gathering. Teachers and administration at the schools knew about the general research topics I aimed to address.

Interviews

After the classroom observation, I conducted informal semi-structured interviews with the two teachers. Each interview was approximately one hour in length. Interviews were not recorded, notes were typed or written. Written notes were always typed into a word document after the interview ended. The interviews were conversational. Teachers were able to provide additional comments about the cultural backgrounds of their students, intercultural communication and intercultural communicative competence, and the role of culture in the classroom during short one-on-one conversations. They were asked informally to talk about these topics and their knowledge and perspectives on these while I took notes. Each conversation touched on these topics; however, the questions asked were not standardized. It was important that the teacher felt free to lead the conversation and express their true opinions on the topics that were brought up.

Reflection

After completing observations and interviews, a reflection questionnaire was filled out and notes were reviewed to be sure they were as in-depth as possible. These questions helped to frame the data gathered in the context of the study. This questionnaire helped to organize data and begin to make sense of the things learned from each classroom experience.

Analysis

I reviewed data collected during all of the interviews and transcribed all notes into a word document. This data was coded through thematic analysis for topics relating to cultural content, teacher's perceptions of their students' cultural backgrounds, barriers to communication, and the use of intercultural communication. The teaching methods at each school were compared as ideas emerged.

Results

Teacher Background: Mainstream School

The teacher at the mainstream school was from the Memphis area. She went to school at a local college and majored in education because helping young students was important to her. During the time that I worked with her in the spring of 2019, she had been teaching for two decades. For the first several years of her teaching career, she worked in general education elementary school classrooms. While working in general education classrooms, she received quite a few ESL students. She said that she worked well with these students. She worked to provide them with the extra support they needed to thrive in the classroom.

After being in the general education classroom for 17 years she went back to school to get certified in teaching ESL. She says that she dealt with ESL students with compassion before becoming an ESL teacher. It has always been important to her that students from all backgrounds felt safe to learn and grow in her classroom. Teaching ESL allowed her to focus on a student population that she saw as more vulnerable than others. She said that she developed compassion for these students by asking herself, "How would I feel if I came here and didn't know any English?" It was important to her that students felt that her classroom was a safe place within the school in the same way she would want.

Teacher Background: Magnet School

The teacher at the ESL magnet school location was from Texas and been

teaching for nine years. She has taught many subjects in grades from pre-K to middle school. In those classes she worked with general education students with ESL and special-education students mixed in. She says that her lessons had to accommodate for all student types in the classroom. While in this position she saw a need for ESL teachers that cared about students and their development.

She had an ESL endorsement because it was a requirement in the location where she received her education degree. Later she decided that she would like to work with students like the ELLs that she had had in classrooms. She has been with the ESL magnet school since it opened two years ago. When she heard about the school and its focus on ELL students who were new to the country, she knew that addressing that need was important. She says, “It’s been nice to start with something and help build it.” She also noted that coming from another state and understanding the ways teachers perceive and treat ELL students gave her unique knowledge about how to deal with issues in the classroom that have not been addressed in Memphis classrooms.

Perceptions of Students’ Cultural Backgrounds: Mainstream School

The majority of students in the mainstream classroom come from Mexico or other Latin American countries. However, there are also some from areas such as Yemen, Vietnam, and Cambodia. The teacher says that of the Spanish-speaking students in the classroom most were born within the United States, but come from households where Spanish is the primary or only language spoken. She also says that the students who speak languages other than Spanish were not born here, they immigrated. Of the students enrolled in ESL, the teacher tells me that there is one whose first language is English. The student is Jamaican, but she says that her “broken English” is what qualified her for the ESL program.

In the mainstream school, the teacher addressed concerns about how teachers treat students of different cultural backgrounds. She says, “You would be surprised at the prejudice that I receive, or the students receive from other teachers. I’ve heard ‘their parents need to learn English’... They’ll say that in front of the child.” She describes general education teachers within the school as culturally insensitive towards ESL students. They believe that the parents of students in ESL are at fault for not teaching children English. The mainstream ESL teacher believes teachers should work alongside parents and students to make goals for the student together. Involving parents and students in this planning allows the teacher to meet the student where they are and maintain respect.

The mainstream teacher's goal is that students of any culture feel safe and heard in her classroom. It is important that students are never shamed about their identity. She says, "This [classroom] is the safest place in this building for them." Students must have a place where they feel it is okay to make mistakes. She reminds students that making mistakes is a part of the learning process. They must also understand that when they make mistakes they will not be judged or made fun of.

Perceptions of Students' Cultural Backgrounds: Magnet School

At the magnet school there are students from a wide range of countries and cultures. They come from areas in the Middle East, Asia, Latin America, and parts of Africa and speaking languages such as Swahili, Spanish, Arabic, French, Tagalog, and Nepali. To qualify for admission into the magnet school students must have resided in the United States for less than one calendar year. Most students become a part of the magnet school program because they are recommended or referred by local immigrant organizations. Typically, the students remain in the program for a year before moving to their local school, but there are some exceptions.

The ESL magnet teacher speaks fluent Spanish, which allows her to connect with students who are also from Hispanic backgrounds. During class she often repeats instructions in Spanish to help students understand the task that they are going to be working on. The majority of students in the classroom speak Spanish as a first language, so this is valuable. Students who speak other languages do not have this additional support, but accommodations such as translation dictionaries are available for every language that students at the school speak. Laptops are another resource that students have available.

It is important to the teacher at the ESL magnet school that her students feel relaxed and safe within the classroom. They must know that their culture is respected and that they have a role to play within the classroom. The teacher believes that each student in the classroom acts as a cultural ambassador. She tells them that in the United States they will sometimes face situations in which they are the only person from their country. In this situation, they must represent their country and their culture. She stresses the idea that students begin to play that role within the classroom, where they interact with people from many different cultures. They must be aware of cultural differences of others and cognizant of the role that they have in representing their own culture.

Navigating the Intercultural Classroom: Mainstream School

The mainstream ESL teacher noted how general education teachers fail to meet ESL students halfway. She voiced concern that teachers in the general education classrooms did not give ESL students the support that they needed. She says, “You’d be so surprised by how other teachers will go out of their way to fail ESL students knowing that they are not accommodating or modifying their work.” She says meeting students halfway is an important part of connecting with them. Understanding students and connecting with them is an important part of being able to communicate effectively with them.

She tells me that intercultural communication “means what we do together and how we communicate together. It doesn’t matter that one student is from Mexico and one is from Yemen, but that we work together and communicate together.” Collaboration promotes unity and understanding within the group of students. She focuses on the group as a whole and their ability to work together instead of the cultural differences that might divide them. During the first class session I observed, she split students into three groups for an exercise on types of energy. The teacher mixes the groups so that students get the chance to work with people that they do not usually sit with. This variety is important because collaboration is a major part of the carousel activity that is planned for the day. In two of the three carousel stations that are set up, students work together to fill out worksheets on energy. In the third station, each student works separately to film a video of themselves talking about the forms of energy. When a student at a table raises their hand to ask a question the teacher comes to the table and asks if he has asked his group members the same question and emphasizes that they are all sitting together to help each other. When she answers the question she makes sure that everyone in the group hears the answer, not only the student that originally asked the question. In this way, the teacher emphasizes that students in the class are a team that should work together to problem-solve and assist each other.

The teacher focuses on unity and collaboration in the content of the course. One text that her group read in the past year was called *Esperanza Rising*, a story about a girl who immigrates with her family from Mexico during the Great Depression. They read the book to help students develop an understanding that they all come from different backgrounds and that they should accept others’ backgrounds and accept students for who they are. It helped them to see that everyone’s story is not the same, but everyone’s story and background is valuable.

Navigating the Intercultural Classroom: Magnet School

The teacher points out that even the Hispanic students come from very different cultures, despite being grouped by language. What is most important to the teacher in this situation is that a “culture of respect” is maintained. To her, this means communicating in ways that show that the home culture of students is valued and respected. She works to promote this culture by mixing groups of people in the classroom. When group activities are scheduled, she ensures that students are not working with the same group of students each time. When they first sit down in the classroom students sit with groups of people that are familiar to them, often with students who speak the same first language. The teacher introduces variety and diversity to student groups by asking people to move around before beginning a group activity or by assigning students to groups herself. The seating chart changes frequently, and with these changes she likes to have people from diverse cultures work closely alongside each other. It is her goal that students in her class exit prepared to represent themselves and their culture outside of the classroom.

She stresses the importance of helping students to feel relaxed in the classroom. She says once they’re relaxed, they feel safe and “intercultural communication promotes that safety.” She also helps to promote a safe classroom environment by showing students that their culture and language are valued. She notes that it is important that everyone will not always agree with each other but that they always show that respect anyway. She tells the story of a young girl and boy in her classroom who had come from the same country to live here. Before each class students must grab their journals from the wall before sitting. In this case, the boy would sit, and it was the girl’s responsibility to grab both of their journals and sharpen his pencil if needed. She would grab their journals from the bin on the wall and return to sit beside him for class. Thinking back on the experience, the teacher notes, “As a teacher I can’t be upset with that.” Over time, she says, the two students have become friends, and this isn’t something that they do anymore.

Barriers to Teacher/Student Communication: Mainstream School

The ESL mainstream teacher believes that anxiety about leaving their comfort zone can be a huge barrier for students. It is hard to give themselves the freedom to make mistakes if they feel unsafe or have any fear of being judged. She wants students to feel safe in her classroom and she says,

I let down all the barriers in this room. It's just the students and me, we don't make fun of the way we talk. If you mispronounce words, it's okay. If you make mistakes, I'm okay with that. I don't mind teaching and correcting them, it's not a harsh correction... There's no sarcasm, no put-downs, we're all about helping each other.

She knows that reducing fear and anxiety plays a huge role in breaking down barriers to communication with students.

The teacher also addresses the communication barrier that arises with new ESL students. When she is interacting with a student who doesn't speak any English, yet the mainstream teacher stresses the importance of using TPR, total physical response. To her, this means using lots of gestures and slowing down speech. She says this is part of an effort to meet students where they are. It allows her to connect with them and attempt and provide foundational language skills. During one observation session, the teacher holds a class meeting in which the students and teacher discuss the lesson from the previous day and give their opinions on what went well and what behaviors need to be improved. When she gives feedback on the lesson the teacher says, "I don't think we listen to each other," and holds up a cupped hand to her ear. She asked students to also make the gesture then asked, "Why don't we listen to each other?" This is a gesture that she uses a few times throughout the conversation to ensure that students began to associate the gesture with the word listen. Each time she said the word listen she would make the gesture and students would follow along. She also used gestures for the word 'talking,' and when she made the point that students were talking over each other she made a talking gesture with both hands and waved her arms about while getting louder.

The teacher also knows sign language and first attempts to teach and use modified signs with new students. Many teachers at this mainstream school know sign language, and she says that her hope is if a student can gain some knowledge of sign language other teachers might use this skill to help ESL students with simple instruction in their general education classrooms.

Barriers to Teacher/Student Communication: Magnet School

Similar to the mainstream teacher, the teacher at the magnet school says nonverbal communication can be extremely useful when working with students from other cultures. It is a tool that she uses often with students who do not speak any English or Spanish. They were recently able to obtain dictionaries for all languages that are spoken in the school. Each student has a translation dictionary from their first language into English and they carry it around from class to class every day. This is a valuable way to

support students who do not yet have the English language skills they need to navigate the classroom environment.

Discussion

The teachers in both of these classrooms showed respect for the cultural backgrounds of their students in different ways and had different levels of engagement using intercultural competence. The magnet school teacher was able to connect with students of different Hispanic cultures because of their shared language. She acted as an example of an intercultural communicator. She believed that it was important to respect the diverse backgrounds of her students and acknowledge the way these backgrounds impact the classroom environment.

The mainstream teacher also believed it was important for students' backgrounds to be respected. However, instead of encouraging students to take on the role of cultural ambassadors, she perceived differences in culture as a barrier to equality and classroom communication. The mainstream teacher reinforced the ways in which students were all the same as a way of preventing barriers from disrupting the classroom environment. The magnet school teacher encouraged students to understand the impact that their cultural background will have in different intercultural settings in the future. She understood the value of providing students with intercultural experiences which allow them to build the skill of intercultural communication. She purposely organized her classroom so that groups of students from diverse backgrounds were able to work closely with one another.

Conclusion

For the magnet school teacher connecting with students of diverse cultural backgrounds seemed to come easy. The teacher used methods such as TPR and exaggerated gestures and movements to explain concepts to students, which was valuable. However, her background of being Hispanic and speaking fluent Spanish was invaluable to her students. She was able to connect with her students of Hispanic backgrounds in a way that was not possible for the mainstream teacher. When she spoke Spanish in the classroom it allowed students who knew little-to-no English to feel as though their teacher had a vested interest in bridging the gap and meeting them where they were. It also allowed students who only spoke Spanish to come to her with questions or concerns they had without the need for translation or dictionaries.

The students in this class who spoke Spanish as a first language were able to communicate with the teacher from their very first day. Students who spoke another language faced barriers common to many other ESL settings.

They relied on other methods of communicating with the teacher before they developed English skills. They were provided with translation dictionaries or allowed to use laptops or phones as a translation device if needed. The teacher used gestures when speaking to them and worked closely with them to provide support where she could. Because the student population was largely Hispanic and many of the teachers were bilingual, it was not uncommon for students to pick up Spanish at the same time that they were learning English. Creating situations in which, for instance, a Senegalese student whose first language was French will learn basic phrases and slang in Spanish from peers concurrently with English vocab. Culture and language are shared freely.

The students in the mainstream course did not have the extra support of having a teacher who spoke their home language. Spanish and Arabic speaking students alike faced barriers to communication with the mainstream teacher. It was important to the mainstream teacher that these students knew that their backgrounds should not create barriers between them in the classroom. She did not focus on how differences can be respectfully addressed in the classroom, but instead encouraged students to be aware of all the ways that they are the same. Part of fostering intercultural communication and respect is understanding that culture and expectations are important to their background and identity. Because of this, the magnet school teacher had a different approach to classroom differences.

The magnet teacher pointed out that even the Hispanic students in her class come from very different cultures, despite being grouped by language. What is most important to the magnet school teacher in this situation is that a culture of respect is maintained. To her, this means communicating in ways that show that the home culture of students is valued and respected. She works to promote this culture by mixing groups of people in the classroom. The seating chart changes frequently and with these changes she likes to have people from diverse cultures working closely alongside each other. She wants students to be prepared to represent themselves and their culture outside of the classroom.

Unlike the mainstream teacher, the magnet school teacher does not shy away from acknowledging the cultural differences in her student population. She is always aware of the cultural backgrounds present and acknowledges the differences that make up the classroom. She uses the experience to prepare students to be great intercultural communicators both in and out of class.

Future Implications

The number of students in Memphis city schools who do not speak English as a first language continues to rise. It is as important as ever that these students feel as though they have a safe and supportive learning environment. Teachers who have strong intercultural communication skills are an essential part of cultivating that environment.

Working with ESL teachers to provide education on the needs of a supportive intercultural environment is important to the future success of the ESL students within Memphis. Long-term, multiple-site studies on teachers' knowledge of intercultural communication and how they implement it into their classroom structure and curriculum are needed to see the full scope of this issue across the school system. The information gathered during this research and in future studies should act as a measure for determining what assets and education ESL teachers in Memphis must be provided to assist them in navigating their intercultural classrooms and supporting diverse student populations.

References

- "English Language Learners In Tennessee Public Schools". OREA, 2012, https://www.comptroller.tn.gov/content/dam/cot/orea/documents/orea-reports-2012/2012_OREA_EnglishLearners.pdf. Accessed 12 Mar 2019.
- Byram, M (1997). *Teaching and assessing intercultural competence*. Clevedon, UK: Multilingual Matters.
- Data USA. "Memphis, TN". *Data USA*, <https://datausa.io/profile/geo/memphis-tn/>. Accessed 10 Dec 2018.
- Fogle, Lyn Wright, and Kelly Moser. "Language Teacher Identities in the Southern United States: Transforming Rural Schools." *Journal of Language, Identity & Education*, vol. 16, no. 2, Mar. 2017, pp. 65–79. EBSCOhost, doi:10.1080/15348458.2016.1277147.
- Kebede, Laura Faith, and Caroline Bauman. "With Students Arriving Every Day, Memphis Seeks To Join Other Cities With Newcomer Programs For English Language Learners". *Chalkbeat*, 2017, <https://www.chalkbeat.org/posts/tn/2017/04/26/with-students-arriving-every-day-memphis-seeks-to-join-other-cities-with-newcomer-programs-for-english-language-learners/>. Accessed 11 Dec 2018.
- Language Network for Quality Assurance (LanQua). "Intercultural Communication". Lanqua.Eu, <https://www.lanqua.eu/theme/intercultural-communication/>. Accessed 10 Dec 2018.
- López-Rocha, S. (2016). *Intercultural communicative competence: creating awareness and promoting skills in the language classroom*. In C. Gorla, O. Speicher, & S. Stollhans (Eds), *Innovative language teaching and learning at university: enhancing participation and collaboration* (pp. 105-111). Dublin:
- Lynch, Matthew. "Bilingual Education: 5 Reasons It Should Be Required - The Edvocate". *The Edvocate*, 2018, <https://www.theedvocate.org/bilingual-education-5-reasons-it-should-be-required/>. Accessed 12 Dec 2018.
- Magnet Schools of America. "What are Magnet Schools". Magnet Schools of America (MSA). <https://magnet.edu/about/what-are-magnet-schools#1499667889100-039b81ce-813c>

- Nagle, Nicholas et al. "A Profile Of Hispanic Population In The State Of Tennessee". *Cber.Bus.Utk.Edu*, 2012, <http://cber.bus.utk.edu/census/hisp/bfox288.pdf>. Accessed 10 Dec 2018.
- National Center for Education Statistics. "English Language Learners In Public Schools". *Nces.Ed.Gov*, 2017, https://nces.ed.gov/programs/coe/pdf/Indicator_CGF/coe_cgf_2017_05.pdf. Accessed 10 Dec 2018.
- National Center for Education Statistics. "English Language Learners In Public Schools". *Nces.Ed.Gov*, 2018, https://nces.ed.gov/programs/coe/indicator_cgf.asp. Accessed 10 Dec 2019.
- National Center for Education Statistics. "Fast Facts". *Nces.Ed.Gov*, 2018, <https://nces.ed.gov/fastfacts/display.asp?id=96>. Accessed 11 Dec 2018. Research-publishing.net. <http://dx.doi.org/10.14705/rpnet.2016.000411>
- Sanchez, Claudio. "English Language Learners: How Your State Is Doing". *Npr.Org*, 2018, <https://www.npr.org/sections/ed/2017/02/23/512451228/5-million-english-language-learners-a-vast-pool-of-talent-at-risk>. Accessed 11 Dec 2018.
- Thao, Tran Quoc, and Pham Tan Tai. "The Importance Of Intercultural Communicative Competence In English Language Teaching And Learning". HCMC Open University, 2017. Research Gate, https://www.researchgate.net/publication/320491458_THE_IMPORTANCE_OF_INTERCULTURAL_COMMUNICATIVE_COMPETENCE_IN_ENGLISH_LANGUAGE_TEACHING_AND_LEARNING/stats. Accessed 13 Mar 2019.
- The Spring Institute. "What's The Difference Between Multicultural, Intercultural, And Cross-Cultural Communication? - The Spring Institute". The Spring Institute, 2018, <https://springinstitute.org/whats-difference-multicultural-intercultural-cross-cultural-communication/>. Accessed 12 Dec 2018.
- Zhang, Yechun. "A Study on ESL Teachers' Intercultural Communication Competence." *English Language Teaching*, vol. 10, no. 11, Jan. 2017, pp. 229–235. EBSCOhost, ezproxy.memphis.edu/login?url=http://search.ebscohost.com/login.aspx?direct=true&db=eric&AN=EJ1160969&site=eds-live&scope=site.

Image Sources

Figure 1: Center for Applied Second Language Studies (CASLS). "Intercom - View Content". Caslsintercom.Uoregon.Edu, 2016, <http://caslsintercom.uoregon.edu/content/21228>. Accessed 10 Mar 2019.

Faculty Review Board

Dr. Gustav Borstad
Instructor
Department of Physics

Dr. Colin Chapell
Instructor
College of Professional & Liberal Studies

Dr. David Freeman
Associate Professor
Department of Biological Sciences

Dr. Ronald Fuentes
Assistant Professor
Department of English

Dr. Arleen Hill
Professor
Earth Sciences

Dr. Jessica Jennings
Assistant Professor
Biomedical Engineering

Dr. Sanjay Mishra
Professor
Department of Physics

Dr. Max Paquette
Associate Professor
School of Health Studies

Dr. Melissa Puppa
Assistant Professor
School of Health Studies

Dr. Kris-Stella Trump
Assistant Professor
Department of Political Science

Submission Guidelines

Eligibility

QuaesitUM considers submissions from any current University of Memphis undergraduate student; eligibility also extends to those who have graduated within the last two semesters. Research must reflect University of Memphis student projects. Manuscripts may be single or co-authored, but the primary author must have been a University of Memphis undergraduate student during the time the research was conducted. Faculty members and graduate students are not eligible.

Content

Papers should present analytical research performed by the author(s). Submissions should include a section in which data and research methodology are described in detail.

All submitted text is to be the sole creation of the author(s) with the exception of correctly cited paraphrases and properly indicated quotations. In the case of collaborative research with faculty, papers should represent the student's contribution to the larger project.

Any research involving human subjects must have approval from the appropriate Institutional Review Board. Submitting authors are responsible for adhering to IRB guidelines. Check with your faculty advisor for further information.

While there is no minimum or maximum length for articles, 8,000 words or less is preferred. We understand academic disciplines have different norms, and we take this into account.

Copyright

Submissions may not be under review for publication elsewhere.

Authors retain copyright of their work. Authors may publish their papers elsewhere later so long as the requirements of all involved parties are satisfied. Given the hard work that our editorial team puts into each paper prior to publication, we ask that if you publish the work elsewhere, you include an acknowledgement of *Quaesitum* and its editorial staff.

Formatting

1. Remove all occurrences of author(s) names from the manuscript.
2. Include a cover sheet as a separate document that contains author name(s), title, faculty sponsor*, date, citation style, and one of the following categories:
 - Life and Health Sciences
 - Physical and Applied Sciences
 - Math/Computer Science/Engineering
 - Social and Behavioral Sciences
 - Humanities
 - Professional

*The faculty sponsor is someone who gave feedback on your paper, taught the class for which you conducted the research, or provided some form of guidance for the paper.

3. Include an abstract of 150 words or less.
4. Upload your manuscript as a .docx or .doc file (Let us know if your academic discipline uses a different format). The manuscript should be formatted as follows:
 - Single-space the body of the text.
 - Use 12 point Times New Roman.
 - Number pages.
 - Properly cite all referenced works.

5. Figures and Tables

- Use greyscale when possible.
- Tables in Word/Excel should be no more than 5 inches wide according to the Word/Excel ruler.
- Avoid extremely small letters/details whenever possible. These can become too small to read if we have to shrink the figure/table to fit within the 5" page width.
- Place figures and tables in your manuscript.
- Number and title all figures and tables in your manuscript.
- Upload a separate, high quality file for each table and figure.

6. Carefully check that each item in your references section follows the punctuation, capitalization, and italicization conventions of your citation style (APA, MLA, etc.).

Review Process

Submissions are uploaded to the Quaesitum submission manager, Scholastica (see the link on the next page). After submission, articles are screened by the Quaesitum editorial staff. Manuscripts meeting and exceeding the panel's criteria are then forwarded to volunteer faculty reviewers who have expertise in a field of research relevant to the manuscript. This is a double-blind process: both authors and faculty reviewers remain anonymous. Final selection decisions are left to the editorial staff.

Revision Process

After the review process is complete (usually mid-March), authors will be notified of the review board's decision. Authors whose papers are selected for publication will receive suggestions for revision from the faculty reviewers and editorial board. Authors are required to revise their manuscript before final publication.

Deadline for Submissions

For publication in Issue 8, papers should be submitted by January 19, 2021.

Submit Your Research Paper

Upload your manuscript to our Scholastica page:

<https://submissions.scholasticahq.com/sites/quaesitum/for-authors>

Questions

Contact us at quaesitum@memphis.edu with any questions.